Title	Organic geochemical study on the life history of lichen and fungi: Search for the molecular fossils and the reconstruction of fungal flora evolution
Author(s)	,
Citation	. ( ) 15281
Issue Date	2023-03-23
DOI	10.14943/doctoral.k15281
Doc URL	http://hdl.handle.net/2115/89550
Type	theses (doctoral)
File Information	Masashi_Ikeda.pdf

Instructions for use

Ph.D. dissertation

Organic geochemical study on the life history of lichen and fungi: Search for the molecular fossils and the reconstruction of fungal flora evolution

地衣類・菌類の有機地球化学的手法による地球生命史研究
：分子化石の探索と菌類フロラの変遷史復元

Masashi Ikeda

Department of Natural History Sciences,
Graduate School of Science, Hokkaido University

March 2023

ABSTRACT

Lichens are organisms that have adapted to extreme environments by forming symbioses between fungi and algae, and are known as typical pioneer plants that expand into bare ground at the beginning of plant succession. The appearance of lichens is ancient, and fossil records indicate that they were already present in the early Devonian (Taylor et al., 1995a,b; Honegger et al., 2013a,b). Recently, molecular phylogenetic analyses have reported that many lichens diversified with environmental changes during the Cretaceous; Gaya et al. (2015) used molecular phylogenetic analyses to report that the pigment phenotype of the lichen family Teloschistaceae changed during the Mid-Cretaceous, which may have resulted in strong UV tolerance, expansion and diversification into bare ground. On the other hand, the fossil record itself is rare in its production due to factors such as habitats that are difficult to preserve and biases such as the observation of microstructures necessary for identification and separation from sedimentary rocks. Therefore, paleoecological studies of lichens at the earth-history level have been limited to studies using extant lichens. Therefore, the objectives of this study were to search for lichen biomarkers, develop lichen vegetation indices and reconstruct paleoecology. As a first step, lipid analysis of extant lichens was performed to examine indicator organic molecules. As a result, we found that the lichens contained aliphatic hydrocarbons, including *n*-alkanes, alkenes, and long-chain branched alkanes, fernenes, diploptene, and hop-21-ene. Lichens with a green algae photobiont (photosynthetic symbiotic algae) contained 1,8-heptadecadiene or 6,9-heptadecadiene and 8- and 7-heptadecene, whereas lichens with cyanobacteria as a photobiont did not contain the heptadecadienes but did contain octadecene, nonadecene and nonadecadiene. These differences in characteristics could be attributed to phylogenetic differences in the photobionts that comprised the lichens, indicating that the alkene composition could be used for lichen chemotaxonomy. These results suggest a previously unknown origin for the C_{17}–C_{19} alkenes in sediments and implied that these components could be used to reconstruct the past composition of lichens. As a next step, we focused on lichen secondary metabolites, known as lichen-specific components. Among oxygen-containing aromatic compounds, dibenzofurans has been reported as a universal compound in lichens, and lichens are known to be the main producers in nature. Since lichens in nature have a methyl group specifically in the first

position of methyl dibenzofuran, this study examined 1-methyl dibenzofuran as a lichen biomarker and indicator. As a results for, The 1-MDBF index showed no abrupt changes at both sites. The ratios of aromatic terpenoids to perylene and higher plant origin terpenoids indicated a relative increase during the decay period of fungi and higher plants. The cold weather event is known to occur in the North American samples during the through-phase, suggesting that lichens of 1-MDBF origin are highly tolerant to environmental changes and are not affected by environmental fluctuations. Based on the findings obtained, we also evaluated the usefulness of oxygen-containing aromatic compounds as lichen tracers. Several aromatic furans were detected in the Mesoproterozoic (1.2-1.0 Ga) sedimentary rocks of the Qaanaaq Fm. in northwestern Greenland. The isomer ratios and abundances of the aromatic furans detected varied from stratigraphic level to stratigraphic level. This may be attributed to changes in the contribution of the source material at the time of deposition, rather than to the effect of maturity. Aromatic furans are suggested to be possible terrestrial sources, and these compounds in the Mesoproterozoic may be important evidence in discussing the evolutionary history of ecosystems and life at that time.

Acknowledgement

Contents

1.1. Fungi and Lichen

1.2. Earth History of Fungi and Lichens

1.3. Organic Geochemical Studies on Fungi and Lichens

1.4. Summary of Chapter and Objectives of This Study

2.1. Introduction

2.2. Samples and methods

   2.2.1. Sample

   2.2.2. Extraction and fractionation

   2.2.3. Formation of DMDS adducts

   2.2.4. Lipid assignment and quantification

   2.2.5 Statistical analysis

2.3. Results and discussion

   2.3.1. Mass spectral characteristics of dimethyl disulfide (DMDS)
          derivatives of C_{17}–C_{20} alkenes

   2.3.2. Composition and concentration of aliphatic compounds

   2.3.3. Taxonomic variability of aliphatic components

   2.3.4. Potential biomarkers of lichen

2.4. Conclusions

CHAPTER 1
Introduction and General Background

1.1. Fungi and Lichen

Fungi, once regarded as a group of plants as "cryptophytes," are now known to be organisms with a diversity far surpassing that of higher plants. According to some research, there are an estimated 400,000 species of higher plants (Paton et al., 2008; Joppa et al., 2017), while there are more than 2.2 to 3.8 million species of fungi on earth (Hawksworth and Lücking, 2017). In the past, Myxomycetes, such as slime molds, and Oomycetes, including water molds, were treated as fungi. However, nowadays, they are called "Pseudofungi" and are considered to be a distinct lineage from the fungi. Recent developments in molecular genetics have shown that the lineage is more closely related to animals than plants, and fungi, along with animals, are now classified as Supergroup, Opisthokonta. Although the classification is still debated, fungi are broadly classified into Microsporidia, Chytridiomycota, Zygomycota, Glomeromycota, Ascomycota, and Basidiomycota (Fig.1.1). Many species of Microsporidia were once considered protozoa, and the Chytridiomycota species were generally considered to be the most primitive of the fungi, as they are often aquatic fungi. The species formerly referred to as "Zygomycota" were also considered primitive because of their simple structures. However, they are strongly independent of each other and are being considered for dissection into multiple taxa (cf. Blackwell, 2011). For example, some of them, initially included in the Zygomycota, have become independent Glomeromycota. On the other hand, Basidiomycota, which include most of what is commonly called mushrooms, and Ascomycota, which include species such as yeast and blue-green mold, are also called "higher fungi(Dikarya)" because they have a more complex structure and ecology than the phyla mentioned above. These higher fungi comprise the majority of fungi and are known to be highly diverse in terms of habitat and morphology. In general, fungi are heterotrophs and, together with prokaryotic bacteria, are known to play the role of "decomposers" in the ecosystem.

On the other hand, among the higher fungi, there is a group of organisms called lichens, which have acquired a unique mode of nutritional acquisition. Lichens are obligate symbioses between fungi (mycobiont) and photosynthetic microalgae, including green algae and cyanobacteria (photobiont). Lichenization, in which fungi establish a symbiotic relationship with algae, is one of the most important fungal lifestyles. There are more than 19,000 species of lichenized fungi, accounting for

approximately 20% of all fungi and 30% of all basidiomycetes (Feuerer and Hawksworth, 2007; Lücking et al., 2016). Approximately 85% of lichens contain green algal photobionts (chlorolichens), 10% contain cyanobacterial photobionts (cyanolichens), and approximately 4% contain both simultaneously (tripartite lichens) (Honegger et al., 2008). Lichens are found in a wide variety of terrestrial habitats and play important roles in terrestrial ecosystems (Elbert et al., 2012; Asplund and Wardle, 2017; Harris et al., 2018). Lichens are one of the most abundant life forms. According to Larson (1987) lichens dominate the vegetation on 8% of the Lichens are one of the most abundant life forms.
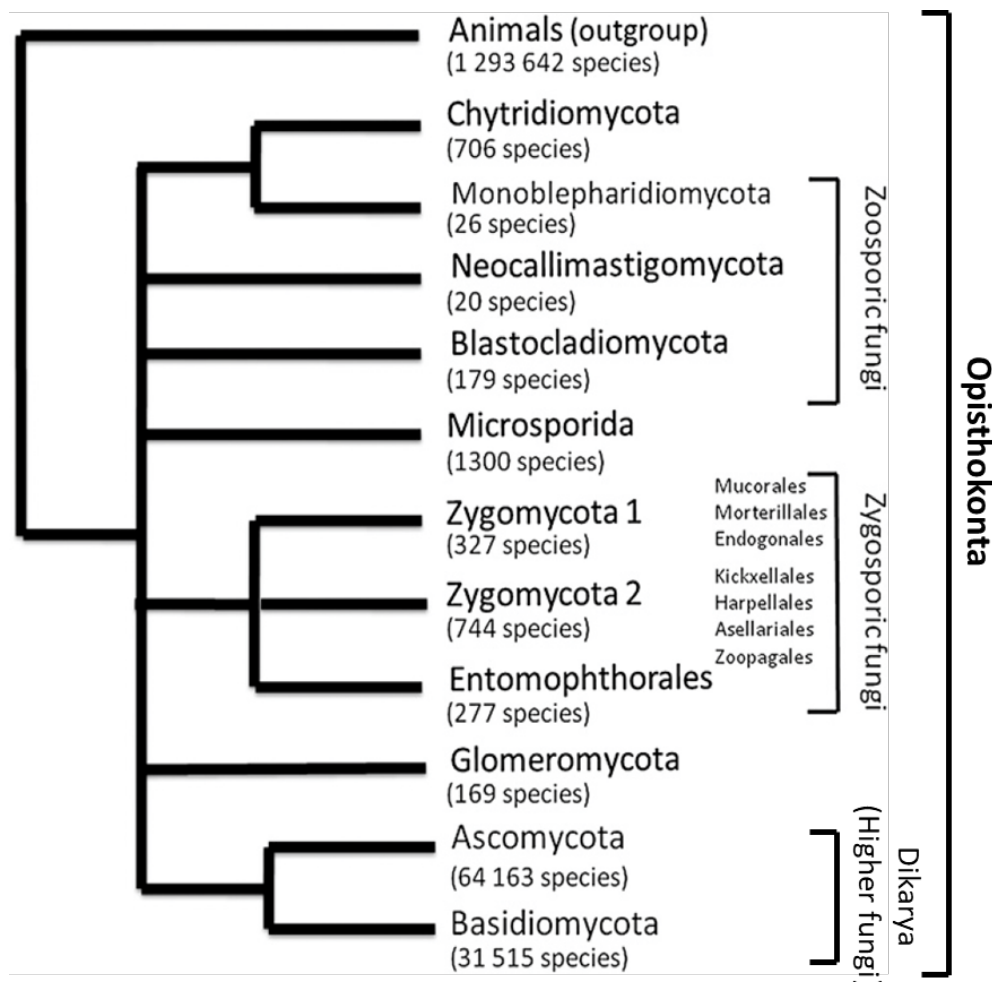
Fig.1.1 Fungal phyla and approximate number of species in each group.
(modified from Blackwell, 2011)

1.2. Earth History of Fungi and Lichens

Fungi and lichens are considered to have appeared very early in the earth's history because of their high diversity, a wide range of habitats, and symbiotic relationships with many plants and animals. Molecular phylogenetic analysis indicates that animals and fungi diverged around 760 - 1060 Ma, and lichens appeared between 200 - 300 Ma (Lücking et al., 2009; Prieto and Wedin, 2013; Beimforde et al., 2014). However, unlike other organisms that multiple fossil records have calibrated, the fossil records for fungi and lichens are very scarce, and their appearance dates are subject to change significantly.

Although many researchers have believed that fungi may have been involved in the emergence of terrestrial plants, there was no direct evidence strongly supporting this hypothesis until Redecker et al. (2000) reported fossils of Glomalean fungi from the Ordovician. Especially in older samples, the debate often centers on whether the observed fossils are fungi. Recently, with the introduction of techniques such as electron microscopy and FTIR microspectroscopy, Loron et al. (2019) reported the oldest fossil fungi, *Orasphaira giraldae*, from a stratum of about 1000 Ma in the Canadian polar region (Fig. 1.2).

Life history studies of fungi are often mentioned based on their current role in terrestrial ecosystems and mathematical simulations. Arbuscular mycorrhizal (AM) fungi are known to be endophytic parasites of many plants. Taylor et al. (2009, 2011) proposed that in addition to AM fungi, ectomycorrhizal (EM) fungi, which increased rapidly coincident with the rise in angiosperms in the earliest Cretaceous, promoted weathering and contributed significantly to the reduction of atmospheric CO_2 since the middle Cretaceous (Fig. 1.3). The involvement of fungi in the carbon cycle has recently been discussed, and Pieńkowski et al. (2016) pointed out the possibility that the accelerated decomposition of organic carbon by terrestrial fungi during the Jurassic marine anoxic event accelerated warming during the Jurassic based on the results of palynomorph (organic microfossil) analysis. Similarly, palynomorph analyses suggest that fungi temporarily increased on land after the mass extinction during the P-T and K-Pg boundary periods and decomposed biological remains (e.g., Vajda and McLoughlin, 2004; Rampino and Eshet, 2018) (Fig. 1.4).

The fossil record of lichens is much smaller than the reported cases of fungal fossils, even including fossils suggested to be lichens. Researchers have mentioned that three conditions are required to be recognized as lichen fossils: (1) the presence of both fungi and photobionts, (2) evidence of physiological interactions (interdependence) between the two organisms, and (3) a body plan that is

different from either symbiont(Stein et al., 1993; Taylor et al., 1997; Taylor and Krings, 2005). Although reports of fossil lichens are scattered over a wide range of periods (Fig. 1.5), it is clear that the conditions are highly dependent on the state of preservation to be considered lichen. The oldest lichen fossils reported to date are *Chlorolichenomycites salopensis* and *Cyanolichenomycites devonicus* reported by Honegger et al. (2013a,b) at ca. 415 Ma (Early Devonian). The time lag between the fossil record and the molecular phylogenetic analysis may be due not only to the time calibration method but also to the fact that different fungal species from the present lichens constituted the early lichens. The lichen *Winfrenatia reticulata*, described by Taylor et al. (1997) from the Early Devonian, was subsequently reported to be composed of fungi related to Glomeromycota and two types of cyanobacteria, unlike Ascomycota and Basidiomycota that make up the lichens of today (Taylor et al., 2004; Karatygin et al., 2009).

Some reports have proposed that lichen-like organisms existed in the Precambrian (Hallbauer et al., 1977; Retallack 1994, 1995, 2007, 2012), while others have proposed the "Protolichen hypothesis" that early lichens, so-called Protolichens, appeared before 450 Ma, giving rise to a non-lichen lineage (Eriksson, 2005). Recently, the Protolichen hypothesis has received attention due to the discovery of lichen fossils *Chlorolichenomycites salopensis* and *Cyanolichenomycites devonicus*. On the other hand, Nelsen et al. (2019) reported that the appearance of lichen-forming fungi probably occurred at least after the appearance of Tracheophytes (425 Ma), based on the results of a molecular phylogenetic analysis that took into account new findings, and the timing of lichen appearance is still under debate. In addition to discussions of the timing of lichen emergence, many studies of lichens in the earth's history have been reported using molecular phylogenetic techniques in recent years. Gaya et al. (2015) reported that the pigment phenotype of the lichen family Teloschistaceae changed during the Middle Cretaceous and acquired UV tolerance, resulting in increased expansion and diversity on bare ground (Fig. 1.6).

Huang et al. (2019) also reported that molecular phylogenetic analyses suggest that lichen diversification may have accelerated from the Middle Cretaceous to the Paleogene, and that major environmental changes such as the Cretaceous Terrestrial Revolution, which is an event that led to rapid diversification of angiosperms, (KTR; from 125 to 80 Ma), the K-Pg event, and PETM, may have been a factor. On the other hand, the authors also mention the methods' limitations, noting that discrepancies in the time of spread between studies may be due to differences in strategies of phylogenetic taxon sampling and geological time among researchers and the need for further experimentation.
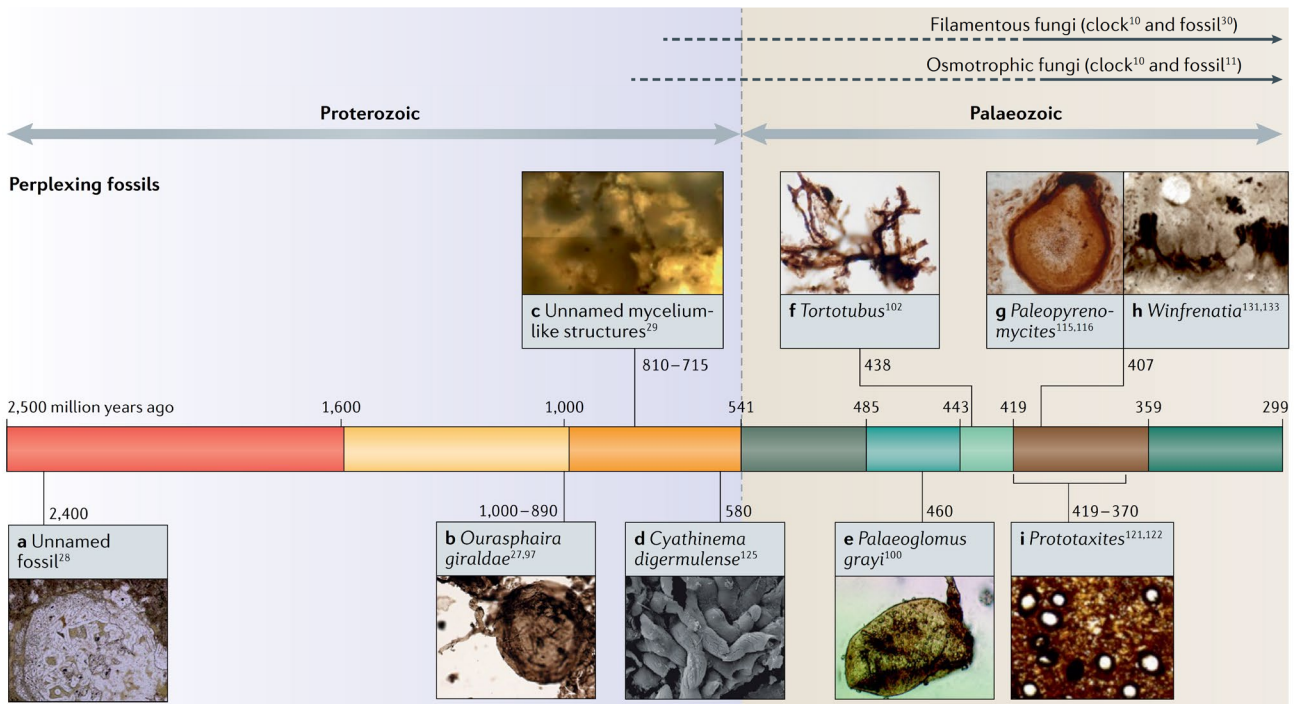
Fig.1.2 Geological ages of fungi. Estimates from molecular clocks (dashed lines) and fossil record (solid lines). Perplexing fungal fossils are shown below the geological timeline. Some fossil records are not reflected in the upper age columns because of controversy over whether they are fungi or not and the possibility of contaminants. (from Berbee et al., 2020)
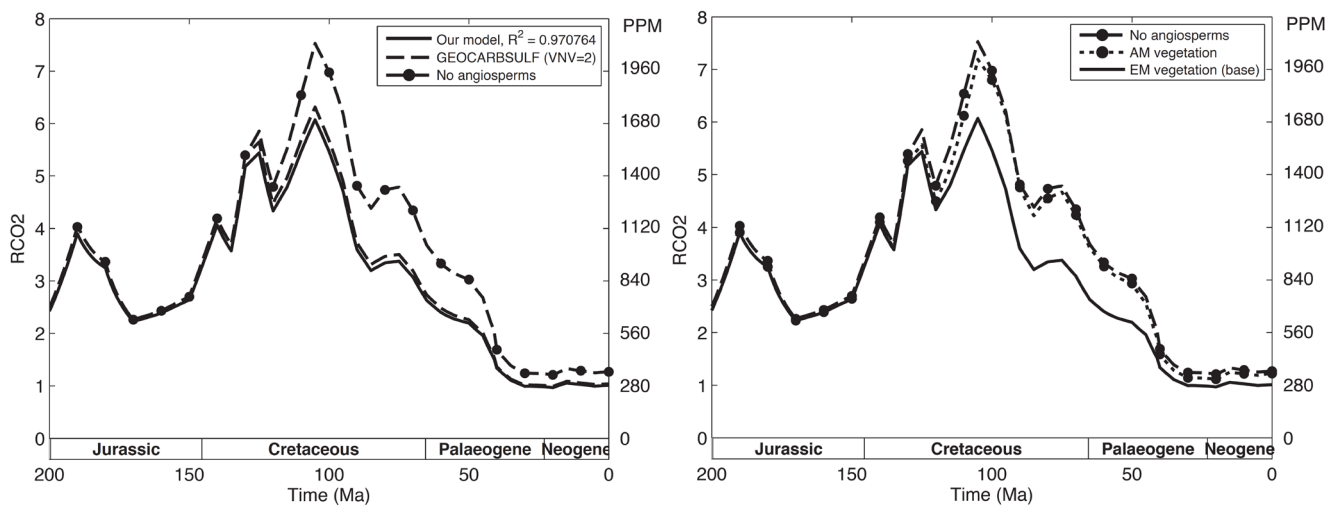
Fig.1.3 Effects of changes in terrestrial vegetation on atmospheric CO_2 concentrations over the past 200 million years. RCO_2 is the atmospheric CO_2 concentration relative to modern values. "No angiosperm" represents the case for considering only gymnosperm; "EM vegetation" represents the case for considering AM and EM assisted weathering; "AM vegetation" represents the case only AM assisted weathering. The RCO_2 variability reconstructed by "EM vegetation" in the right panel matches the RCO_2 variability of GEOCARBSULF in the left panel. (modified from Taylor et al., 2011)
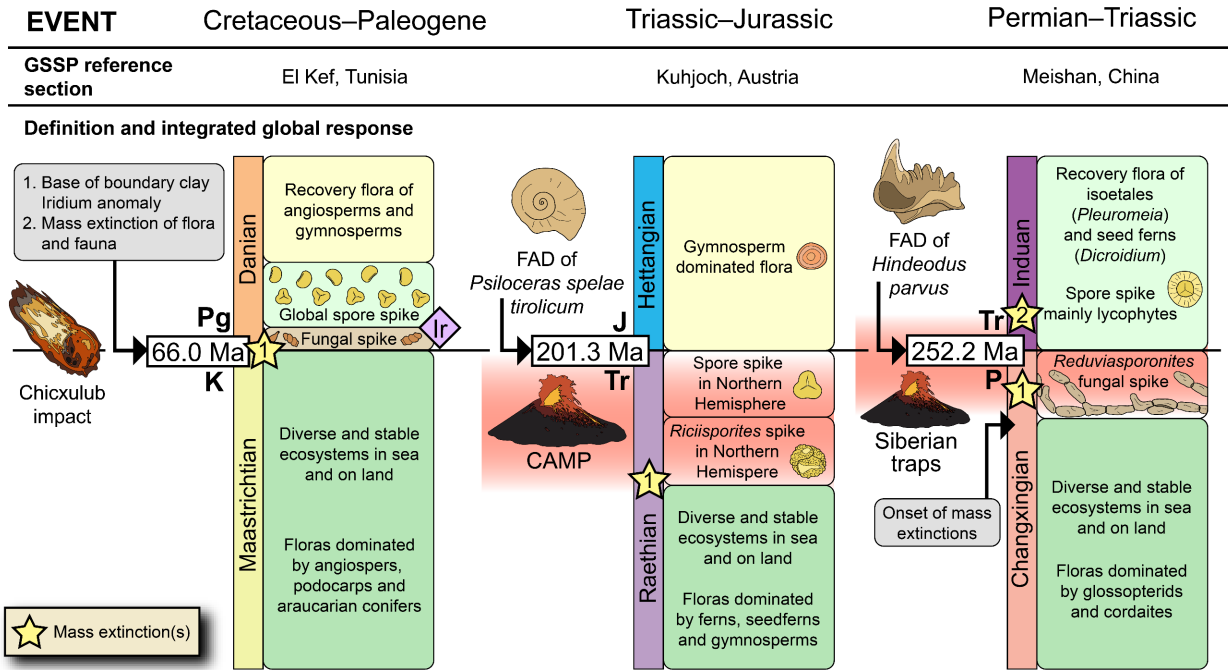
Fig.1.4 Schematic illustration of the mass extinction period, with Fungal spike reported at the P-T and K-Pg boundary. (from Vajda and Bercovici, 2014)
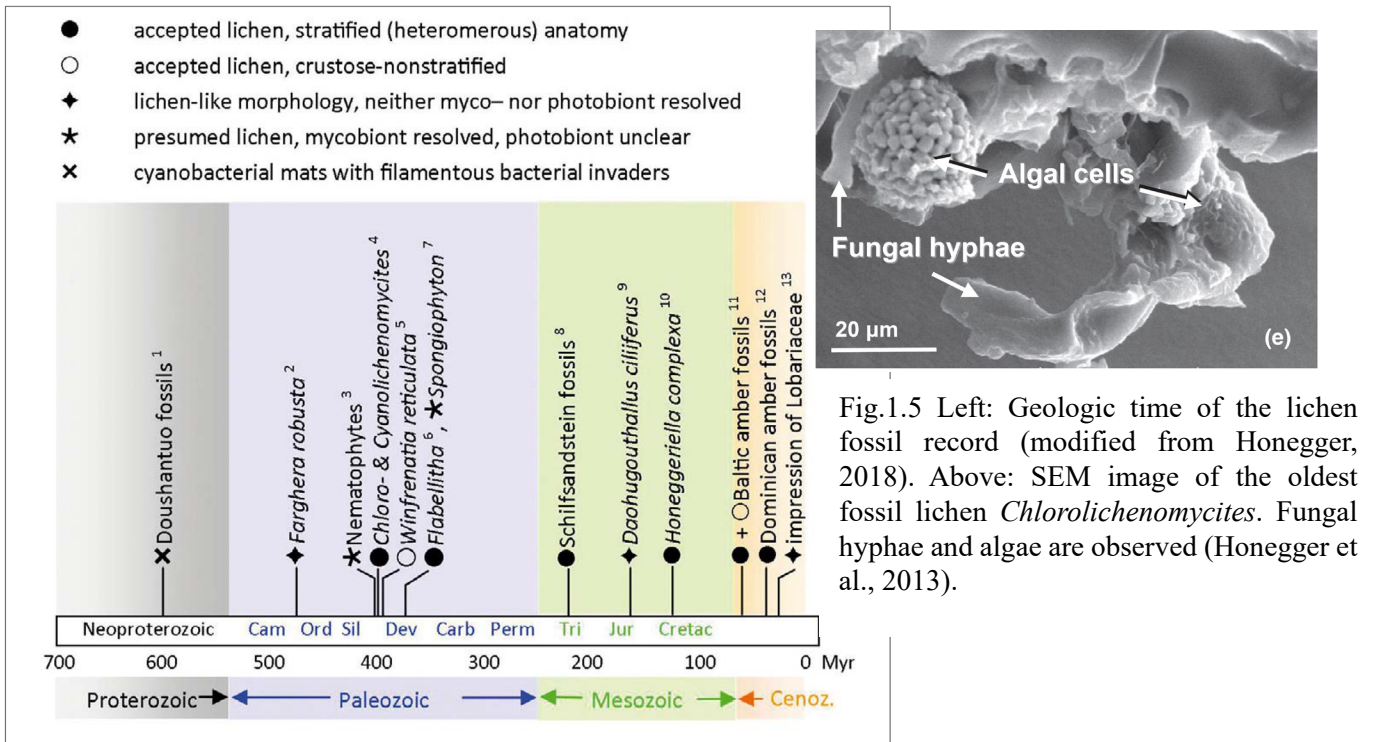
Fig.1.5 Left: Geologic time of the lichen fossil record (modified from Honegger, 2018). Above: SEM image of the oldest fossil lichen *Chlorolichenomycites*. Fungal hyphae and algae are observed (Honegger et al., 2013).

6
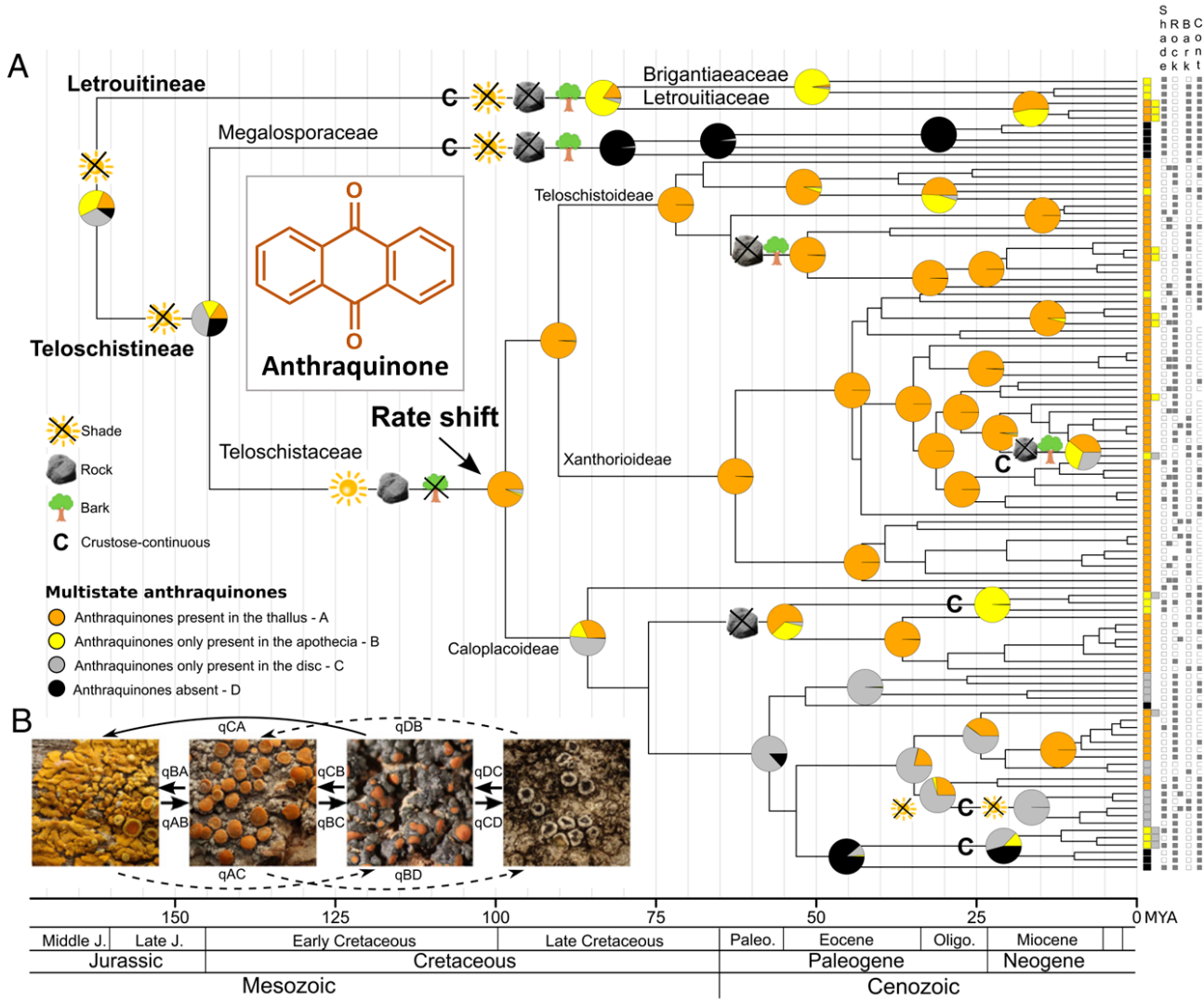
Fig.1.6 Time-calibrated phylogeny of the order Teloschistales of anthraquinone evolution. The colored squares on the right side of the tree represent phenotypes, the same classification as the colors indicated in the tree pie chart. The square next to it also indicates the presence or absence of the trait with black and white.

From left, a sun for light exposure (shade column), a rock for rock substrate (rock column), a tree for epiphtism (bark column), and a letter C for growth form crustose-continuous (cont column). (modified from Gaya et al., 2015)

1.3. Organic Geochemical Studies on Fungi and Lichens

Organic geochemical approaches to studying the paleoecology of fungi include palynomorph analysis, as described above. However, except for studies in terrestrial sediments such as peat deposits, palynomorph analyses from marine sediments rarely preserve species-specific structures and makeup such a small proportion of the total palynomorphs that most discussions are limited to the extent that they indicate terrestrial input (e.g., Nakagawa et al., 2022). On the other hand, biomarker (molecular fossil) studies have reported the behavior of terrestrial fungi using perylene, which is believed to be derived from wood-rotting fungi and mycorrhizal fungi (Grice et al., 2009; Suzuki et al., 2010; Itoh et al., 2012; Marynowski et al., 2013, 2015; Hanke et al., 2019). Marynowski et al. (2013) proposed the conifer wood degradation index (CWDI) as an indicator of the degree of decay of wood fossils using perylene. Itoh et al. (2012) analyzed sediments and sclerotium samples from Lake Biwa. They found 4,9-dihydroxyperylene-3,10-quinone(DHPQ) produced by *Cenococcum geophilum*, a rhizobium parasitic on plants, as one of the origins of perylene. Suzuki et al. (2010) reported that carbon isotope ratios and variations of perylene in sedimentary rocks from the Late Cretaceous to the Paleogene off the coast of Sanriku indicate that perylene is derived from fungi and increases in wet environments.

Many diverse and specific compounds have been reported from the extant lichens. On the other hand, organic geochemical studies of lichens have been mainly limited to studies using recent past peat samples (Ficken et al., 1998; Jia et al., 2008; Schellekens et al., 2015).

Ficken et al. (1998) used *n*-alkane, *n*-alkanol, and *n*-alkanoic acid composition ratios of peat-constituting plants, and Jia et al. (2008) used monosaccharide composition ratios to propose vegetation change indices, including lichens in peat-deposits. However, studies using these ratios use compounds common to many other organisms, so variation in their compositional ratios in sediments is also affected by multiple factors, complicating interpretation. Huang et al. (2012) suggested that C_{23} *n*-alkane and long-chain 3-methylalkanes (*anteiso*-alkanes) could be used as indicators of the paleoenvironmental reconstruction as unique features of lichens based on analysis of extant lichen samples. However, attempts at chemotaxonomy based on *n*-alkane compositions of lichens have been unsuccessful (Zygadlo et al., 1993), and *n*-alkane compositions have been found to vary significantly with the environment, even if among the same species (Piervittori et al., 1996). In addition, it is considered that long-chain 3-methylalkane may be produced under limited conditions, as it may not be detected in some sampling locations, even among the same species in this paper. Schellekens et al. (2015) proposed that 3-methoxy-5-methylphenol could be used as a lichen biomarker based on the

results of pyrolysis product analysis of plants and peat samples. 3-methoxy-5-methylphenol has been reported to be detected in some lichen extracts (ter Heide et al., 1975). Since it was detected in five of the six peat samples they examined, it may be possible to reconstruct lichen vegetation variation in peatlands.

On the other hand, organic geological studies for paleoecological reconstructions of lichens in geologic time using sedimentary rocks are extremely limited. Radke et al. (2000) analyzed alkyldibenzofurans in sedimentary rocks of the Upper Carboniferous from the Sakoa coal basin, Madagascar. They proposed 1-methyl dibenzofuran (1-MDBF) as a potential lichen biomarker because it behaved differently from other isomers. Many researchers agree that aromatic furans, including dibenzofurans in sedimentary rocks, are of terrestrial origin. Among the reports on detecting DBF in sedimentary rocks, the presence of abnormal concentrations of aromatic furans, including dibenzofurans, during the P-T boundary deserve special mention. This case was reported by several sites and is believed to have been a global event. However, the interpretation of this event is under debate. Some studies have supposed the origin of DBFs as thermal maturation products of lignins and polysaccharides from higher plants, which are interpreted as soil erosion events associated with terrestrial disturbance (Sephton et al., 2005; Fenton et al., 2007; Wang and Visscher, 2007; Biswas et al., 2020), while others have supposed the origin of aromatic furans, including DBF, as a lichen origin and interpreted it as an expansion of lichen vegetation event during the terrestrial collapse (Watson et al., 2005; Sawada et al., 2012). Palynomorph analysis has identified a stratigraphic level (Fungal spike) dominated by fungi called *Reduviasporonites* during the P-T boundary (Eshet et al., 1995; Steiner et al., 2003; Visscher et al., 2011; Rampino and Eshet, 2018). Sephton et al. (2009) reported that the detection of DBFs in pyrolysis products of *Reduviasporonites*, so aromatic furans in the P-T boundary might be attributable to fungi *Reduviasporonites*. Whether or not these fungi formed lichens is unknown, but in any case, this is likely a case of fungi (or lichens) responding to a robust environmental disturbance event.
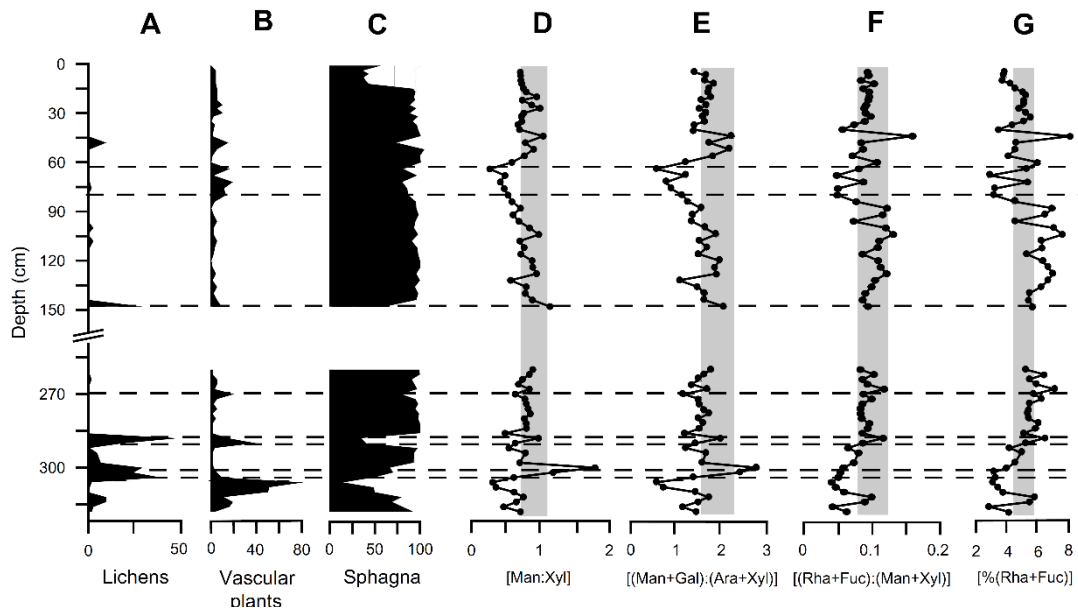
Fig.1.7 Comparison of monosaccharide parameters with macrofossil records. (A) % lichen, (B) % vascular plants, (C) % Sphagna, (D) [Man:Xyl]; (E) [(Man+Gal):(Ara+Xyl)], (F) [(Rha + Fuc):(Man + Xyl)], (G) [%(Rha + Fuc)]. In this study, the proxy [(Man + Gal):(Ara + Xyl)] and [Man:Xyl] indicate the vegetation in the order of decreasing values: lichens > Sphagna > vascular plants. [(Rha + Fuc):(Man + Xyl)] and [%(Rha+Fuc)] are used as proxy for Sphagna. Shaded grey areas denote proxy values for modern Sphagna.
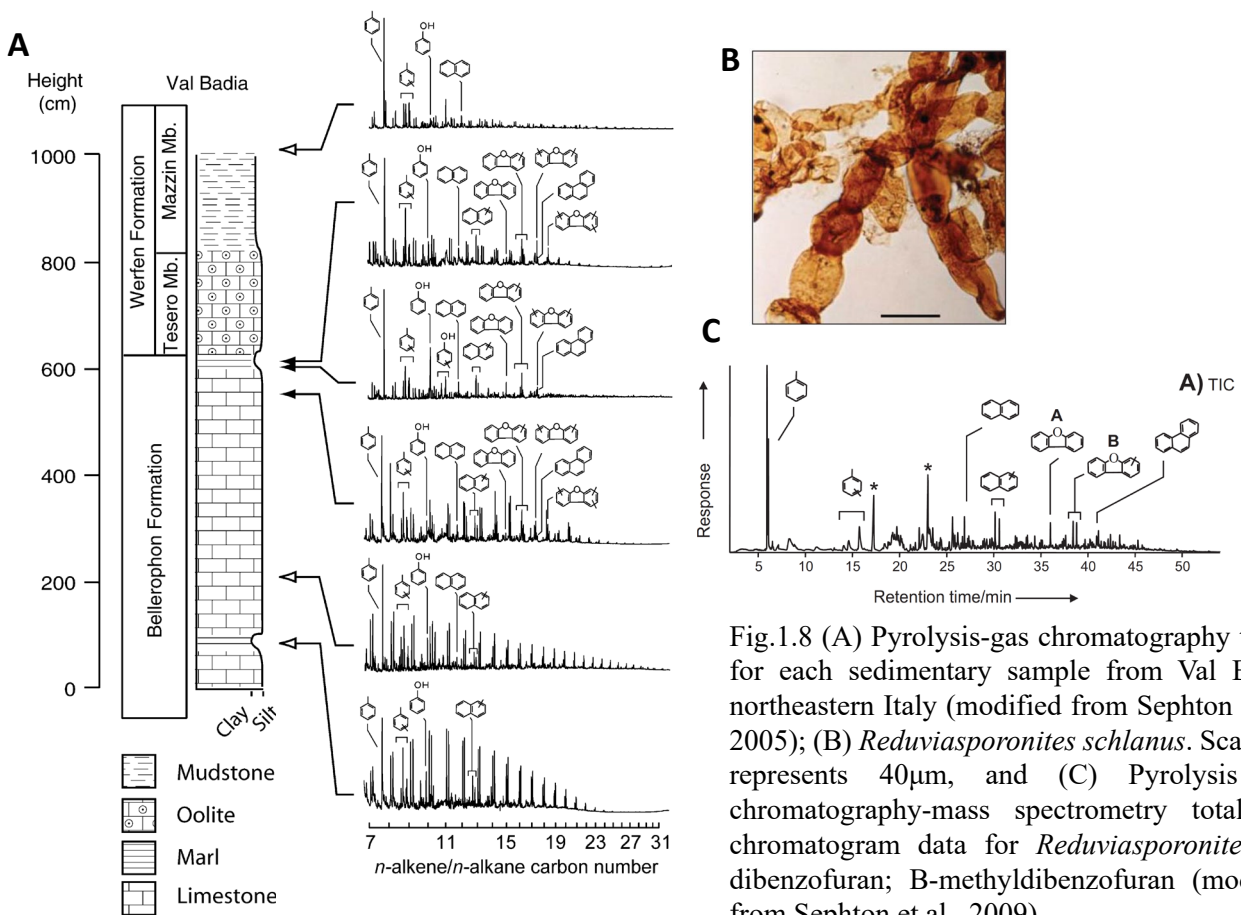
Fig.1.8 (A) Pyrolysis-gas chromatography traces for each sedimentary sample from Val Badia, northeastern Italy (modified from Sephton et al., 2005); (B) *Reduviasporonites schlanus*. Scale bar represents 40μm, and (C) Pyrolysis gas chromatography-mass spectrometry total Ion chromatogram data for *Reduviasporonites*: A-dibenzofuran; B-methyldibenzofuran (modified from Sephton et al., 2009).

1.4. Summary of Chapter and Objectives of This Study

Previous studies on the Earth's history of fungi and lichens have been based mainly on molecular clocks and fossils. However, as noted above, the estimation of the timing of evolution and diversification by molecular clocks is still subject to inconsistencies among studies due to differences in methods. Moreover, the reporting of new fossil evidence forces calibration of timing. In addition, especially in lichen fossils, taphonomy studies of extant lichens indicate that critical features of lichen thalli have been destroyed, suggesting that breakthrough fossils are unlikely to be obtained (Tomescu et al., 2010; Honegger et al., 2013; Graham et al., 2017; Lücking and Nelsen, 2018).

The survival strategy of lichenization, in which fungi associate with algae, is important in the evolutionary history of fungi, and it has long been pointed out that lichens may have had a significant impact on paleo-terrestrial ecosystems. However, many parts are still shrouded in mystery. Therefore, this study aimed to examine molecular fossils, develop indices using organic geochemical methods, and approach the reading of the evolutionary history of lichens and fungi from a new perspective.

CHAPTER 2
Searching for lichen biomarkers using lipid analysis of extant lichen samples

2.1. Introduction

Lichens are obligate symbioses between fungi (mycobiont) and photosynthetic microalgae, including green algae and cyanobacteria (photobiont). Lichenization, in which fungi establish a symbiotic relationship with algae, is one of the most important fungal lifestyles. There are more than 19,000 species of lichenized fungi, accounting for one out of every five recognized fungal species (Feuerer and Hawksworth, 2007; Lucking et al., 2016). Approximately 85% of lichens contain green algal photobionts (chlorolichens), 10% contain cyanobacterial photobionts (cyanolichens), and approximately 4% contain both simultaneously (tripartite lichens) (Honegger et al., 2008). Lichens are found in a wide variety of terrestrial habitats and play important roles in terrestrial ecosystems (Elbert et al., 2012; Asplund and Wardle, 2017; Harris et al., 2018). The earliest known lichen fossils date back to the Early Devonian period (415 Ma) (Honegger et al., 2013a, b), but the exact date of the first appearance of lichen is uncertain (e.g., Nelsen et al., 2020). Reports of lichen fossils are extremely rare because these remains are easily decomposed; consequently, most studies of their evolutionary history and response to the paleoenvironment have relied on a molecular clock approach (Printzen et al., 2000; Gaya et al., 2015; Kraichak et al., 2015; Huang et al., 2019; Nelsen et al., 2020).

Several studies have attempted to reconstruct the paleoclimatic responses of lichens by employing biomarkers. Various components of lichen lipids have been reported, including *n*-alkanes, alkanols, alkanoic acid, neutral monosaccharides, lichen secondary metabolites, carotenoids, steroids, and terpenoids (Huneck and Yoshimura, 1996), and certain compounds such as lichen secondary metabolites, *n*-alkanes, and alkanoic acid have been considered for use in the chemical classification of lichens (e.g., Zygadlo et al., 1993; Sassaki et al., 2001; Santos et al., 2015). Several studies have reported that lichens contain abundant *n*-alkenes (Corbier and Teisseire, 1974; Gavin et al., 1978; Solberg, 1986, 1987; Ikeda et al., 2018, 2021), but little has been reported regarding their composition. Through the analytical measurement of *n*-alkanes, *n*-alkanols, and *n*-alkanoic acids in Scottish peat samples and peat-forming plants, Ficken et al. (1998) demonstrated that the lichen contribution to past biomass may have been greater than that

estimated by the fossil record. The authors concluded that the lichen contributions estimated by these lipid analyses were higher than previous quantitative estimations. Jia et al. (2008) used the composition of neutral monosaccharides in peat cores to reconstruct the variations in vegetation of the major peat-forming plants, including lichens. However, neutral monosaccharides are susceptible to microbial degradation (e.g., Amon et al., 2001), and there are many selective compositional changes of each monosaccharide, as indicated by the different degradation orders reported in previous studies (Hedges et al., 1985; Opsahl and Benner, 1999; Panagiotopoulos and Sempéré, 2007).

In this study, we comprehensively analyzed aliphatic compounds, especially *n*-alkenes, in samples of lichen belonging to Lecanoromycetes and examined their potential for use as biomarkers and as a chemotaxonomic tool.

2.2. Samples and methods

2.2.1. Samples

The 29 samples analyzed contained 27 species of lichens from the class Lecanoromycetes (orders Lecanorales, 16 species; Teloschistales, one species; Caliciales, four species; Peltigerales, six species) (Table 2.1). These specimens were collected from several locations in Japan. Lichen species were identified based on morphological and biochemical techniques. Chemical spot tests with paraphenylenediamine, potassium hydroxide, and calcium hypochlorite were used to determine the biochemical characteristics. A microcrystallization technique (Asahina and Shibata, 1954; Huneck and Yoshimura, 1996) was also used to identify some specimens. These characteristics were compared to the descriptions of the species provided by Yoshimura (1994) and Yamamoto (2017). The nomenclature used followed the AlgaeBase (Guiry and Guiry, 2022) for symbiotic algae, and the MycoBank (http://www.mycobank.org/) for the lichenized fungi. Following collection, the samples were stored at −30°C in our laboratory. At the time of analysis, any non-lichen debris impurities were removed with tweezers, and the samples were washed with distilled water and lyophilized.

2.2.2. Extraction and fractionation

Lipid extraction and separation were performed according to Sawada et al. (2013) and Nakamura et al. (2015). To extract the free compounds, crushed samples were steeped with methanol and a mixture of methanol/dichloromethane (1:1, v/v) overnight. Tetracosane-d_{50} was

added to the crude extract as an internal standard. After adding distilled water, the combined extracts were shaken and centrifuged to separate the neutral lipids into the organic solvent layer, while water-soluble compounds were separated into the aqueous layer. The organic solvent layer was siphoned off and passed through an anhydrous Na_2SO_4 column. The eluate neutral lipids were dried in a rotary evaporator, re-dissolved in *n*-hexane, and then passed through a 95% activated silica gel column: hexane for alkane fraction, hexane and toluene (3:1, v:v) for aromatic fraction, hexane and ethyl acetate (EtOAc) (9:1, v:v) and MeOH and EtOAc (1:1, v:v) for polar fraction. The polar fractions were silylated by adding BSTFA [N,O – bis(trimethylsilyl)trifluoroacetamine] and heating at 70ºC for 30 min. After this treatment, a gas chromatography–mass spectrometry (GC-MS) analysis was conducted.

2.2.3. Formation of DMDS adducts

As described by Carlson et al. (1989), the hydrocarbon fraction was dissolved in hexane (200 μL) and incubated at 40 °C for 4 h with 200 μL DMDS and 100 μL iodine solution (60 mg in 1 mL diethyl ether). After adding $Na_2S_2O_3$ to stop the reaction, the DMDS adducts were extracted three times with hexane.

2.2.4. Lipid assignment and quantification

Lipids were identified by GC-MS using an Agilent 7890B GC instrument equipped with a 30 m × 0.25 mm i.d. DB-5HT fused silica column (Agilent, Santa Clara, CA, USA) directly coupled to an Agilent 5977A MSD quadruple mass spectrometer (electron voltage, 70 eV; scan range, *m/z* 50–650 in 1.3 s). The oven temperature was programmed as follows: 50°C (held for 4 min) to 310 C at 4°C/min (held for 20 min). The injection temperature was 310°C and the instrument was run in splitless mode with helium as the carrier gas. Alkanes and alkenes were quantified using a GC-2025 GC-flame ionization detector (Shimadzu, Kyoto, Japan) equipped with the same DB-5HT column as that used for the GC-MS analysis. The injection temperature, temperature program, and carrier gas used were identical to those used in the GC-MS analysis. The precision of the measurements was calculated for some samples based on triplicate or quadruplicate analyses of the same lichen samples.

2.2.5. Statistical analysis

The statistical analysis and data visualization were performed in R version 4.2.0 (R Core Team,

2022). The optimal number of clusters was determined with the fpc package (Hennig, 2020), and a clustered heatmap was created using the pheatmap package (Kolde, 2019).

2.3. Results and discussion

2.3.1. Mass spectral characteristics of dimethyl disulfide (DMDS) derivatives of C_{17}–C_{20} alkenes

Various C_{16}–C_{29} mono-, di-, and tri-unsaturated alkenes were detected in apolar fractions (Fig. 2.1). C_{17} alkadienes were particularly abundant in the Lecanorales, Teloschistales, and Peltigerales lichen samples. The positions of the double bonds in the alkenes and alkadienes (**1–10**) were determined by analyzing DMDS adducts via gas chromatography–mass spectrometry (GC-MS) (Carlson et al., 1989; Rieley et al., 1998; Nakamura et al., 2015). Determining the double bond positions of unsaturated hydrocarbons by MS is challenging due to double bond migration during ionization (Wolff et al., 1966). To facilitate double bond detection, we applied a DMDS adduction method to attach methyl sulfides to the double bonds; this way, cleavage occurred between the two methyl sulfide groups during ionization, enabling deduction of the double bond positions (Fig. 2.2). The mass spectra of the DMDS adducts of the most abundant C_{17} alkadiene in *Xanthoria mandschurica* (Zahlbr.) Asahina indicated that methyl sulfides were attached to two double bonds in the alkadiene following DMDS adduction, and that one of the two double bonds was at position C-8 (ions at *m/z* 173 [C^+], 251 [AB^+], 203 [$(AB-48)^+$], 157 [$(AB-94)^+$], and 155 [$(AB-96)^+$]) (Table 2.2, Fig. 2.2 and 2.3). The other double bond was assumed to be at position C-1 (ions at *m/z* 61 [A^+], 363 [BC^+], 315 [$(BC-48)^+$; i.e., $BC-CH_3SH$], 269 [$(BC-94)^+$; i.e., $BC-DMDS$], and 267 [$(BC-96)^+$; i.e., $BC-2CH_3SH$]) (Table 2.2, Fig. 2.2 and 2.3). Although the ion at *m/z* 61 is universally found in mass fragments of DMDS adducts (Francis and Veland, 1981), the absence of prominent mass fragments originating from cleavage at potential positions other than C-1 suggests that the major C_{17} alkadiene in *X. mandschurica* was a 1,8-heptadecadiene (**1**). Although we could not determine the geometric structure of the double bonds of this compound in this study, an (8*Z*)-1,8-heptadecadiene was identified in lichens in previous studies (Corbier and Tesseire, 1974; Gavin et al., 1978). Thus, we expected the double bonds of this compound to be in the *cis* configuration. The mass spectra of DMDS adducts of the most abundant C_{17} alkadiene in *Cladonia scabriuscula* (Delise) Nyl. were obtained from derivatives containing methyl sulfide groups attached to one of the two double bonds. Tetrakis-type adducts, including the DMDS adduct of 1,8-heptadecadiene (**1**), can only form when there are at least four methylene groups between each double bond; therefore, methyl sulfides can only

attach to one of two adjacent double bonds (three methylene groups or fewer between each double bond) (Carlson et al., 1989; Yamamoto et al., 1991; Shibamoto et al., 2016). Shibamoto et al. (2016) found that methyl sulfides only attach to one of two adjacent double bonds in unsaturated fatty acid methyl esters during DMDS adduction due to steric inhibition. In this study, the molecular ion at *m/z* 330 and the high intensity of the ions at *m/z* 282 [(M − 48)$^+$; i.e., M - CH$_3$SH] and *m/z* 235 [(M − 95)$^+$; i.e., M - CH$_3$SH − CH$_3$S•] suggest that the methyl sulfides attached to one double bond; the presence of stable conjugated ions further indicate the presence of an unreacted double bond. The double bonds in the *Cl. scabriuscula* alkadiene were located at positions C-6 (ions at *m/z* 131 [A$^+$] and 199 [C$^+$]) and C-9 (ions at *m/z* 171 [A$^+$] and 159 [C$^+$]) (Table 2.2, Fig. 2.2 and 2.3), and thus were identified as 6,9-heptadecadiene (**2**). C$_{17}$ alkenes (monoenes; **3**–**6**) were another major group of compounds detected, and the positions of the monoene double bonds were again determined by DMDS adduction. The most abundant C$_{17}$ monoenes in *Cl. scabriuscula* (**3**,**4**) initially appeared to be a single compound, but subsequently generated two peaks after DMDS adduction, suggesting the co-elution of two compounds . The positions of the double bonds in the C$_{17}$ monoenes (**3**, **4**) were C-7 (ions at *m/z* 159 [A$^+$] and 173 [C$^+$]) and C-8 (ions at *m/z* 145 [A$^+$] and 187 [C$^+$]) (Table 2.2, Fig. 2.2 and 2.3). The double bond positions of two C$_{17}$ monoenes in *X. mandschurica* (**5**, **6**) were determined to be C-1 (ions at *m/z* 61 [A$^+$] and 271 [C$^+$]) and C-3 (ions at *m/z* 89 [A$^+$] and 243 [C$^+$]) (Table 2.2, Fig. 2.2 and 2.3), respectively. In several Peltigerales lichen samples, C$_{18}$–C$_{20}$ mono-unsaturated alkenes were found to be major compounds (**7**–**9**). The C$_{18}$ monoene that was detected in *Collema furfuraceum* Du Rietz (**7**) was identified as a 1-octadecene, as the mass spectrum of its DMDS adducts revealed a double bond at position C-1 (ions at *m/z* 61 [A$^+$] and 285 [C$^+$]) (Table 2.2, Fig. 2.2 and 2.3). The position of the double bond in the C$_{18}$ monoene found in *Peltigera degenii* Gyeln. was C-4 (ions at *m/z* 103 [A$^+$] and 243 [C$^+$]) and was identified as 4-octadecene (**8**). Furthermore, the double bond in the most abundant *P. degenii* C$_{19}$ monoene was found at position C-5 (ions at *m/z* 117 [A$^+$] and 243 [C$^+$]) (Table 2.2, Fig. 2.2 and 2.3), producing 5-nonadecene (**9**). The double bond position of the most abundant C$_{20}$ monoene detected in *P. degenii* is C-6 (ions at *m/z* 131 [A+] and 243 [C+]) (Table 2.2, Fig. 2.2 and 2.3) and was identified as 6-eicosene (**10**).

2.3.2. Composition and concentration of aliphatic compounds

2.3.2.1. *n*-Alkanes

n-Alkanes with carbon numbers ranging between C_{13} and C_{42} were detected in all lichen samples (Fig. 3, Table 2, Table S1). All samples had an odd carbon number dominance of the long-chain *n*-alkanes ($> C_{24}$), but the carbon number of the most prominent *n*-alkane varied (Fig. 2.4, Table 2.3). In some samples, medium long-chain *n*-alkanes (C_{21}–C_{23}) were predominant, whereas a bimodal distribution with long-chain *n*-alkanes was observed in others. Among the short-chain *n*-alkanes, there were also samples with a prominent *n*-C_{17} peak, which exhibited bimodal/trimodal distributions along with the long-chain and medium long-chain *n*-alkanes. The *n*-C_{17} alkane was frequently detected in the cyanobacteria symbiotic genera *Lobaria*, *Peltigera*, and *Collema*, which may be attributed to the symbiotic alga *Nostoc* sp. Many cyanobacteria produce the *n*-C_{17} alkane (Gelpi et al., 1970; Ladygina et al., 2006; Coates et al., 2014), and the genus *Nostoc* is a prominent producer of the *n*-C_{17} alkane (e.g., Liu et al., 2013; Coates et al., 2014). Based on separate cultures of the photobiont and mycobiont of *Xanthoria parietina*, Torres et al. (2003) reported that the medium- to long-chain *n*-alkanes are primarily derived from fungi, with the *n*-C_{17} alkane content being insignificant. The composition of short-chain *n*-alkanes in lichens is primarily influenced by the differences in photobiont species. In our samples, the genera *Peltigera* and *Collema*, which contain cyanobacteria as their exclusive photosymbiont, were more *n*-C_{17} dominant than the genus *Lobaria*, which has green algae as its primary photosymbiont and secondary photobiont cyanobacteria restricted to small structures called cephalodia that occur sporadically within their tissues. These results suggest that these structures were introduced by the symbiotic algae *Nostoc* sp.

The differences in the distribution of long-chain *n*-alkanes may be influenced not only by mycobionts but also by environmental factors. According to Huang et al. (2012), the $\delta^{13}C$ values of *n*-alkanes in some lichen samples from Dajiuhu and Qizimei, China, indicated that the $> C_{23}$ *n*-alkane homologs were derived from mycobionts, with a small contribution from photobionts. They also demonstrated that lichen-derived *n*-alkanes exhibited two distinct patterns depending on their environment, either a predominance of *n*-C_{29} alkanes or a bimodal distribution of *n*-C_{23} and *n*-C_{29} alkanes. Similarly, Piervittori et al. (1996) reported that the *n*-alkane composition of lichens varied depending on the environmental variability. In our study, multiple distribution patterns were observed among samples collected at the same time and location, indicating that

differences in multiple parameters, such as interspecific chemotaxonomy and the microenvironment, may influence the *n*-alkane composition.

2.3.2.2. *n*-Alkenes

In our study, lichens were found to contain C_{16}–C_{29} alkenes (Fig. 2.1, Tables 2.3, Table S2). The structural identification of the major alkenes was previously addressed in Ikeda et al. (2021). In most samples, 1,8-heptadecadiene or 6,9-heptadecadiene and 8- and 7-heptadecene were the most prominent peaks in the aliphatic fraction (Fig. 2.1, Table 2.3). In contrast, 4-octadecene and 5-nonadecene were the most abundant alkenes in the genus *Peltigera*, while 1-octadecene and the $C_{19:2}$ alkene were the most abundant alkenes in the genus *Collema*. Although there are few reports of alkenes in lichens, 1,8-heptadecadiene has been widely detected in the Parmeliaceae species *Evernia prunastri* and *Cetraria islandica* (Corbier and Teisseire, 1974; Gavin et al., 1978; Solberg, 1986). Solberg (1987) additionally detected heptadecadiene and heptadecene in four Parmeliaceae lichens: *Cetraria delisei*, *Lobaria pulmonaria*, *Stereocaulon tomentosum*, and *Usnea hirta*. As discussed in Section 2.3.2.1, the *n*-alkane composition in lichen is susceptible to environmental influences. Similarly, a clear seasonal variation in the fatty acid composition of lichens has also been reported (e.g., Dembitsky et al., 1994a, b; Piervittori et al., 1995). In our study, the heptadecadiene and heptadecene compositions in *Xanthoria mandschurica* and *Lobaria orientalis* samples collected at two different sites were similar, although the concentrations of these compounds differed substantially between the two sites. These results indicate that the alkene composition of lichens may be more affected by taxonomic variations than environmental effects.

2.3.2.3. Branched alkanes

Long-chain (C_{20}–C_{31}) *anteiso*-(3-methyl)-alkanes were identified in several lichens (Fig. 2.1, Table 2.3). The *anteiso*-alkanes were most prevalent in the genus *Cladonia*, while *Stereocaulon japonicum*, *Ramalina yasudae*, *Pyxine endochrysina*, and *Collema complanatum* also contained *anteiso*-alkanes with various chain lengths. Long-chain *anteiso*-alkanes have previously been detected only in the lichens *Ramalina intermediella* and *Siphula ceratites* (Gaskell et al., 1973; Huang et al., 2012). We found a wider occurrence of the compounds among seven species of the genus *Cladonia*. Huang et al. (2012) reported that *R. intermediella* collected from Qizimei Mountain, China, contained C_{24}–C_{32} *anteiso*-alkanes and C_{27}, C_{29}, and C_{31} *iso*-alkanes. In addition,

they also detected long-chain branched alkanes in other lichens from Qizimei, but neither *anteiso*-alkanes nor *iso*-alkanes were detected in *R. intermediella* collected from the Dajiuhu wetland, China. The previous findings suggest that these branched alkanes may be produced under specific environmental conditions, but our findings suggest that the influence of species variations rather than regional (environmental) differences may be more strongly associated with *anteiso*-alkane production. Long-chain *anteiso*-alkanes and *iso*-(2-methyl) alkanes have been detected in lacustrine sediments (Fukushima, 1996, 2005), Antarctic rock (Matsumoto et al., 1992), coal and ancient sediments (Chaffee, 1986; Summons et al., 1988; Cheng et al., 2019), insect wax (Blomquist et al., 1976; Nelson et al., 1981; Bernier et al., 1998), higher plants (Maffei, 1994; Rogge et al., 1994; Kavouras et al, 1998; Reddy et al., 2000; Grice et al., 2008; Pautler et al., 2010; Huang et al., 2011; He et al., 2016), urban aerosol (Rogge et al., 1994; Kavouras et al., 1998; Bi et al., 2005), and modern and Holocene microorganism mats (Shiea et al., 1990; Kenig et al., 1995; He et al., 2015).

A symbiont of fungi and algae in lichen has recently been discovered to have symbiotic relationships with bacteria as a third symbiont (e.g., Cardinale et al., 2006). Bacteria are typical producers of *iso*- and *anteiso*-fatty acids (Kaneda, 1991), and it is possible that specific bacteria or bacterial symbioses synthesize these long-chain *anteiso*-alkanes in lichens. The origin of long-chain *anteiso*-alkanes is unclear, but some higher plants also produce them (e.g., Grice et al., 2008). Remarkably, Matsumoto et al. (1992) detected C_{20}–C_{30} *anteiso*-alkanes in lichen-dominated microbial communities, which were derived from unidentified heterotrophic bacteria or symbiotic processes in distinct microbial communities, growing on Antarctic rocks. Alphaproteobacteria comprise the majority of the internal bacterial communities in lichens (Cardinale et al., 2006, 2008; Bates et al., 2011; Pankratov, 2018). In our study, *Cladonia* lichens were the most prominent producers of the long-chain *anteiso*-alkanes, while some of the other lichens contained these compounds as a minor constituent. It is therefore possible that internal bacterial communities in lichens are responsible for the production of long-chain *anteiso*-alkanes, although the relationship of these bacteria to the mycobionts or photobionts is still unknown.

Other branched alkanes, a squalene, and a compound **c**, were detected in some samples. Solberg (1987) reported the detection of squalene in several lichens, as well as a prominent polyunsaturated branched hydrocarbon in *L. pulmonaria* with an estimated C_{27} homologue. We tentatively identified compound **c** as a polyunsaturated compound with a similar cleavage pattern to the C_{27} polyunsaturated branched hydrocarbon reported by Solberg (1987). As in Solberg

(1987), this compound was found to be prominent in the genus *Lobaria* (Fig. 1), and it was also detected in some other lichen species (Fig. 2.1, Table 2.3).

2.3.2.4. Other apolar compounds

A series of hopanoids were detected in the lichen samples (Fig. 2.1, Table 2.3). Diploptene and its related compound hop-21-ene have been identified in soil, peat, lake, and marine sediments, and are produced by various types of bacteria, including cyanobacteria (Brassell et al., 1980; Brassell and Eglinton, 1981; Volkman et al., 1986; Venkatesan, 1988; van Winden et al., 2012; Méjanelle et al., 2017). This compound has also been found in ferns and mosses (Ageta and Arai, 1983; Toyota et al., 1998; Huang et al., 2010; Li et al., 2022). Li et al. (2022) reported that the diploptene may be provided by the coexisting heterotrophic bacteria, methanotrophs, or methylotrophs on the basis of the carbon isotope ratios of the diploptene and long-chain *n*-alkanes of the epiphytic bryophytes. It is possible that the lichen symbiotic bacteria are involved in the production of hopanoids because these compounds have been detected prominently not only in cyanolichens but also in chlorolichens.

Fernene was also detected as a major terpenoid in all lichen samples. All samples contained varying amounts of two fernene isomers, and some samples contained a trace amount of fernadiene, but with a low reliability of identification. Fernene has been found in terrestrial plants, such as ferns (Ageta and Arai, 1983), gymnosperm *Podocarpus* species (Silva et al., 1972), and extinct pteridosperms (seed ferns) (Paull et al., 1998). However, some bacteria also produce these compounds (Volkman et al., 1986; Douka et al., 2001). It was therefore presumed that the internal bacterial communities in lichens synthesized the fernene compounds as well as diploptene.

2.3.2.5. Polar compounds

Several compounds known as lichen secondary metabolites were detected in the polar fractions (Fig. 2.5). Lichen secondary metabolites are known as compounds that are particularly unique to lichens. Fallacinol and parietin, which have anthraquinone skeletons, were detected in several samples. Anthraquinones provide lichen with strong UV tolerance and are especially characteristic of lichens that thrive on bare soil exposed to intense solar radiation (Boustie et al., 2011). Dibenzofurans were also successfully detected on several occasions, although with low reproducibility. Dibenzofurans, in particular, have been reported as compounds possessed by lichens in general (Millot et al., 2016). However, to the author's knowledge, there were no

reported cases detected by GC-MS because of their highly polar components. At this stage, a permanent method to detect these compounds could not be established.

2.3.3. Taxonomic variability of aliphatic components

Variations in the photobionts rather than the mycobionts were likely responsible for much of the difference in the aliphatic hydrocarbon composition. The predominant alkene in species belonging to the orders Lecanorales, Caliciales, and Teloschistales was 1,8-heptadecadiene (with the exception of the families Cladoniaceae and Stereocaulaceae). Furthermore, 6,9-heptadecadiene was abundant in species belonging to the families Cladoniaceae and Stereocaulaceae in the order Lecanorales, and the genus *Lobaria* in the family Peltigeraceae (Peltigerales). These 6,9-heptadecadiene-producing species were also distinguished by their high concentrations of 8- and 7-heptadecenes. In contrast, the species belonging to Collemataceae and *Peltigera* in the family Peltigeraceae (Peltigerales) were distinguished by their high abundances of C_{18} and C_{19} alkenes and lack of heptadecadienes. Biosynthetic pathways that produce C_{17}–C_{21} alkenes are present in cyanobacteria and eukaryotic microalgae (Coates et al., 2014; Sorigué et al., 2016). Comparing the alkene composition of lichens with the photobiont taxonomies revealed that the C_{17} alkadienes were abundant in lichens with only green algae photobionts, whereas the C_{18} and C_{19} alkenes were more prevalent in lichens with only cyanobacterial photobionts. *Lobaria* species, which can harbor both green algae and cyanobacteria, exhibited a combination of the characteristics of both groups, containing both the C_{17} alkadiene and C_{19} alkene (5-nonadecene). It was therefore presumed that the differences in alkene composition were attributable to taxonomic variations among symbiotic algae. Furthermore, although the photobiont in the majority of chlorolichens was *Trebouxia*, Asterochloris sp. was the photobiont of *Cladonia* and *Stereocaulon* species (Škaloud and Peksa, 2010; Peksa and Škaloud, 2011; Moya et al., 2015; Pino-Bodas and Stenroos, 2021). We therefore hypothesized that the 1,8-heptadecadiene was derived from *Trebouxia*, and the 6,9-heptadecadiene, and 8- and 7-heptadecenes were derived from *Asterochloris*. Previous studies (Dembitsky et al., 1994a, b; Piervittori et al., 1995, 1996; Reis et al., 2005) have found that seasonality and habitats could influence the alkanoic acid and *n*-alkane composition of lichen lipids. However, it is unlikely that the alkene composition varied significantly due to environmental conditions, although our samples were collected from an uncontrolled environment.

We performed a cluster analysis to determine whether the composition of lichen aliphatic hydrocarbons could be used for lichen chemotaxonomy. The cluster analysis using only the *n*-alkene composition, or *n*-alkane and *n*-alkene composition, of each sample resulted in clusters that reflected the differences among symbiotic algae well (Fig. 2.6). In contrast, the cluster analysis using the *n*-alkane composition of each sample did not permit a good interpretation of the cohesiveness of each cluster. The major difference between the two clusters of lichens with only *Trebouxia* as a symbiont may be due to the 1,8-heptadecadiene concentration. Cluster 'C' had high concentrations of 1,8-heptadecadiene (145.74–56.68 µg/g), whereas Cluster 'D' had relatively low concentrations (41.93–14.81 µg/g), indicating a difference between these two clusters. The amounts of the alkene produced by the mycobiont may have been influenced by other factors, given that two *X. mandschurica* samples from different collection sites were classified into distinct clusters despite containing identical symbiotic algae. The presence or absence of the two heptadecadienes and the major C_{17}–C_{19} alkenes was a major cause of the differences between these clusters. Consequently, the differences in the alkene composition of the lichen samples was the primary factor reflecting the differences in lichen taxa, particularly the photobiont, rather than environmental factors.

2.3.4. Potential biomarkers of lichen

Several specific compounds in the lichen samples were determined to be aliphatic hydrocarbons. Huang et al. (2012) proposed that long-chain *anteiso*-alkanes could be used as a biomarker for lichens. We further confirmed the presence of long-chain *anteiso*-alkanes in lichens. These compounds were characteristic for some lichens, especially the genus *Cladonia*, which is an important lichen in polar peatlands and tundra regions (e.g., Payette and Delwaide, 2018), and could be used as a biomarker to evaluate lichen assemblages in peatlands and tundra. Our data showed that chlorolichens produce a substantial amount of alkadiene. Numerous studies have used the alkenes, particularly long-chain alkenes (> C_{20}), preserved in sediments as biomarkers of terrestrial higher plants or algae for paleoenvironmental reconstructions (Matsumoto et al., 1990; Jaffé et al., 1995; Zhang et al., 2004, 2007; Theissen et al., 2005; de Mesmay et al., 2007; van Bree et al., 2014). In contrast, the origin of short- to medium-chain alkenes has not been well documented (Matsumoto et al., 1990; Cardoso et al., 1983; Cranwell et al., 1987; Yongdong et al., 2015; Kaiser et al., 2016). There are few reports of the alkene composition of lichens, but as described in Section 2.3.2.2, lichens with green algae commonly produce heptadecadiene. In

addition, Matsumoto et al. (1992) discovered heptadecadiene in Antarctic rocks colonized by living and fossil cryptoendolithic lichens and fungi. Because heptadecadiene has been detected prominently in lichen in some studies (Corbier and Tesseire, 1974; Gavin et al., 1978; Solberg, 1986, 1987), we propose that chlorolichens universally produce heptadecadienes.

We assumed that the alkenes were produced in lichens by an algal photobiont or as a result of symbiosis with certain species of photobiont because the alkene composition was attributed to phylogenetic differences in the symbiotic algae. Green algae that are symbiotic with lichens, such as *Trebouxia* and *Asterochloris*, have adapted to the terrestrial environment and can occupy a wide variety of habitats as a result of their symbiosis with lichens. Laboratory experiments have shown that these algae have a heterotrophic tendency toward fungi (Ahmadjian, 1993). These green algae, which make up the majority of lichens, are rarely found in nature and are thought to have escaped from damaged lichen thalli (Ahmadjian, 1988). Thus, these alkenes, particularly heptadecadienes, may be used as lichen biomarkers.

2.4. Conclusions

We performed a lipid analysis on 29 samples of lichen belonging to the order Lecanorales. The samples contained alkenes, branched alkanes, and hopanoids in addition to *n*-alkanes. Alkenes were widely detected in all samples, indicating that their composition may have been strongly influenced by the differences in the photosynthetic organisms that make up the lichens. Although there are a limited number of alkene compositions reported for lichens, the compositions identified here were similar to those reported previously, suggesting that these compounds are common to many lichens. The origin of short- to medium-chain homologues in sediments has not been well documented, but our study provides an example of the origin of these organisms and presents a potential new biomarker for determining the past constituents of lichens.

Table 2.1 Mycobiont and photobiont classification of lichens used in the experiment.

Samples	Classification	Photobiont		
		Type	Type (classification)	Reference
Platismatia interrupta	Lecanoromycetes Lecanorales Parmeliaceae	Green algae	*Trebouxia* sp.	[1]; [2]; [3]; [4]
Flavoparmelia caperata [a]	Lecanoromycetes Lecanorales Parmeliaceae	Green algae	*Trebouxia* sp.	[5]
Parmotrema clavuliferum	Lecanoromycetes Lecanorales Parmeliaceae	Green algae	*Trebouxia* sp.	[6]
Usnea bismolliuscula [a]	Lecanoromycetes Lecanorales Parmeliaceae	Green algae	*Trebouxia* sp.	[7]
Usnea rubrotincta	Lecanoromycetes Lecanorales Parmeliaceae	Green algae	*Trebouxia* sp.	[7]
Usnea mutabilis	Lecanoromycetes Lecanorales Parmeliaceae	Green algae	*Trebouxia* sp.	[7]
Cladonia scabriuscula [a, b]	Lecanoromycetes Lecanorales Cladoniaceae	Green algae	*Asterochloris* sp.	[8]; [9]; [10]
Cladonia vulcani [b]	Lecanoromycetes Lecanorales Cladoniaceae	Green algae	*Asterochloris* sp.	[8]; [9]; [10]
Cladonia fruticulosa	Lecanoromycetes Lecanorales Cladoniaceae	Green algae	*Asterochloris* sp.	[8]; [9]; [10]
Cladonia stellaris	Lecanoromycetes Lecanorales Cladoniaceae	Green algae	*Asterochloris* sp.	[8]; [9]; [10]
Cladonia cryptochlorophaea	Lecanoromycetes Lecanorales Cladoniaceae	Green algae	*Asterochloris* sp.	[8]; [9]; [10]
Cladonia ramulosa	Lecanoromycetes Lecanorales Cladoniaceae	Green algae	*Asterochloris* sp.	[8]; [9]; [10]
Cladonia rangiferina	Lecanoromycetes Lecanorales Cladoniaceae	Green algae	*Asterochloris* sp.	[8]; [9]; [10]
Stereocaulon japonicum	Lecanoromycetes Lecanorales Stereocaulaceae	Green algae	*Asterochloris* sp.	[11]
Ramalina sinensis	Lecanoromycetes Lecanorales Ramalinaceae	Green algae	*Trebouxia* sp.	[12]
Ramalina yasudae [a]	Lecanoromycetes Lecanorales Ramalinaceae	Green algae	*Trebouxia* sp.	[12]
Xanthoria mandschurica **1** [a, b]	Lecanoromycetes Teloschistales Teloschistaceae	Green algae	*Trebouxia* sp.	[3]; [13]
Xanthoria mandschurica **2**	Lecanoromycetes Teloschistales Teloschistaceae	Green algae	*Trebouxia* sp.	[3]; [13]
Pyxine endochrysina	Lecanoromycetes Caliciales Caliciaceae	Green algae	*Trebouxia* sp.	[3]
Heterodermia subascendens	Lecanoromycetes Caliciales Physciaceae	Green algae	*Trebouxia* sp.	[3]
Heterodermia obscurata	Lecanoromycetes Caliciales Physciaceae	Green algae	*Trebouxia* sp.	[14]
Anaptychia isidiza	Lecanoromycetes Caliciales Physciaceae	Green algae	*Trebouxia* sp.	[15]
Lobaria spathulata [a, c]	Lecanoromycetes Peltigerales Peltigeraceae	Green algae, Cyanobacteria	*Symbiochloris* sp., *Nostoc* sp.	[3]; [16]; [17]; [18]
Lobaria orientalis **1** [c]	Lecanoromycetes Peltigerales Peltigeraceae	Green algae, Cyanobacteria	*Symbiochloris* sp., *Nostoc* sp.	[3]; [16]; [17]; [18]
Lobaria orientalis **2** [c]	Lecanoromycetes Peltigerales Peltigeraceae	Green algae, Cyanobacteria	*Symbiochloris* sp., *Nostoc* sp.	[3]; [16]; [17]; [18]
Lobaria tuberculata [c]	Lecanoromycetes Peltigerales Peltigeraceae	Green algae, Cyanobacteria	*Symbiochloris* sp., *Nostoc* sp.	[3]; [16]; [17]; [18]
Peltigera degenii [a]	Lecanoromycetes Peltigerales Peltigeraceae	Cyanobacteria	*Nostoc* sp.	[3]; [19]; [20]; [21]
Collema furfuraceum [a]	Lecanoromycetes Peltigerales Collemataceae	Cyanobacteria	*Nostoc* sp.	[3]; [22]
Collema complanatum	Lecanoromycetes Peltigerales Collemataceae	Cyanobacteria	*Nostoc* sp.	[3]; [22]

[a] Ikeda et al., 2021. [b] Ikeda et al., 2018. [c] Green algae as the primary photobiont and with localized cyanobacteria in cephalodia.

[1]: Czeczuga & Czeczuga-Semeniuk, 2002; [2]: Miadlikowska et al., 2006; [3]: Miadlikowska et al., 2014; [4]: Palmqvist & Dahlman, 2006; [5]: Beck et al., 1998; [6]: Leavitt et al., 2015; [7]: Rafat et al., 2015; [8] Moya et al., 2015; [9]: Pino-Bodas & Stenroos, 2021; [10]: Škaloud & Peksa, 2010; [11]: Peksa & Škaloud, 2011; [12]: Voytsekhovich & Beck, 2016; [13]: Nyati et al., 2014; [14]: Xu et al., 2022; [15]: Dahlkild et al., 2001; [16]: Cornejo & Scheidegger, 2015; [17]: Dal Grande et al., 2014; [18]: Škaloud et al., 2016; [19]: Myllys et al., 2007; [20]: O'Brien et al., 2005; [21]: Rikkinen et al., 2002; [22]: Otálora et
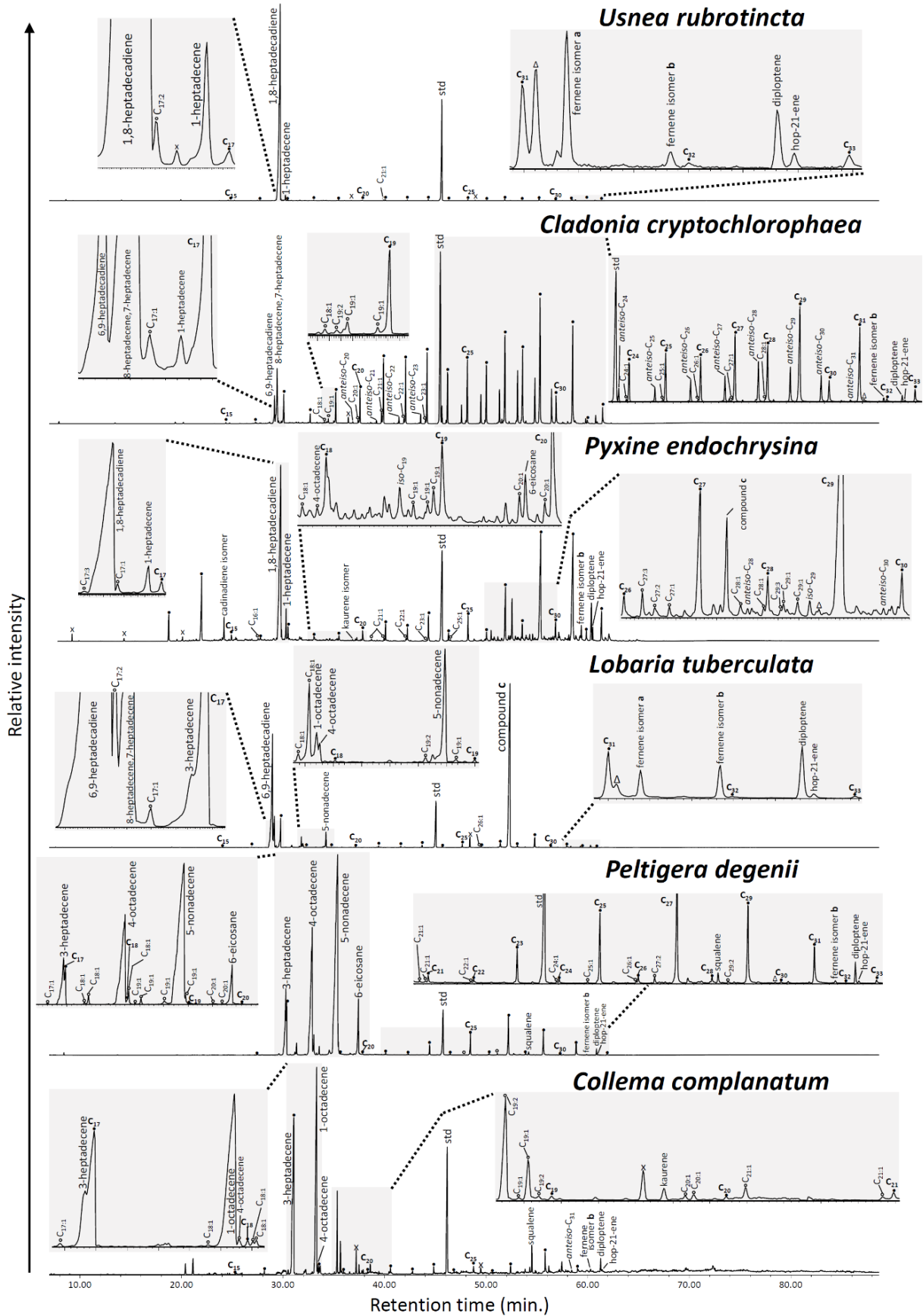
Fig.2.1 Total ion chromatograms showing the distribution of aliphatic hydrocarbons detected from *Usnea rubrotincta*, *Cladonia cryptochlorophaea*, *Pyxine endochrysina*, *Lobaria tuberculata*, *Peltigera degenii* (after Ikeda et al., 2021), and *Collema complanatum*. std, standard (tetracosane-d$_{50}$); •, n-alkanes; ○, n-alkenes with unknown double bond positions; x, contamination; Δ, hopanoid.
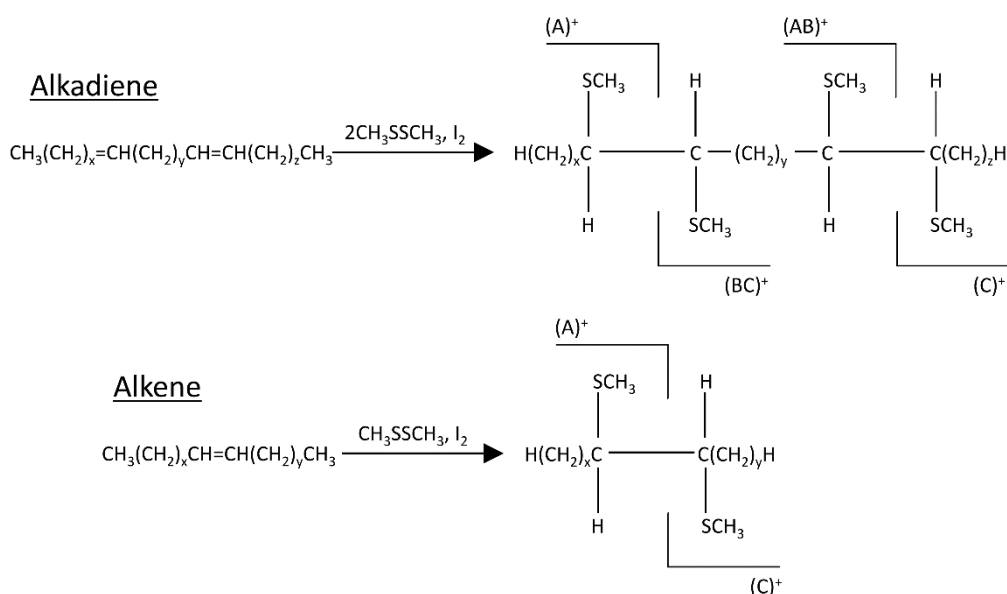
Fig.2.2 Fragmentation scheme for the formation of DMDS adducts of alkenes
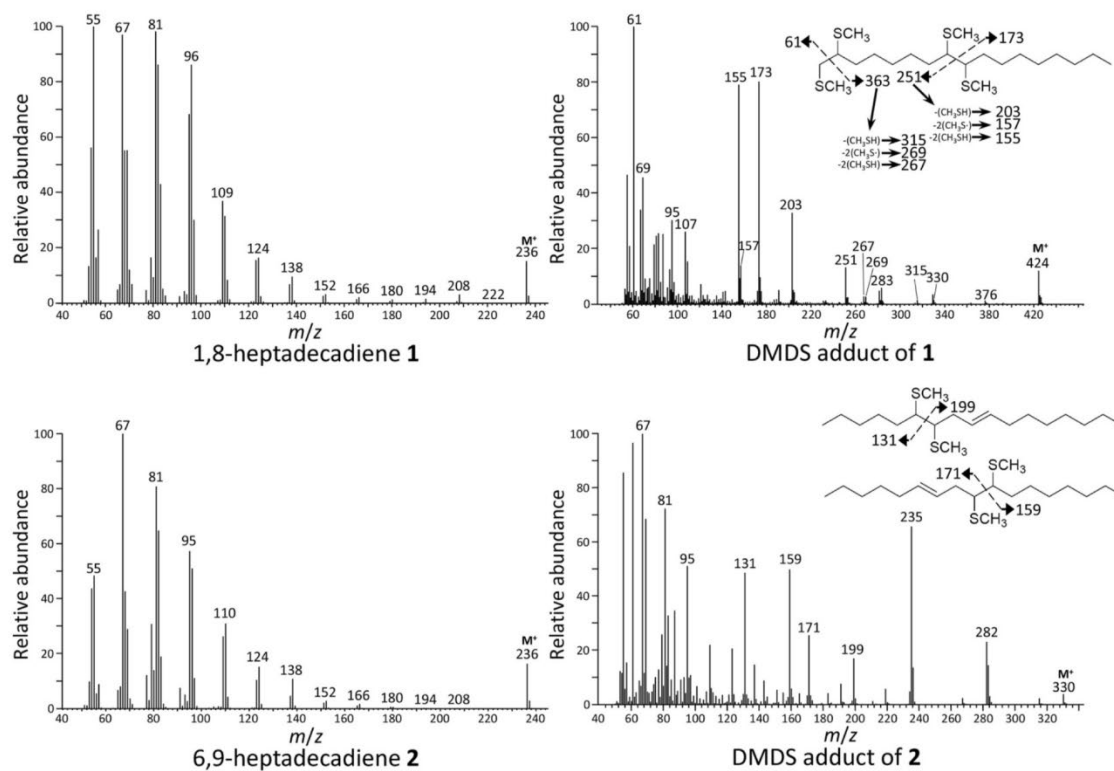
Fig.2.3 Mass spectra of 1,8-heptadecadiene (**1**), 6,9-heptadecadiene (**2**), 8-heptadecene (**3**), 7-heptadecene (**4**), 1-heptadecene (**5**), 3-heptadecene (**6**), 1-octadecene (**7**), 4-octadecene (**8**), 5-nonadecene (**9**), and 6-eicosene (**10**) from lichens and mass spectra of their DMDS adducts.
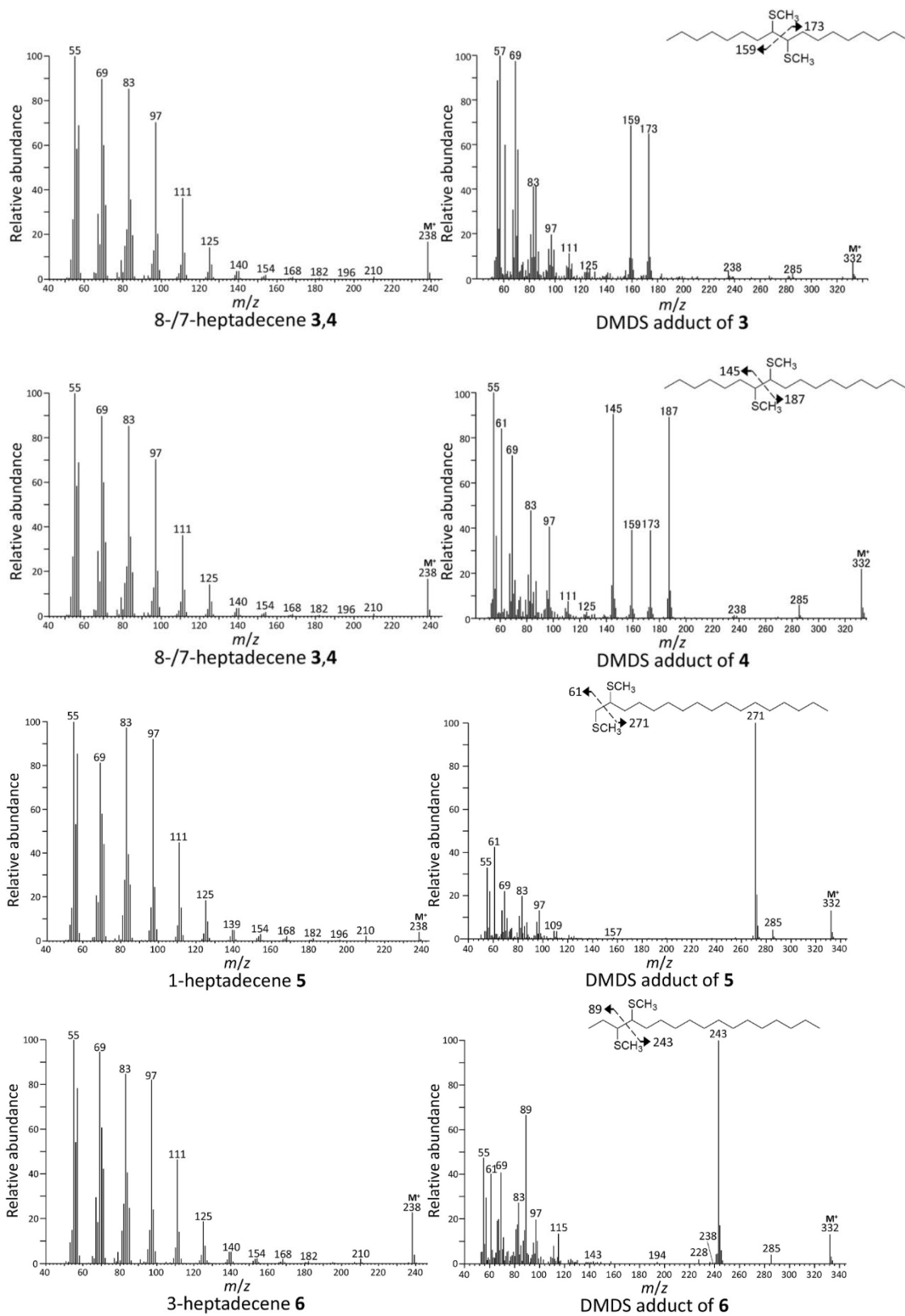
Fig.2.3 (*continued*).
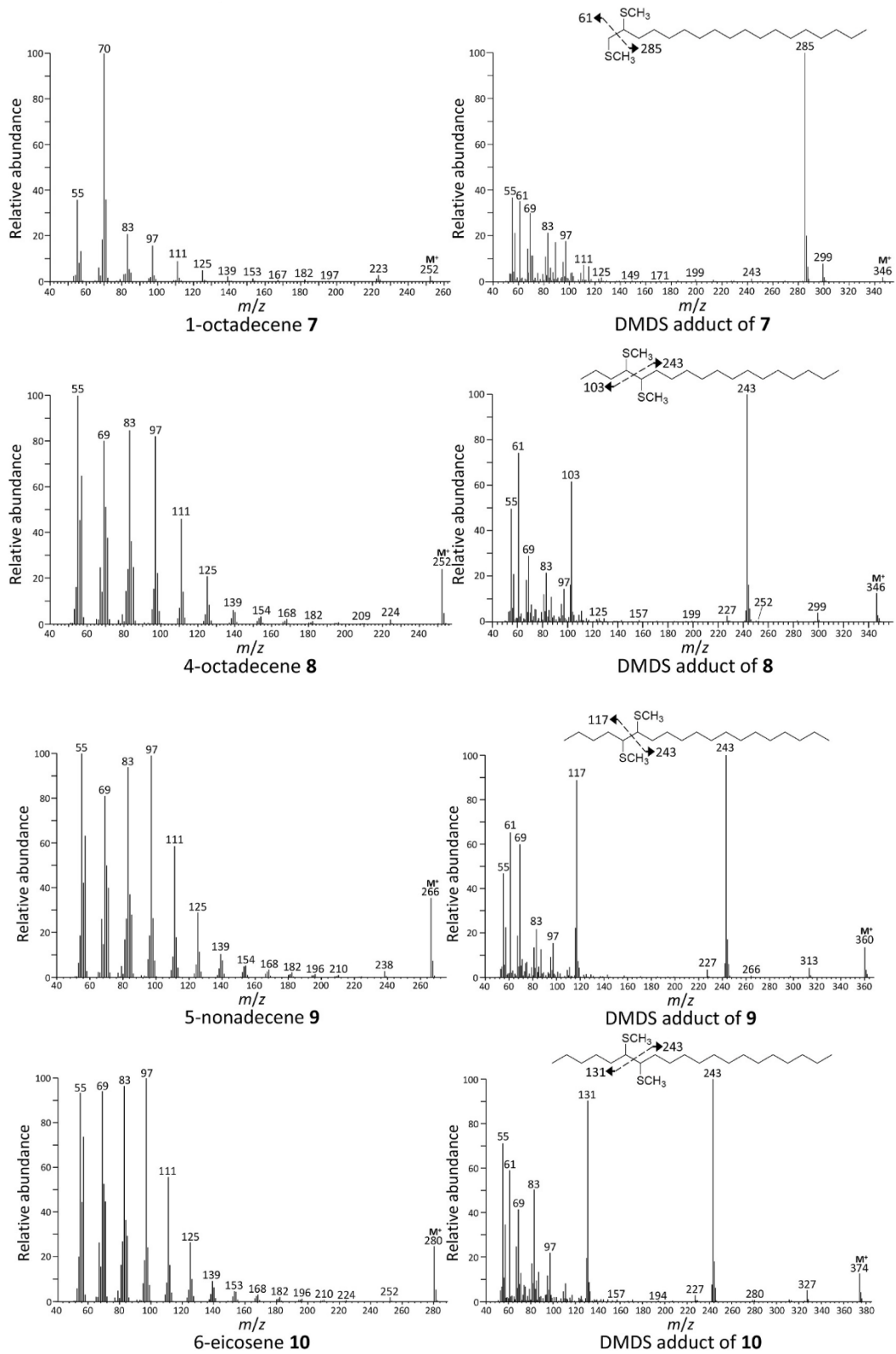
Fig.2.3 (*continued*).

Table 2.2.

Mass-to-charge ratio (% relative abundance) of key ions in the mass spectra of the DMDS derivatives of alkene isomers from lichen samples.

Compound	m/z														
	x#	y#	z#	[A]+	[C]+	[BC - 48]-	[BC - 94]+	[AB - 48]+	[AB - 94]+	[M - 141]+	[M - 95]+	[M - 94]+	[M - 48]-	[M - 47]-	[M]+
Alkadiene															
1,8-heptadecadiene **1**	0	5	8	61(100)	173(80)	315(2)	269(3)	203(33)	157(14)	283(6)		330(2)	376(1)		424(12)
6,9-heptadecadiene **2**	5	1	7	131(49)	199(17)						235(66)		282(23)		330(4)
				171(26)	159(50)						235(66)		282(23)		330(4)
Alkene															
7-heptadecene **3**	6	9		145(91)	187(89)							238(1)		285(6)	332(22)
8-heptadecene **4**	7	8		159(69)	173(65)							238(1)		285(2)	332(7)
1-heptadecene **5**	0	15		61(43)	271(100)							–		285(4)	332(13)
3-heptadecene **6**	2	13		89(67)	243(100)							238(1)		285(4)	332(13)
1-octadecene **7**	0	16		61(35)	285(100)							–		299(8)	346(2)
4-octadecene **8**	3	13		103(62)	243(100)							252(1)		299(4)	346(13)
5-nonadecene **9**	4	13		117(89)	243(100)							266(1)		313(4)	360(14)
6-eicosene **10**	5	13		131(90)	243(100)							280(1)		327(5)	374(13)

#: x, y, z represent partial chain lengths shown in the chemical formula H(CH2)xCH = CH(CH2)yCH = CH(CH2)zH in alkadiene and H(CH2)xCH = CH(CH2)yH in alkene for interpretation.

29
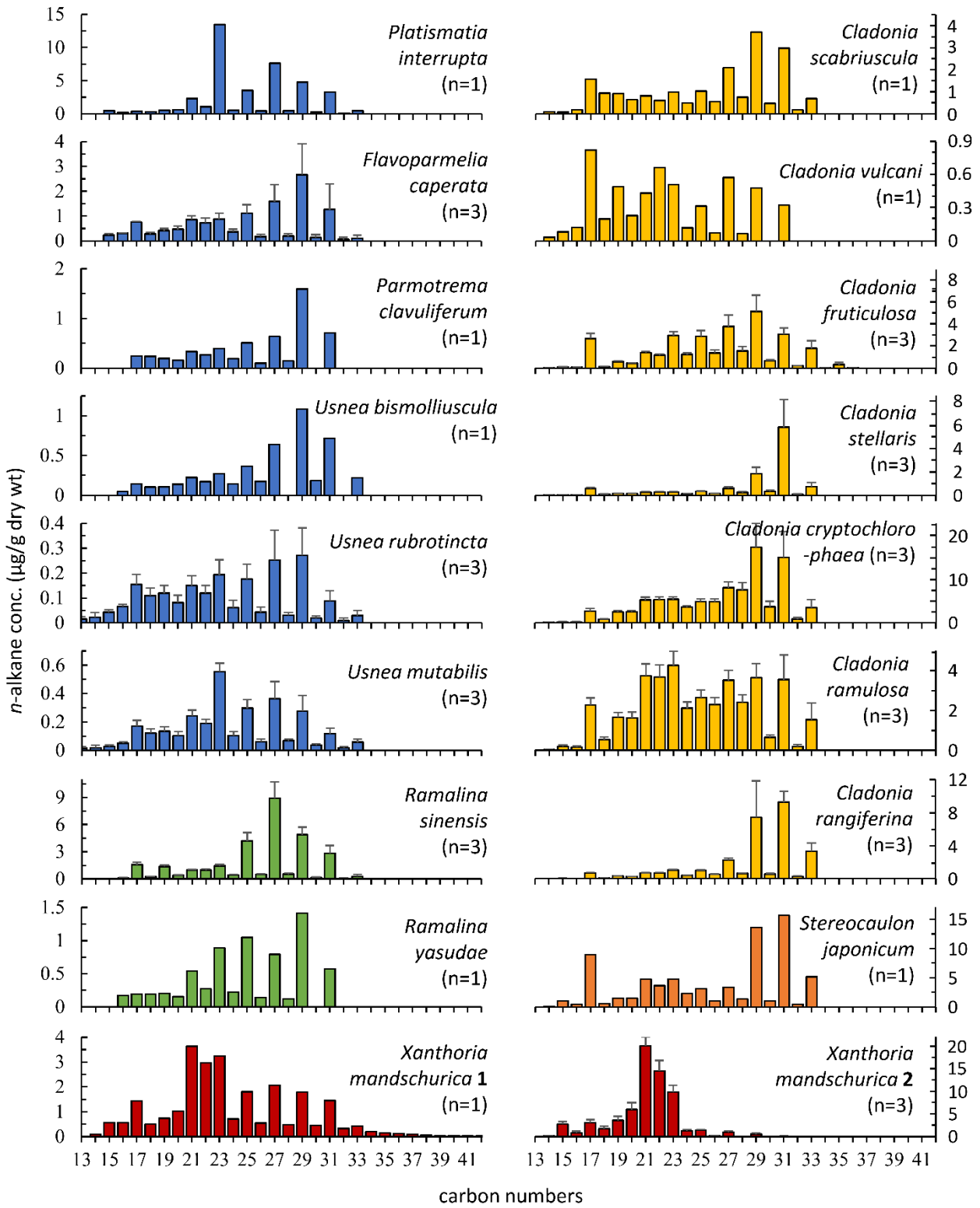
Fig.2.4. *n*-Alkane distributions in lichens showing the averaged distribution values with the mean standard deviation of each sample.
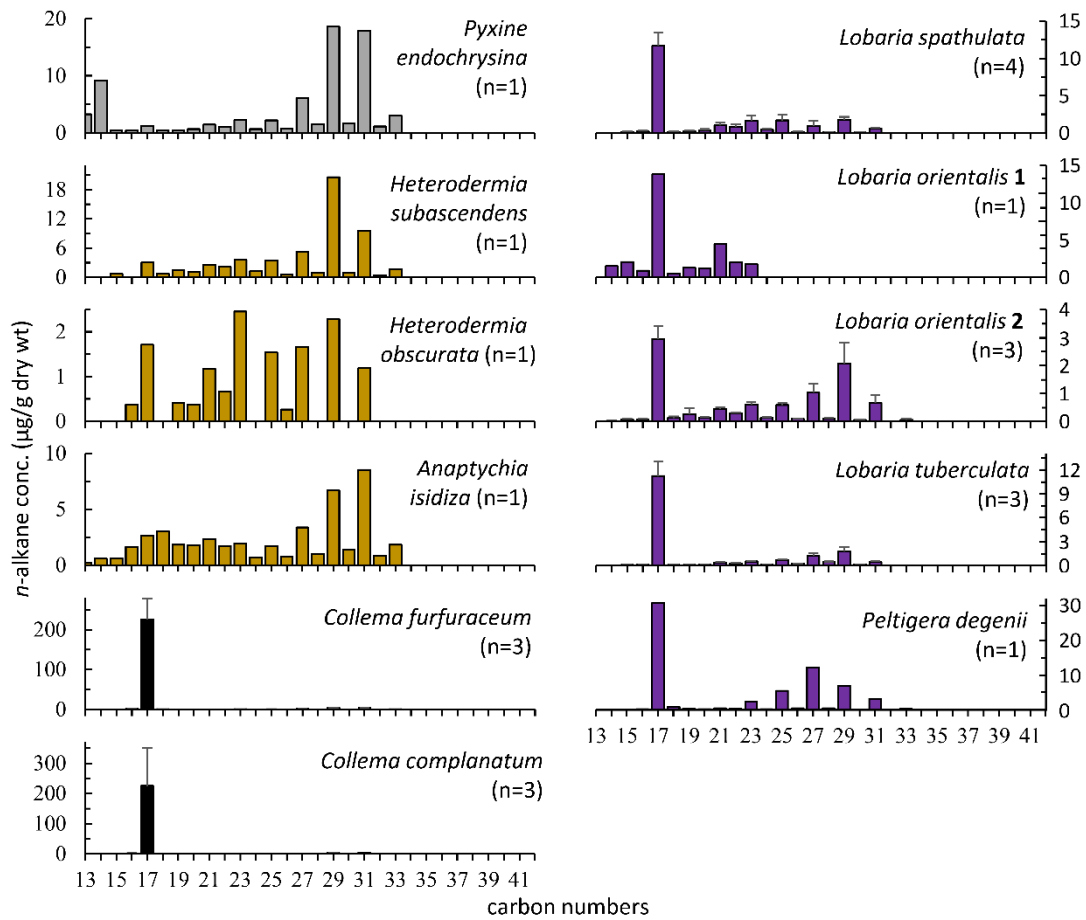
Fig.2.4 (*continued*).
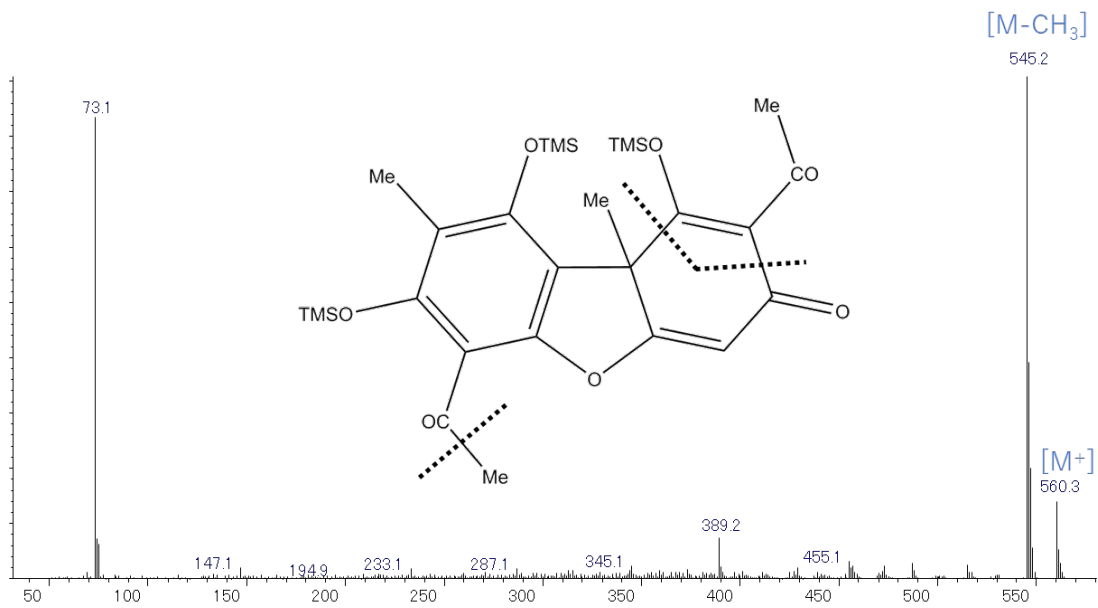
Fig.2.5 (Captions are on the next page)
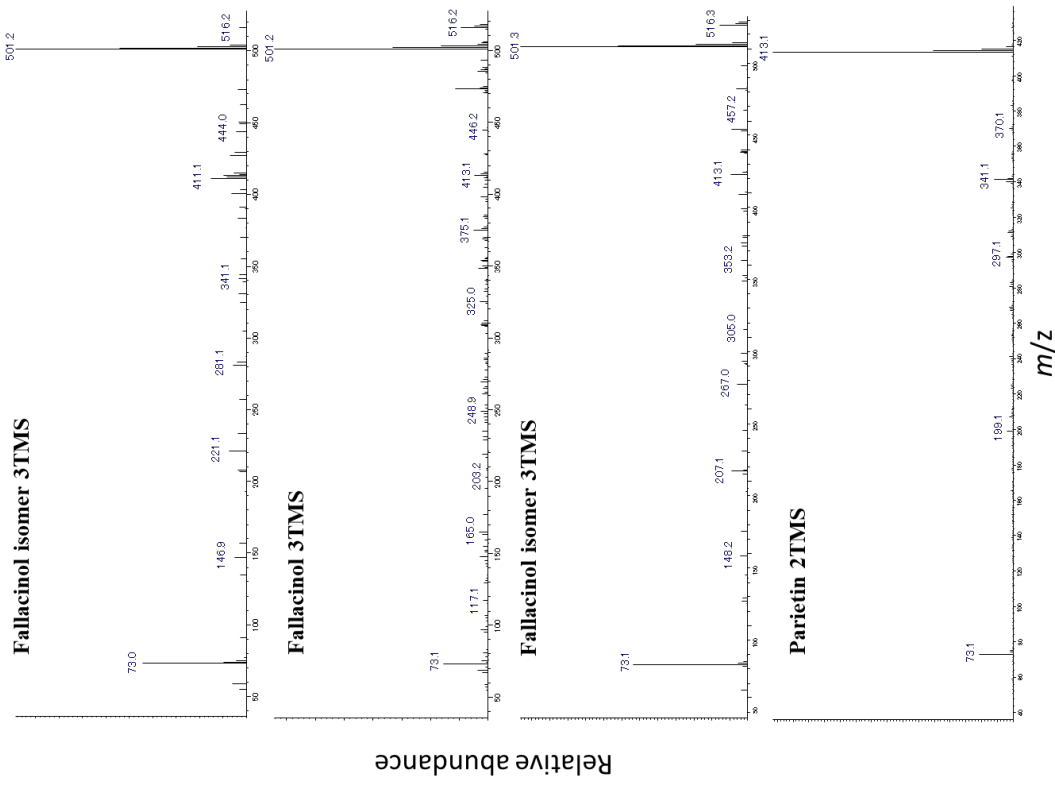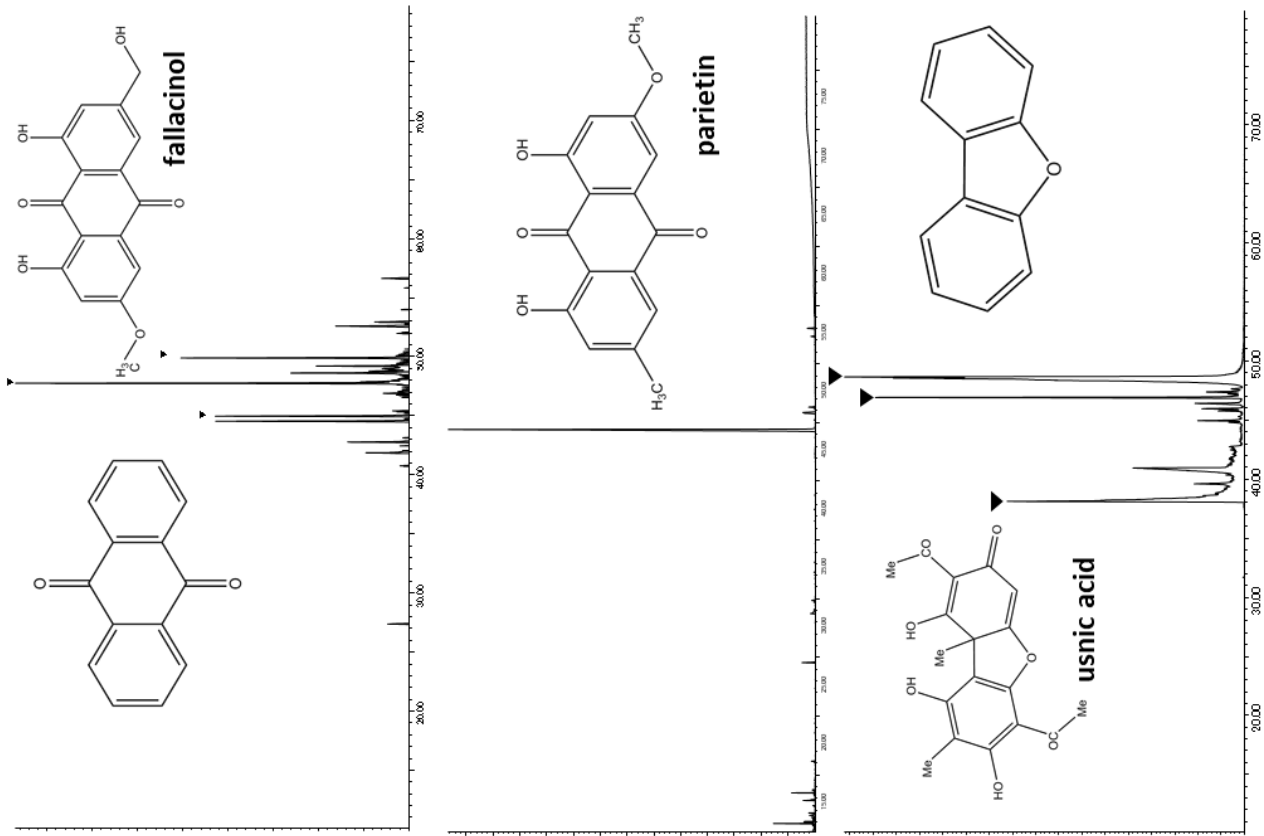
Fig.2.5 TIC of polar fractions and mass spectra of oxygen-containing aromatic compounds detected from some lichen samples.
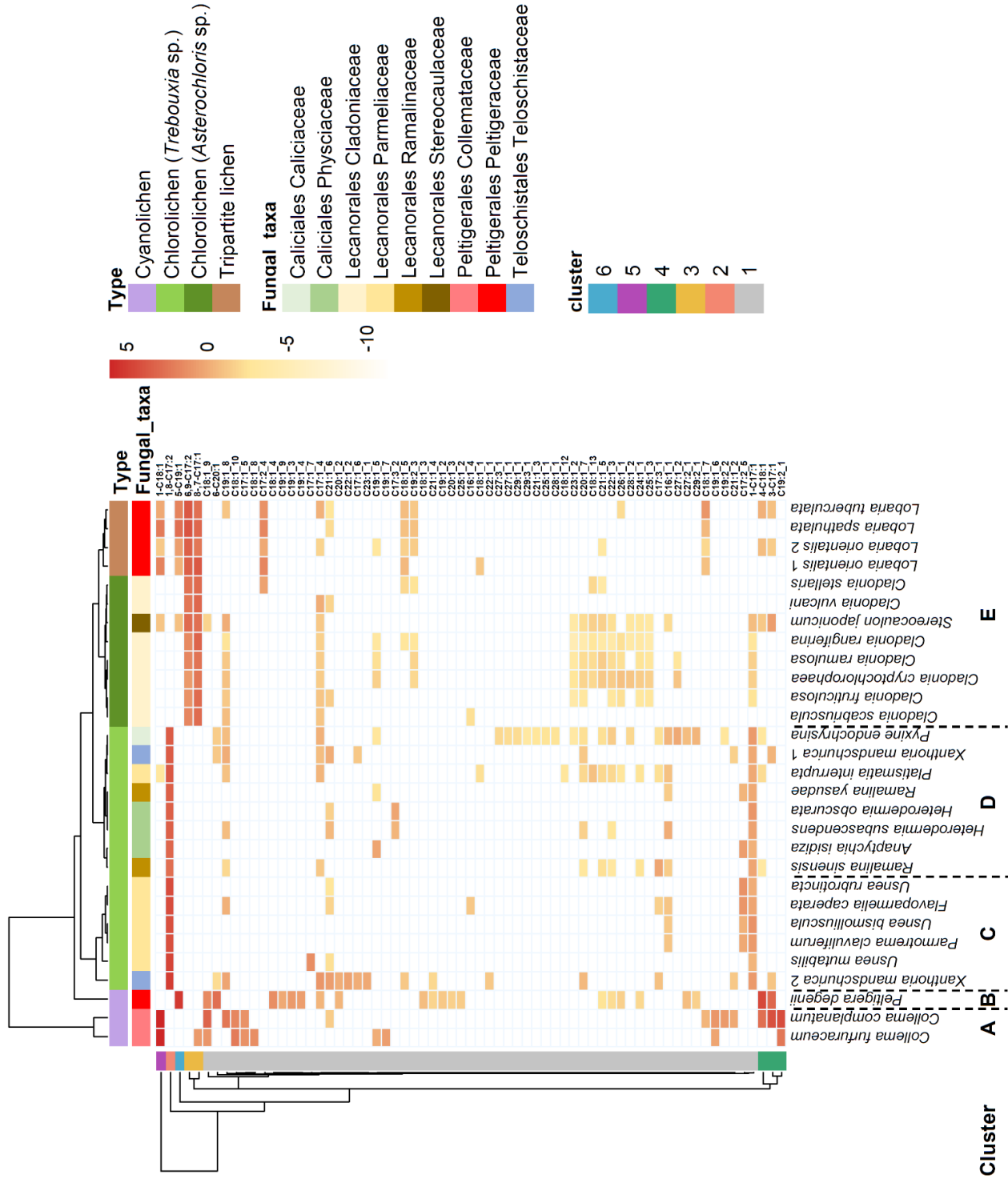
Fig. 2.6. Heatmap of the log$_e$-transformed alkene concentration in lichens. Species (columns) and alkenes (rows) are clustered based on the Euclidean distance and Ward D2 minimum variance clustering. For convenience, log$_e$(0), i.e., not detected, is indicated on the heatmap with a value one order of magnitude smaller than the smallest value.

Table 2.3. Distribution of major components

Samples	n-Alkane conc. (μg/g dry wt.)	ACL	CPI (24-32)	range	Alkene conc. (μg/g dry wt.)	main contents	anteiso-alkanes	Squalene	compound c
Platismatia interrupta [a]	40.75	25.93	13.07	C$_{15}$-C$_{33}$	45.51	1,8-C$_{17:2}$	n.d.		
Flavoparmelia caperata [a]	12.61	27.69	9.16	C$_{15}$-C$_{33}$	73.37	1,8-C$_{17:2}$	n.d.	x	x
Parmotrema clavuliferum [a]	5.71	27.88	10.00	C$_{17}$-C$_{31}$	60.19	1,8-C$_{17:2}$	n.d.	x	xx
Usnea bismolliuscula [a]	4.73	28.38	6.61	C$_{16}$-C$_{33}$	62.4	1,8-C$_{17:2}$	n.d.	x	x
Usnea rubroincta	2.05	26.96	6.32	C$_{13}$-C$_{33}$	74.27	1,8-C$_{17:2}$	n.d.		
Usnea mutabilis	3.02	26.16	4.61	C$_{13}$-C$_{33}$	102.84	1,8-C$_{17:2}$	n.d.		
Cladonia scabriuscula [a, b]	19.77	28.51	4.67	C$_{14}$-C$_{33}$	23.52	6,9-C$_{17:2}$, 8-, 7-C$_{17:1}$	C$_{28}$-C$_{30}$	x	
Cladonia vulcani [b]	5.55	26.80	8.50	C$_{14}$-C$_{31}$	33.82	6,9-C$_{17:2}$, 8-, 7-C$_{17:1}$	n.d.	x	
Cladonia fruticulosa	31.74	27.80	3.44	C$_{14}$-C$_{36}$	20.87	6,9-C$_{17:2}$, 8-, 7-C$_{17:1}$	C$_{26}$-C$_{30}$		
Cladonia stellaris	12.4	30.07	9.86	C$_{14}$-C$_{33}$	32.37	6,9-C$_{17:2}$, 8-, 7-C$_{17:1}$	C$_{25}$-C$_{30}$		
Cladonia cryptochlorophaea	94.01	28.56	2.49	C$_{14}$-C$_{33}$	15.07	6,9-C$_{17:2}$, 8-, 7-C$_{17:1}$	C$_{20}$-C$_{31}$		
Cladonia ramulosa	40.62	27.43	2.06	C$_{14}$-C$_{33}$	18.69	6,9-C$_{17:2}$, 8-, 7-C$_{17:1}$	C$_{20}$-C$_{31}$		
Cladonia rangiferina	29.14	29.71	10.00	C$_{15}$-C$_{33}$	31.51	6,9-C$_{17:2}$, 8-, 7-C$_{17:1}$	C$_{22}$-C$_{30}$		
Stereocaulon japonicum	74.2	29.09	7.57	C$_{14}$-C$_{33}$	37.31	6,9-C$_{17:2}$, 8-, 7-C$_{17:1}$	C$_{28}$, C$_{30}$	x	x
Ramalina sinensis	29.83	27.38	14.84	C$_{16}$-C$_{33}$	18.14	1,8-C$_{17:2}$	n.d.	x	xx
Ramalina yasudae [a]	6.92	26.88	10.32	C$_{16}$-C$_{31}$	32.18	1,8-C$_{17:2}$	C$_{28}$	x	x
Xanthoria mandschurica 1 [a, b]	25.59	26.57	3.56	C$_{14}$-C$_{42}$	42.29	1,8-C$_{17:2}$	n.d.	x	
Xanthoria mandschurica 2	66.84	23.85	3.38	C$_{14}$-C$_{33}$	159.67	1,8-C$_{17:2}$	n.d.		
Pyxine endochrysina	74.61	29.27	9.17	C$_{13}$-C$_{33}$	44.95	1,8-C$_{17:2}$	C$_{28}$, C$_{30}$		x
Heterodermia subascendens	60.05	28.55	11.69	C$_{15}$-C$_{33}$	31.22	1,8-C$_{17:2}$	n.d.	x	
Heterodermia obscurata	14.12	26.61	25.69	C$_{16}$-C$_{31}$	34.85	1,8-C$_{17:2}$	n.d.	x	
Anaptychia isidiza	45.39	28.96	5.08	C$_{13}$-C$_{33}$	22.95	1,8-C$_{17:2}$	n.d.		
Lobaria spathulata [a]	21.87	26.39	11.35	C$_{15}$-C$_{31}$	94.49	6,9-C$_{17:2}$, 8-, 7-C$_{17:1}$, 5-C$_{19:1}$	n.d.	x	xx
Lobaria orientalis 1	15.67	23.00	NA	C$_{14}$-C$_{23}$	84.6	6,9-C$_{17:2}$, 8-, 7-C$_{17:1}$	n.d.		xx
Lobaria orientalis 2	9.86	27.71	13.27	C$_{14}$-C$_{33}$	41.95	6,9-C$_{17:2}$, 8-, 7-C$_{17:1}$	n.d.		xx
Lobaria tuberculata	18.24	27.38	4.60	C$_{15}$-C$_{33}$	75.14	6,9-C$_{17:2}$, 8-, 7-C$_{17:1}$	n.d.		xx
Peltigera degenii [a]	65.47	27.26	23.08	C$_{15}$-C$_{33}$	307.79	4-C$_{18:1}$, 5-C$_{19:1}$	n.d.	x	
Collema furfuraceum [a]	243.77	28.96	8.54	C$_{13}$-C$_{33}$	417.74	1-C$_{18:1}$	n.d.	x	
Collema complanatum	199.35	25.34	11.75	C$_{15}$-C$_{29}$	646.17	1-C$_{18:1}$, C$_{19:2}$	C$_{31}$	x	

[a] Ikeda et al., 2021. [b] Ikeda et al., 2018

$ACL = (23[C_{23}] + 25[C_{25}] + 27[C_{27}] + 29[C_{29}] + 31[C_{31}] + 33[C_{33}])/([C_{23}] + [C_{25}] + [C_{27}] + [C_{29}] + [C_{31}] + [C_{33}])$ [C$_x$]: concentrations of n-C$_x$ alkanes (Poynter & Eglinton, 1990; Zhang et al., 2004)

$CPI = 2([C_{25}] + [C_{27}] + [C_{29}] + [C_{31}])/([[C_{24}] + [C_{26}] + [C_{28}] + [C_{30}]) + ([C_{26}] + [C_{28}] + [C_{30}] + [C_{32}]])]$, [C$_x$]: concentrations of n-C$_x$ alkanes (Bray & Evans, 1961)

x: detected ; xx: abundant

CHAPTER 3
Lichen and fungal biomarker analysis of the sediments deposited across the Cenomanian/Turonian boundary: Reconstruction of fungal flora changes

3.1. Introduction

The Cretaceous is an interval of great interest for understanding the ecological evolution in terrestrial areas under hothouse conditions. There were no ice sheets in the polar regions, and especially the Late Cenomanian-Early Turonian was the Cretaceous ocean surface temperature maximum, known as the "Cretaceous thermal maximum" (Norris et al., 2002; Forster et al., 2007; O'Brien et al., 2017). A large environmental disturbance event, oceanic anoxic event (OAE2: ~94 Ma), is known to have occurred during the Cenomanian-Turonian boundary period and has been linked with large igneous province (LIP) volcanic activity. This environmental disturbance event occurred globally and lasted approximately 600-900 kyr, although studies vary in duration (Sageman et al., 2006; Eldrett et al., 2015; Jenkyns et al., 2017; Li et al., 2017; Jones et al., 2019). The mechanism of marine anoxic events is thought to be the increase in biological production in the ocean surface layer due to igneous activity, resulting in the expansion of anoxic water masses and the deposition of large amounts of organic matter without decomposition. Black shales formed by the deposition of organic matter are distributed worldwide. Because large-scale igneous activity and subsequent deposition of organic matter also significantly impacted the carbon cycle, OAE2 has been used as a stratigraphic contrast tool even in areas where black shales cannot be identified, with positive isotopic excursions of carbonate and organic carbon being reported. OAE2 is the most studied of the Cretaceous OAEs and is subdivided into five stages based on variations in $\delta^{13}C$ values. $\delta^{13}C$ shows a positive shift at the beginning of OAE2 (1st build-up), followed by a negative spike (Trough interval), then a second positive shift (2nd build-up), and keeps to a heavier carbon isotope ratio (Plateau) and finally return to a lighter value (Recovery). The negative shift is synchronous with LIPs activity, and the positive shift is thought to be related to increased oceanic production. The Trough period is known to have experienced a "Plenus Cold Event," a cooling event caused by a decrease in pCO2. It is estimated that 33-55% of marine ecosystem species became extinct (Sepkoski, 1989), and the extinction of planktonic foraminifera, especially those that inhabit the ocean surface, suggests that the effects of the OAE extended to the ocean surface. Limited research suggests that this significant carbon cycle change event may have also

strongly affected terrestrial ecosystems (Eaton et al., 1997; Kuypers et al., 1999; Hay et al., 2012; Heimhofer et al., 2018). Heimhofer et al. (2018) used a palynomorph analysis of terrestrial paleovegetation changes during OAE2 in southern France. The results indicate that vegetation in southern France changed from a cold and dry savanna climate to a warmer and wetter climate and conifer-dominated forests during the OAE.

As noted in Chapter 1, fungi, especially lichens, may have promoted diversification and allowed lichens to explore niche spaces during the mid-Cretaceous period. However, the only fossil record of lichens in the Cretaceous is the *Honeggeriella complexa*, reported in Matsunaga et al. (2013), and there is no direct evidence of environmental response and expansion of lichens. Therefore, this study examined lichen indicators using aromatic furans to elucidate the environmental response of lichens during the OAE2 period, which is known to have undergone major environmental changes.

3.2. Samples and methods

3.2.1. Omagarisawa River Section

The samples are sedimentary rocks of the Yezo Group, which are distributed in the Omagarisawa River (OMZ) in the Tomamae area (Fig. 3.1). The Yezo Group, which is distributed north-south along the mid-axis of Hokkaido, is thought to have been deposited in the forearc basin on the eastern margin of the Asian continent from the mid-Cretaceous to the early Paleogene, with a total thickness of approximately 10,000 m (Takashima et al., 2004). This sample was collected during a joint survey with Professor Takashima of Tohoku University. The samples are sedimentary rocks collected during the August 2017 survey, some of which were previously collected and provided by Dr. Ando of Akita University. The Saku Formation of the Yezo Group exposed in the study area contains the OAE2 equivalent formation that occurred near the Cenomanian-Turonian boundary, and the behavior of δ^{13}C values of wood chips in sedimentary rocks and comparison with other areas indicate that the OAE2 formation in this study area extends about 700 m thick. Plant fragments from terrestrial sources in the Yezo Formation are considered to have been intensely mixed during transport from terrestrial areas to the Yezo forearc basin. In addition, about 100 years have been mixed and averaged by bioturbation (Hasegawa, 2001; Hasegawa et al., 2003). The Saku Formation is composed of mudstone-dominated turbidite sandstone-mudstone alternation. As with other Yezo Formation samples, a detailed record of terrestrial vegetation changes during OAE2 events is expected because of the large terrestrial contribution and low maturity (Ando et al., 2017). The study area consisted mainly of alternating layers of sand and mud, and only mudstone was sampled.

3.2.2. North Fork Cottonwood Creek Section

The samples are sedimentary rocks of the Budden Canyon Formation of the Great Valley Sequence (GVS) in the North Fork Cottonwood Creek (NFCC), northern California, U.S.A (Fig. 3.1). The GVS is a typical forearc basin sedimentary sequence deposited on the continental margin of North America at ~30-40°N. The Budden Canyon Formation records sedimentary deposits from the Berriasian to the Turonian. The Cenomanian-Turonian boundary stratigraphy at this site is dominated by dark-gray organic-rich terrigenous mudstone interbedded with some thin turbidite beds and minor conglomerate sandstone. The sample used in this study was provided by Prof. Takashima of Tohoku University and reported by Du Vivier et al. (2015) and Takashima et al. (2011), which compared each phase of OAE2 with other sites.

3.2.3. Biomarker analysis

Extraction and separation of bitumen were performed as described by Sawada et al. (1996). Sediments were extracted with methanol (MeOH), dichloromethane (DCM) and DCM/MeOH (1/1, v/v). As an internal standard, tetracosane-d_{50} was added, and the extract was dried in a rotary evaporator and re- dissolved in hexane. The hexane extract was passed through a silica gel column (95% activated); the aliphatic and aromatic hydrocarbon fractions were eluted consecutively with hexane and hexane/toluene (3/1, v/v) and analyzed using gas chromatography-mass spectrometry (GC-MS). Lipids were identified by GC-MS using an Agilent 7890B GC instrument equipped with a 30 m × 0.25 mm i.d. DB-5HT fused silica column (Agilent, Santa Clara, CA, USA) directly coupled to an Agilent 5977A MSD quadruple mass spectrometer (electron voltage, 70 eV; scan range, *m/z* 50–650 in 1.3 s). The oven temperature was programmed as follows: 50°C (held for 4 min) to 310 C at 4°C/min (held for 20 min). The injection temperature was 310°C and the instrument was run in splitless mode with helium as the carrier gas.

3.3. Results and discussion

3.3.1. Maturity and depositional environment indicator of biomarker

All samples detected ββ hopane characteristics of low maturity samples. The C_{32} 22S/(22S+22R) hopane ratio, an indicator of maturity, ranged from 0.13 to 0.39 for OMZ samples and from 0.07 to 0.32 for CNFF samples. The ββ hopane ratios (ββ/(ββ+αβ+βα) C_{30} hopane) were 0.17-0.26 and 0.18-0.48, respectively. Both were very low maturity, approximately 0.4% Ro when converted to vitrinite

reflectance.

   The pristane (Pr)/phytane (Ph) ratio is commonly used as a redox indicator. It is known that phytol, formed from chlorophyll, undergoes oxidation and decarboxylation to become pristane   under oxidative conditions and becomes phytane by reduction and dehydration reactions under anoxic conditions by diagenetic processes (Didyk et al. 1978). While excessive input of terrestrial organic matter also increases Pr/Ph values (Powell, 1988). In this study, following Waseda and Nishita (1998) and Sawada (2006), we estimated the depositional environment by plotting the values of the $C_{27}/(C_{27}+C_{29})$ regular sterane ratio and Pr/Ph ratio, which is used as an indicator of terrestrial/marine ratio (Fig. 3.2). The results indicate a high contribution of terrigenous organic matter at both sites, except for some of the OMZ samples. These results are also consistent with previous studies (e.g., Hasegawa, 2001; Fernando et al., 2011) that have found a high contribution from terrestrial source sediments.

   3.3.2. Reconstruction of paleovegetation based on biomarker analysis

   In this study, two vegetation indices were used to reconstruct the vegetation changes of terrestrial higher plants.

   The first, ar-AGI (Nakamura et al., 2010), indicates the ratio of aromatic triterpenoids (ar-TTs) of angiosperm origin to aromatic diterpenoids (ar-DTs) of gymnosperm origin and is an indicator of the angiosperm/ gymnosperm ratio (Fig.3.3). The second, HPP (Higher Plant Parameter) (van Aarssen et al., 2000) is the ratio of Retene, which is mainly derived from conifers, to Cadalene, which is a common present in higher plants, and is an indicator of the expansion of coniferous vegetation.

   In the OMZ, the ar-AGI values were high in the middle of the 1st build-up and decreased sharply at the end; in the Trough, they decreased temporarily in the middle but increased gradually; in the 2nd build-up, they decreased temporarily in the early phase; in the Plateau, maintained high values, and returned to the same value as before OAE in the Recovery. The HPP values in the OMZ varied as follows: in the 1st build-up, decreasing in the middle and rapidly increasing in the end: gradually decreasing in the Trough phase; in the 2nd build-up, rapidly increasing in the end; taking a low value in the Plateau phase; and stabilizing at a slightly higher value in the Recovery phase. The opposite trend of ar-AGI and HPP from 1st build-up to Trough suggests that there may have been environmental changes (e.g., aridification) at the end of the 1st build-up that resulted in strong environmental disturbances on land that led to the dominance of gymnosperms, especially conifers. van Aarssen et al. (2000) reconstructed HPP variability in Jurassic Australian marine sedimentary rocks. They

proposed HPP as an indicator of global climate change because it is synchronized with other paleoclimate data and global sea-level changes. Subsequently, Hautevelle et al. (2006) reported that retenes are derived primarily from drought-tolerant Pinaceae, and that other paleoclimate data showed increased HPP in response to desiccation. The trend of the rapid increase in HPP at the end of the 2nd build-up was not in sync with the change in ar-AGI. This case may indicate an increase in the relative share of conifers due to the attenuation of terrestrial plants other than seed plants (Bryophytes, Lycophytes, and Pteridophytes). More detailed studies are needed, but in any case, the results suggest that in the OMZ section, some environmental changes at the end of the 1st build-up and 2nd build-up strongly affected the terrestrial vegetation as well.

In the NFCC, ar-AGI values were temporarily high in the middle of the 1st build-up phase, then declined sharply in the last phase; in the Trough, fluctuated violently but increased progressively; in the 2nd build-up, declined in the middle of the phase then increased sharply; in the Plateau, remained high; declined sharply in the middle of the Recovery phase, and stabilized at lower values than before OAE. The HPP values in the NFCC showed an inverse trend to ar-AGI, behaving as follows: in the 1st build-up, decreased in the middle and rapidly increased at the end of the phase: took a low value in the Trough phase; in the 2nd build-up, temporarily increased in the middle; remained low value from the Plateau phase to the first half of the Recovery phase, increasing rapidly in the second half of the Recovery phase, and then stabilizing at a higher value than before OAE.

The variability of these indices in the NFCC was very high, ranging from 0.12-0.74 for ar-AGI and 0.09-0.83 for HPP in the NFCC, compared to 0.44-0.81 and 0.14-0.64 in the OMZ, respectively. The ar-AGI fluctuations themselves were similar at both sites but differed from the OMZ section in that HPP spiked at the end of the 2nd build-up at OMZ. In contrast, at NFCC, it spiked temporarily in the middle of the 2nd build-up and took a high value after the latter half of the Recovery phase. In particular, the NFCC showed a small range of HPP variability throughout most of the OAE period, and the contribution of conifers increased only after the latter part of the Recovery period. This difference between the OMZ and NFCC sections can be attributed to differences in the original vegetation of the hinterland. As shown in Fig. 3.4, the biomes in the Cenomanian-Turonian are thought to have been warm moist forest vegetation in the OMZ section, while the NFCC section was dry savanna vegetation (Sewall et al., 2007; Heimhofer et al., 2018). This may suggest that the OMZ was a transition of dominant forest species, whereas the NFCC shows the expansion and contraction of conifers in savanna vegetation. Few studies have reconstructed terrestrial vegetation during OAE2. However, Heimhofer et al. (2018) conducted palynomorph and biomarker analyses (TEX_{86}) in the

OAE2 section of the Southern Provençal Basin, France. They found that coniferous vegetation may have expanded due to exceptional warming and wetting caused by OAE2 with a period of temporary interruption due to the expansion of the dominant angiosperm savanna-type vegetation rich in angiosperms caused by a cold event (Plenus Cold Event) during the Trough period. In the NFCC section, the savanna vegetation, probably dominated by non-woody angiosperms, was temporarily dominated by coniferous vegetation in the 1st and 2nd build-ups, and the impact of the exceptional warming caused by the OAE on the terrestrial ecosystem may have promoted a permanent expansion of coniferous vegetation afterward. No major vegetation transition was observed in the OMZ section before and after OAE2, while in the NFCC section, suggesting that a significant vegetation transition with conifer expansion may have occurred after OAE2 by biomarker analysis in this study.

3.3.3. Examination of fungal indices and reconstruction of fungal flora

A prominent perylene peak was detected in the aromatic fraction of samples from both sites (Fig. 3.5). Perylene has been reported to be a biomarker derived from wood-degrading fungi and mycorrhizae (Jiang et al., 2000; Grice et al., 2009; Itoh et al., 2012; Marynowski et al., 2013, 2015; Hanke et al., 2019). In this study, the following indices were used to reconstruct the variation in the contribution of these fungi to terrestrial ecosystems: (1) the perylene/(perylene+pyrene) index, which uses the ratio of perylene to pyrene, a PAH (polycyclic aromatic hydrocarbon) of which perylene is also a class. (2) perylene/(perylene+phenathrene) using the ratio of perylene to phenanthrene, a PAHs (polycyclic aromatic hydrocarbon), and (3) perylene/(perylene+ar-DTs+ar-TTs) using the ratio of perylene to ar-DTs and ar-TTs of higher plant origin to indicate the relative contribution of fungi to higher plants. In the OMZ section, these indicators remained permanently high, and temporarily low in the 1st and 2nd build-up. Notably, these indicators also varied considerably during the period when significant changes in terrestrial vegetation occurred. These all showed similar behavior, suggesting that the fungal activity itself declined during the 1st build-up and especially the 2nd build-up period, rather than relative changes due to the decline of terrestrial vegetation.

In the NFCC section, there was a marked decrease in the middle of the Recovery period in these indicators. This timing coincides with the time between the low value of ar-AGI and the increase in the value of HPP. This may indicate that the plants themselves associated with fungi, such as wood-degrading fungi and ectomycorrhizae, the origin organisms of perylene, have declined, and the contribution of the fungi themselves has also declined. The variation of perylene/(perylene+ar-DTs+ar-TTs) differs from the other two indicators, remaining slightly lower than its value before the

Plateau period even after the conifer expansion and showing a behavior similar to that of ar-AGI. This suggests that the fungi may have been strongly associated with plants that thrived in the pre-Recovery vegetation, or they may have become less active in the new environment with expanded coniferous vegetation. In the NFCC, the decrease in the Recovery phase of these indices was remarkable, but the two indices, which are the ratio of perylene to PAHs, showed a slight decreasing trend from the end of the 1st build-up phase to the Trough phase as well. A strong cold event (Plenus Cold Event; PCE) is known to have occurred in the Tethys Sea, Paleo-Atlantic, and Western Interior Seaway during this period (O'Conner et al., 2019). Although there are no direct reconstructions of this cold event in the Pacific, the temporary decrease in pCO2 associated with the PCE has been recorded in variations in δ^{13}C values at Pacific sites (Nemoto and Hasegawa, 2011; Du Vivier et al., 2015), suggesting that the cold event may have been a global event.The decrease in indicators during the Trough period may indicate a decline in fungal activity due to the effects of this cold event.

3.3.4. Examination of lichen indices and reconstruction of lichen behavior

Several dibenzofuran series were detected in the aromatic fractions of samples from both sites. Each compound was identified as dibenzofuran (DBF), methyl dibenzofuran (4-/2-/3-/1-MDBF), and dimethyldibenzofuran/ethyl dibenzofuran (4-EDBF/4,6-/2,4 -/3,6-/2,7-/1,4- and 1,6-DMDBF) (Fig. 3 Fig. 3.6). The origin of dibenzofurans in sedimentary rocks has been proposed as a terrestrial higher plant origin (Born et al., 1989; Hatcher and Clifford, 1997; Sephton et al., 2005; Fenton et al., 2007; Wang and Visscher, 2007; Biswas et al., 2020), while others have suggested a lichen origin (Radke et al., 2000; Watson et al., 2005; Sawada et al., 2012).

The theory of terrestrial higher plant origin has been proposed based on the synthesis of dibenzofuran in laboratory maturation experiments of polysaccharides and biphenyls produced by higher plants.

Watanabe (2000) showed that dibenzofurans are formed from lignin, cellulose and phenol produced by higher plants through simulated maturation experiments. In contrast, alkyl dibenzofurans were not found to be produced in this study. Radke et al. (2000) used multivariate analysis to estimate the origin of methyl dibenzofurans in sedimentary rocks. Their results suggest that 1-MDBF differs in origin from other dibenzofurans (dibenzofurans, 2-/3-/4-MDBF) in moderately mature samples. They argue that lichen dibenzofurans may be the origin of 1-MDBF because lichen-produced dibenzofurans are the only alkyl dibenzofurans reported to be produced under other natural conditions that have an alkyl chain specifically at position 1 (position 9). In

the samples of our study, the degree of maturity is low, and the phenomenon of increased relative amounts of 1-MDBF isomers (Radke et al., 2000), which is known to occur in the high maturity zone (Ro>1.0 %), is not considered to have occurred. Based on the above, 1-MDBF was examined as an indicator as a lichen biomarker in this study.

The isomer ratio (1-MDBF/(1- +2- +3- +4-MDBF)) index showed a slightly increasing trend toward the top in the samples from both sites, but there were no significant fluctuations in increase or decrease. On the other hand, the 1-MDBF/(1-MDBF+perylene) ratio showed a marked increase during the period when the fungal contribution indicator showed a decrease. The 1-MDBF/(1-MDBF/ar-DTs+ar-TTs) ratio also increased during the same period as the perylene indicator. This suggests that while no expansion or contraction of lichen vegetation occurred, the relative contribution of lichens to the terrestrial ecosystem increased relative to the attenuation of fungi and higher plants.

The increase in the 1-MDBF/(1-MDBF+ar-DTs+ar-TTs) ratio in the NFCC samples during the Trough may indicate that lichens have shown tolerance to certain environmental stresses, such as cold weather, in response to the attenuation of higher plant vegetation itself, which was not captured by ar-AGI or HPP. While several previous studies using lichen fossils have suggested that lichens thrived in warm or wet vegetation (e.g., Wang et al., 2010; Kaasakainen et al., 2017), the present study suggests that lichens in the Mid-Cretaceous were as resistant to environmental stresses as modern lichens.

3.4. Conclusions

Sediments from the North American (NFCC) and eastern margin of Asia (OMZ) sites, which record the mid-Cretaceous environmental disturbance event OAE2, were used to reconstruct vegetation change and fungal and lichen behavior based on biomarker analysis. We found that there were significant vegetation changes during OAE2 at both sites, and that coniferous vegetation in the OMZ temporarily expanded during the 1st and 2nd build-up, suggesting that the contribution of fungi to the vegetation change was also greatly affected by the vegetation change. On the other hand, the lichen index using 1-MDBF indicated that the vegetation increased relative to higher plants and fungi during environmental disturbance and may have been highly tolerant to environmental stresses. The NFCC site showed similar vegetation changes in the 1st and 2nd build-up. On the other hand, unlike the OMZ, vegetation at this site changed significantly before and after the OAE, indicating that coniferous vegetation expanded. This significant vegetation

transition period was detrimental to fungi, which showed significant attenuation, but had little effect on lichens. Paleoecological reconstructions of lichens in geological time have so far been based on limited lichen fossils. In this study, we were able to reconstruct differences in environmental responses from other terrestrial ecosystems at high resolution by using biomarkers.

Fig.3.1. Index map showing location of Tomamae area of Hokkaido and Ono Quadrangle of Shasta County and schematic geological map of study area, respectively.

44
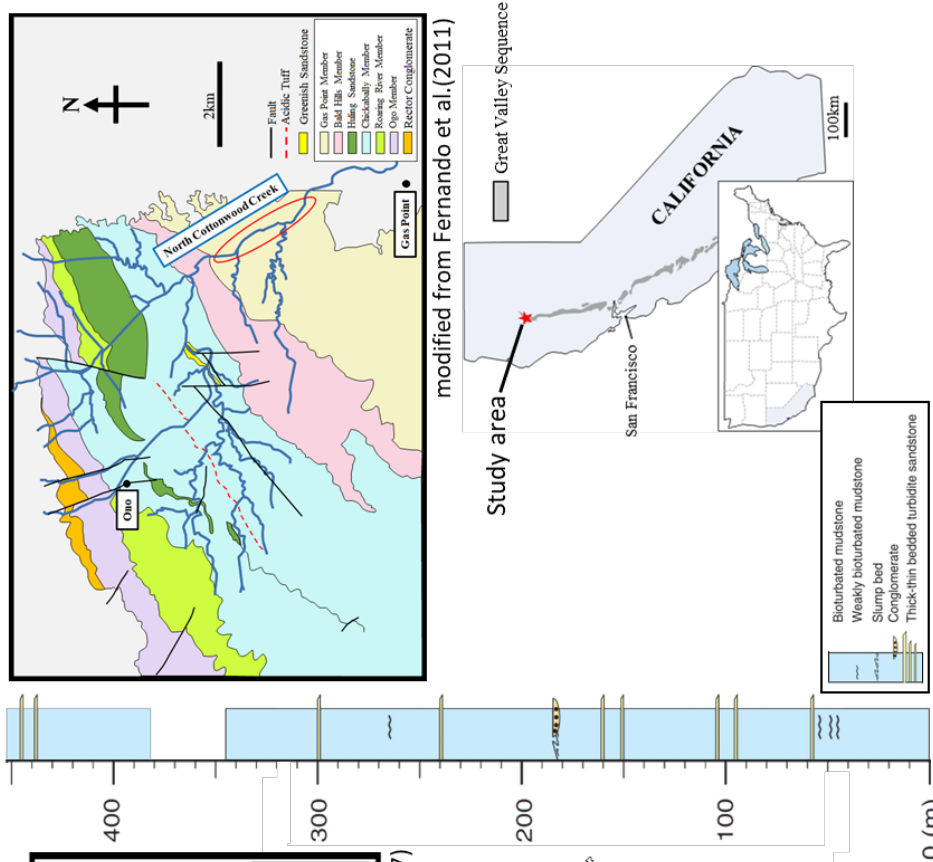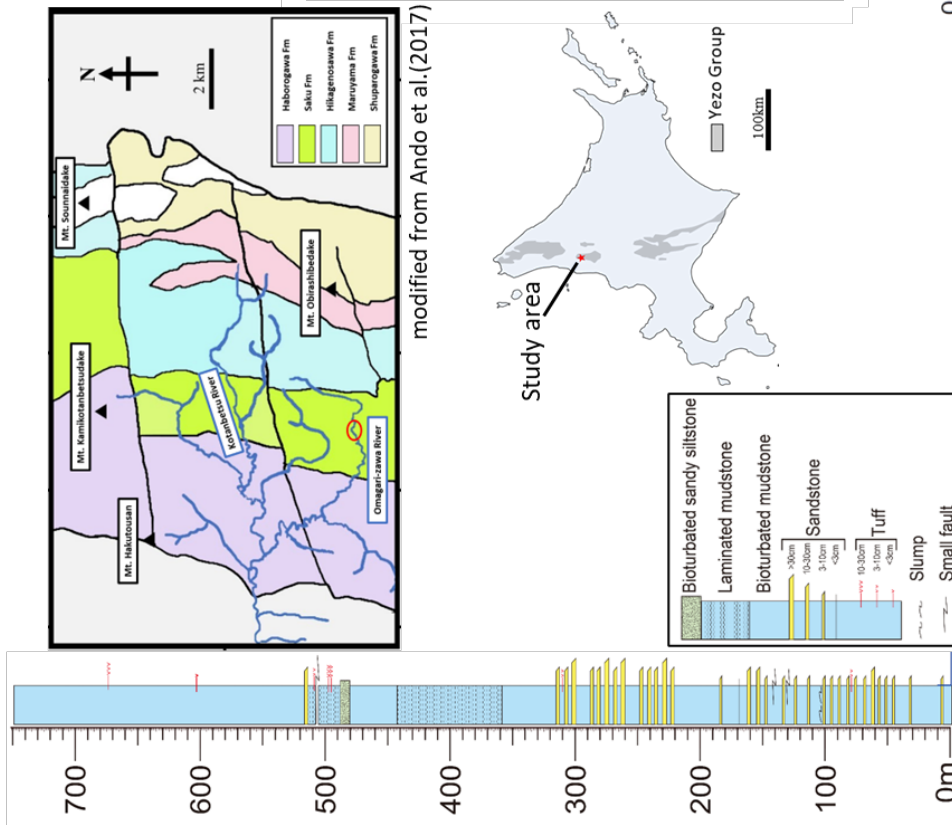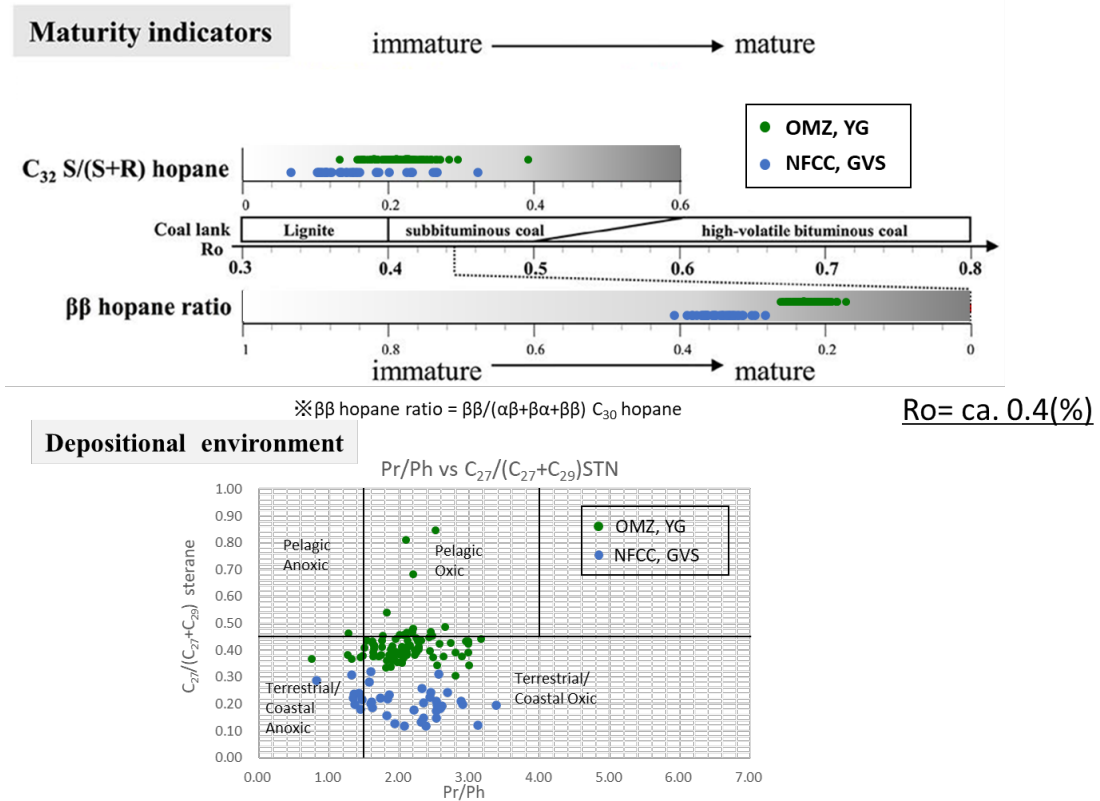
Fig.3.2.(Upper) Maturity indicator and, (below) Depositional environment calculated by biomarker from each sample (modified from Ando et al., 2017).
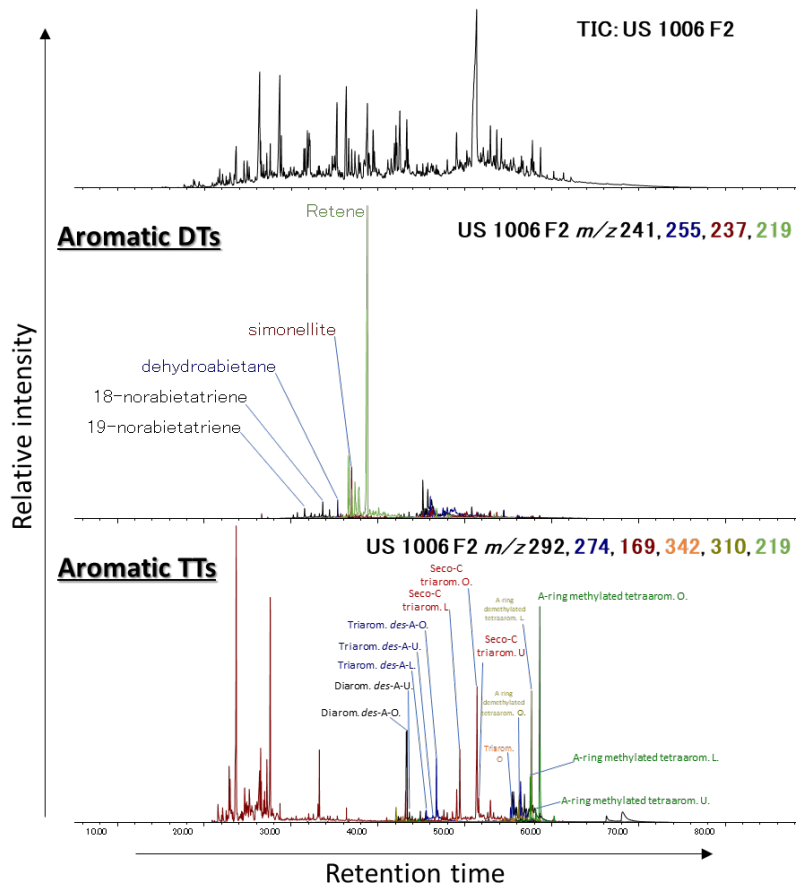
Fig.3.3. Diterpenoids and triterpenoids detected in the samples
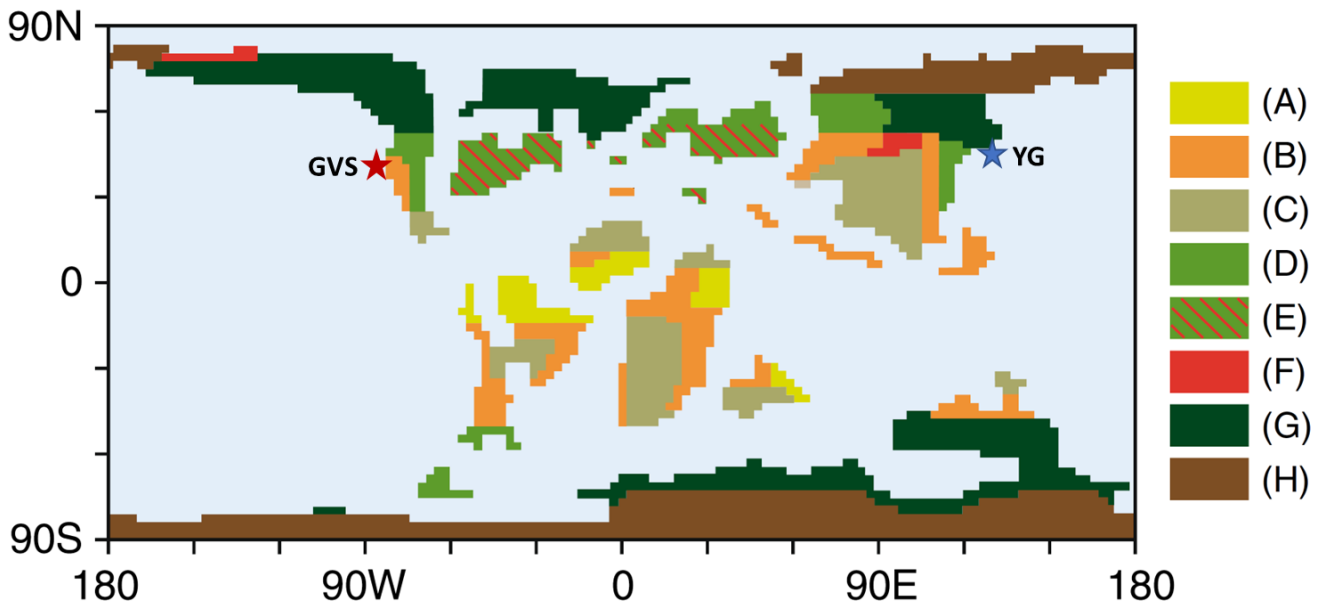
Fig.3.4. Palaeogeographic map illustrating Cenomanian–Turonian biome distribution.
(A)tropical moist, open canopy mixed forest with shrub understory; (B) savanna-type dry low understory with sparse trees; (C) deciduous dry/ warm shrubland; (D) mid-latitude evergreen closed canopy conifer forest; (E) Normapolles province; (F) evergreen wet/cool shrubland; (G) high-latitude moist, open canopy forest with shrub understory; (H) boreal closed canopy conifer forest. (modified from Heimhofer et al., 2018)

4 6
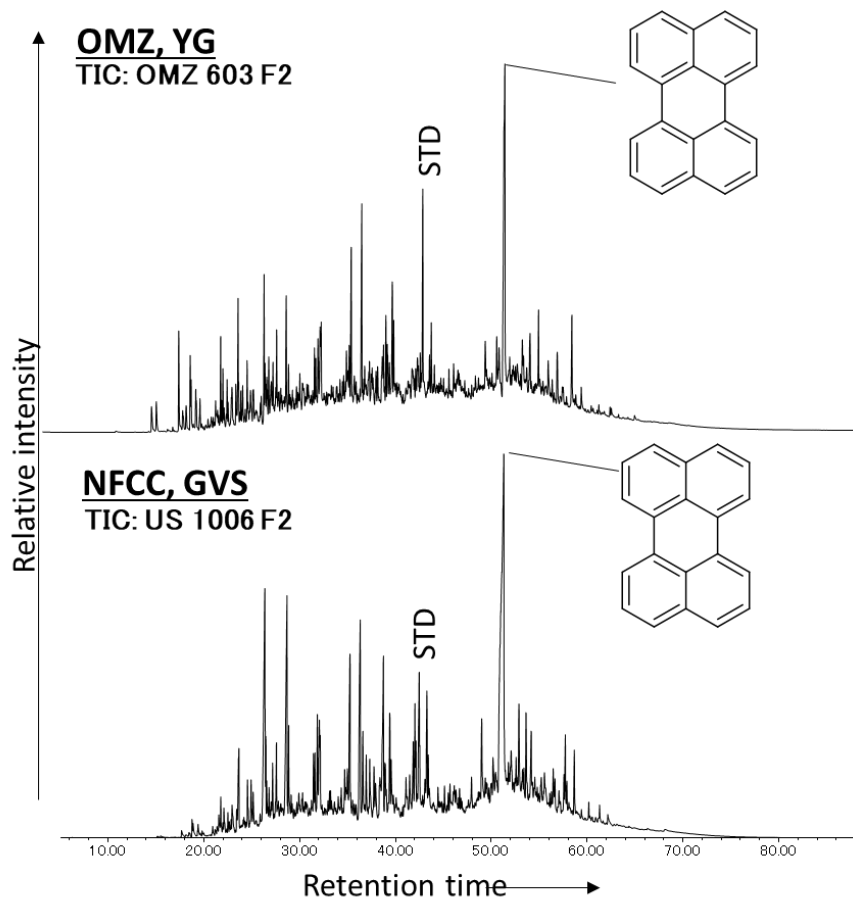
Fig.3.5.TIC of aromatic fraction
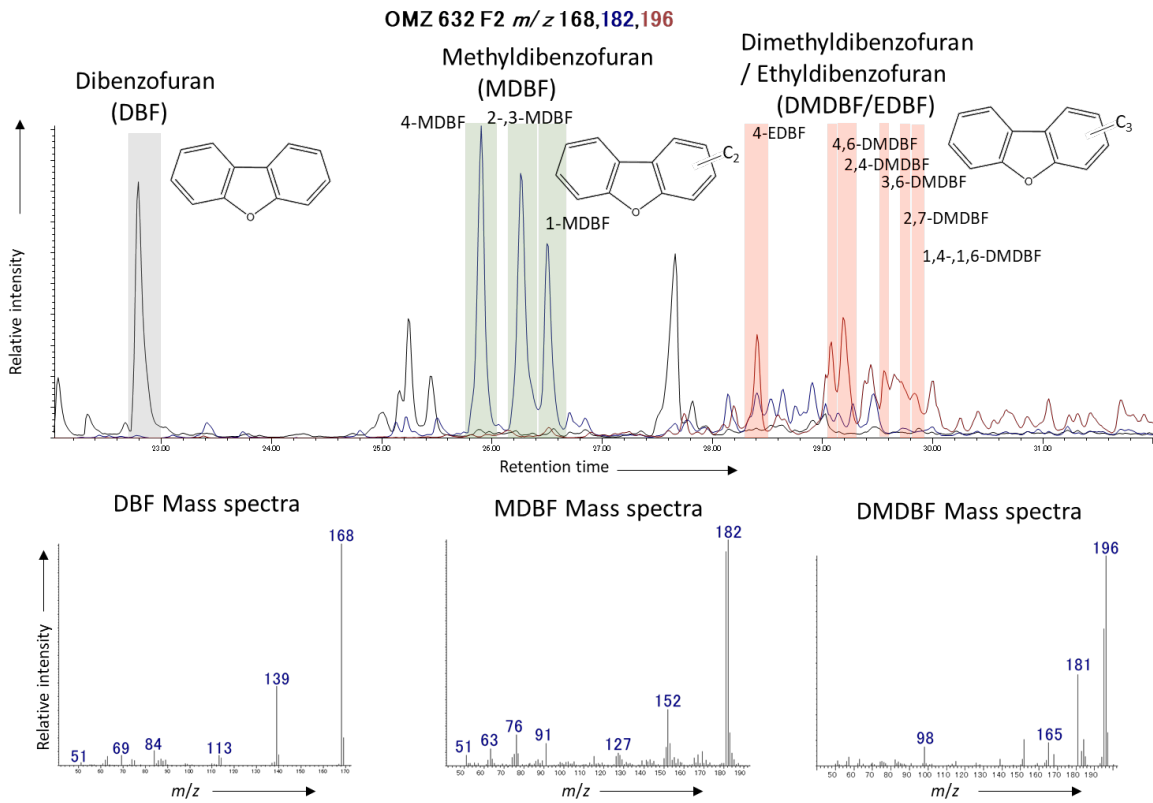
Fig.3.6. Dibenzofuran series detected in the samples.
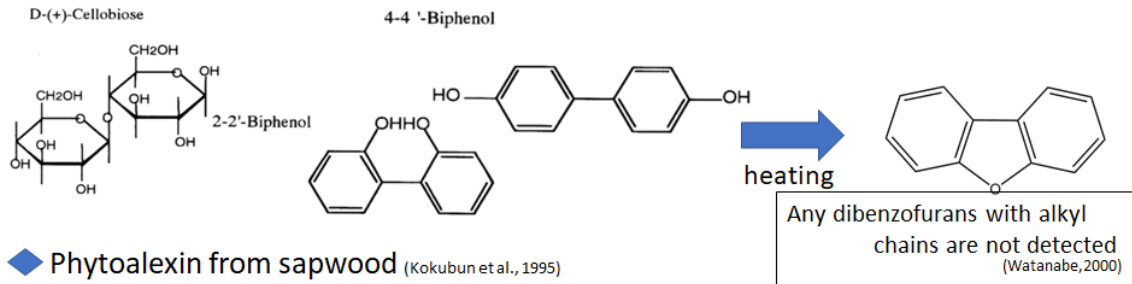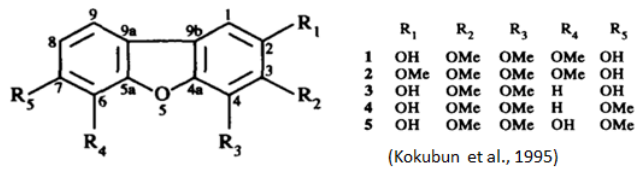
Fig.3.7. Origin of DBF in sedimentary rocks mentioned in previous studies

Fig.3.8. List of $\delta^{13}C$ variation, each phase of OAE2 and behavior of each indicator in OMZ

Fig.3.9. List of $\delta^{13}C$ variation, each phase of OAE2 and behavior of each indicator in NFCC

4 9

Table 3.1. List of indicator values used in this chapter in the OMZ section

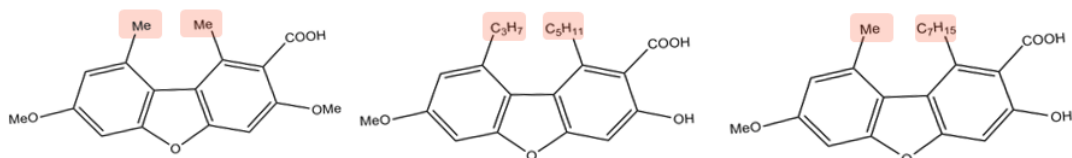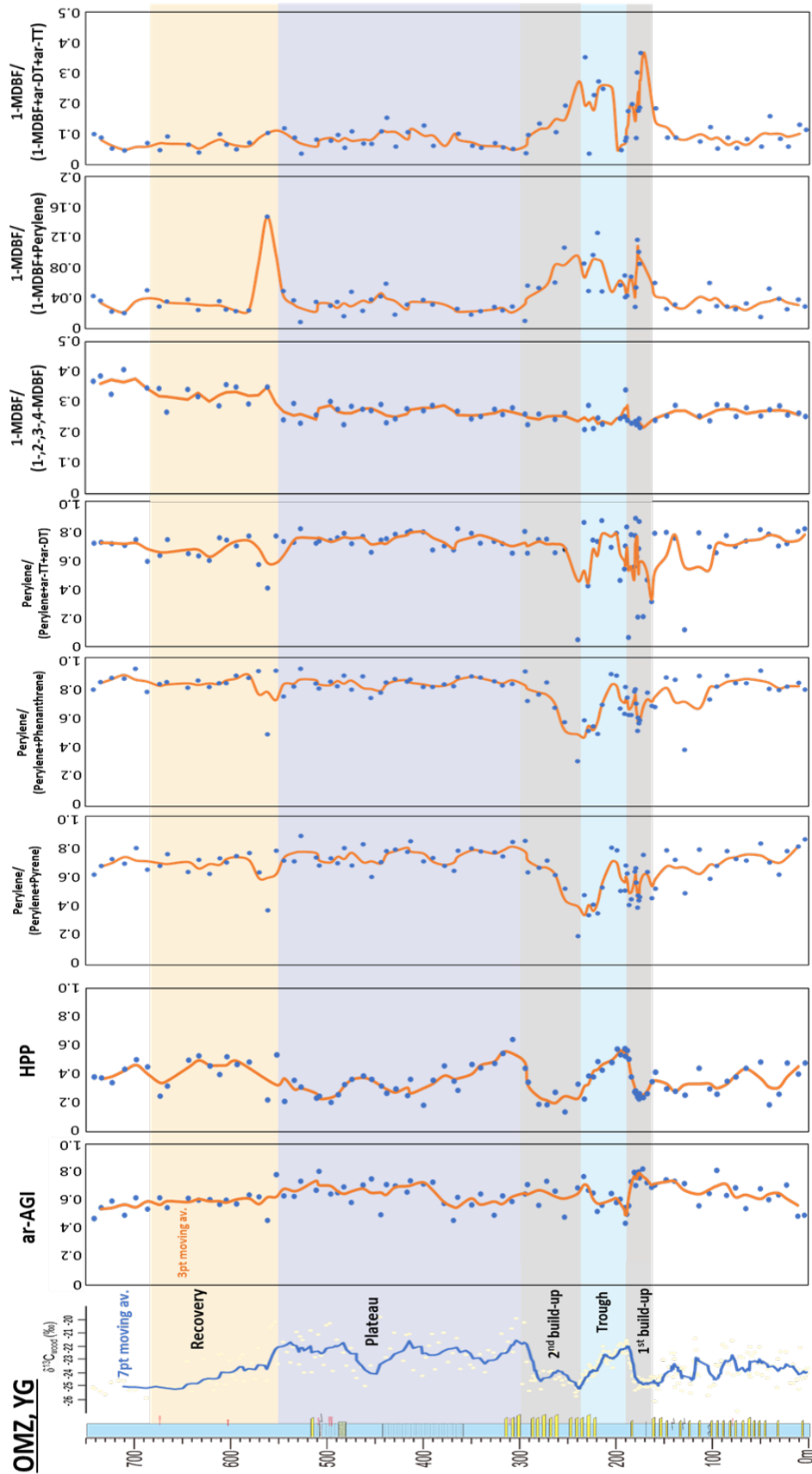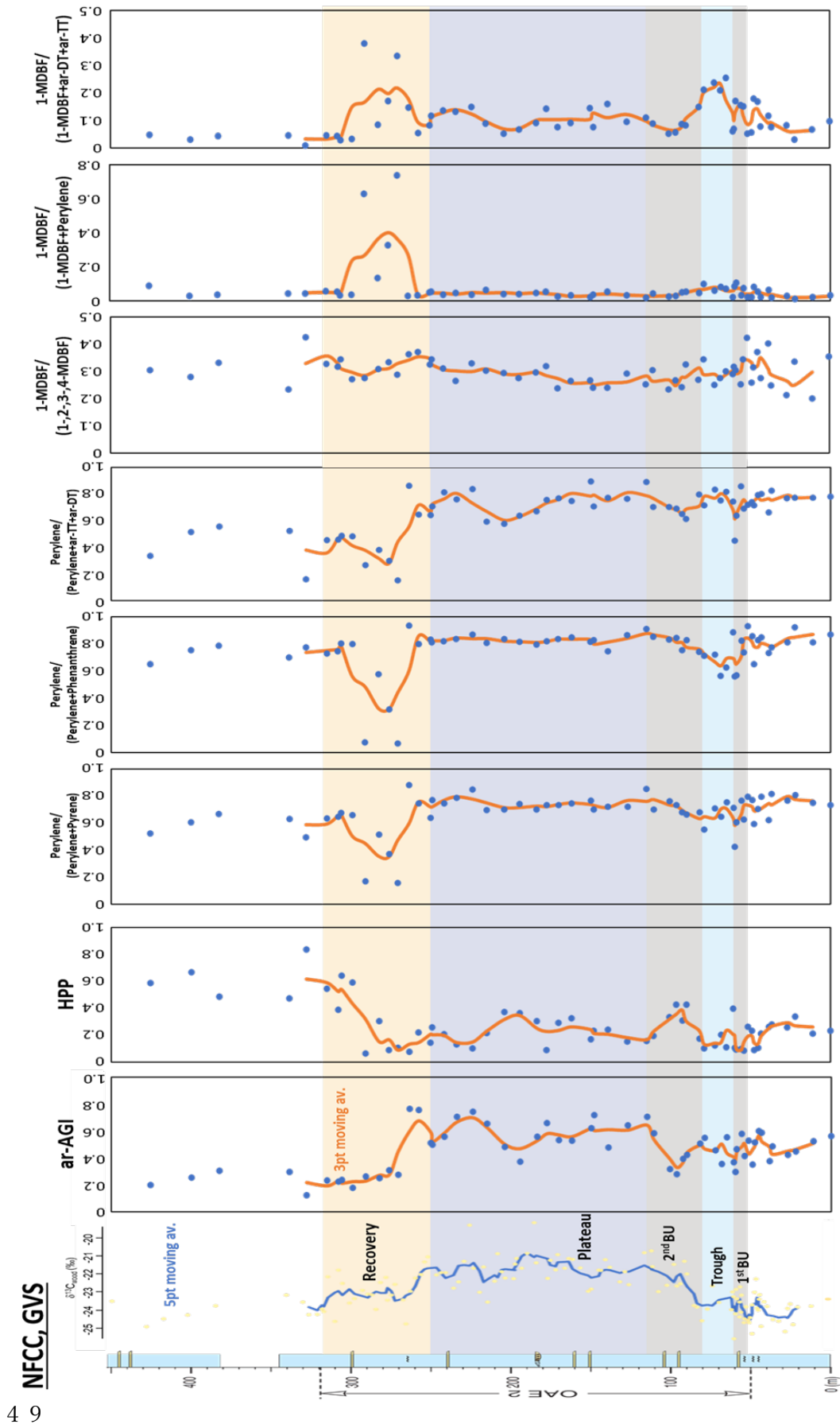| Sampl No.	depth(m)	Phase	S/(S+R) C₃₂ hopane	ββhopan ratio	C₂₇/(C₂₇+C₂₉)STN	Pr/Ph	ar-AGI	HPP	Perylene/(Perylene+Pyrene)	Perylene/(Perylene+Phenanthrene)	Perylene/(Perylene+ar-DT+ar-TT)	1-/(1-,2-,3-,4-MDBF) ration	1-MDBF/(1-MDBF+Perylene)	1-MDBF/(1-MDBF+ar-DT+ar-TT)
OMZ275	741.5	Post-OAE	0.39	0.19	0.41	1.51	0.47	0.38	0.61	0.78	0.71	0.37	0.04	0.10
OMZ273	734.1	Post-OAE	0.21	0.21	0.42	2.15	0.55	0.38	0.67	0.83	0.72	0.39	0.04	0.09
OMZ271	722.8	Post-OAE	0.20	0.22	0.44	2.12	0.59	0.34	0.71	0.86	0.71	0.33	0.02	0.05
OMZ269	709.7	Post-OAE	0.22	0.23	0.34	1.88	0.49	0.44	0.68	0.86	0.70	0.41	0.02	0.05
OMZ267	697.9	Post-OAE	0.21	0.22	0.37	0.75	0.62	0.50	0.78	0.92	0.74	NA	NA	NA
OMZ266	686.0	Post-OAE	0.20	0.22	0.43	2.27	0.54	0.45	0.64	0.77	0.59	0.35	0.05	0.07
OMZ264	673.1	Recovery	0.18	0.22	0.41	2.05	0.61	0.25	0.66	0.82	0.63	0.35	0.03	0.05
OMZ263	665.3	Recovery	0.18	0.20	0.39	2.25	0.55	0.32	0.74	0.83	0.74	0.27	0.04	0.09
OMZ689	643.6	Recovery	0.23	0.20	0.39	2.01	0.62	0.50	0.63	0.80	0.64	0.34	0.04	0.06
OMZ259	632.8	Recovery	0.22	0.19	0.40	2.27	0.60	0.53	0.70	0.84	0.62	0.32	0.02	0.04
OMZ258	621.6	Recovery	0.23	0.18	0.44	1.54	0.59	0.46	0.61	0.80	0.59	NA	NA	NA
OMZ687	611.1	Recovery	0.22	0.21	0.41	2.28	0.57	0.40	0.72	0.83	0.75	0.29	0.04	0.10
OMZ255	603.9	Recovery	0.23	0.19	0.40	1.88	0.60	0.52	0.69	0.83	0.73	0.36	0.02	0.06
OMZ254	593.7	Recovery	0.23	0.20	0.36	1.97	0.57	0.47	0.73	0.88	0.69	0.35	0.02	0.05
OMZ680	580.4	Recovery	0.24	0.19	0.44	1.95	0.64	0.48	0.75	0.86	0.76	0.30	0.02	0.07
OMZ678	570.2	Recovery	0.27	0.21	0.36	NA	0.62	NA	0.62	0.91	0.56	NA	NA	NA
OMZ251	561.3	Recovery	0.27	0.17	0.43	1.62	0.46	0.22	0.37	0.48	0.40	0.35	0.15	0.10
OMZ674	552.2	Recovery	0.26	0.21	0.35	NA	0.78	0.54	0.77	0.91	0.76	NA	NA	NA
OMZ673	544.4	Plateau	0.25	0.22	0.39	2.10	0.62	0.21	0.70	0.74	0.72	0.24	0.05	0.12
OMZ672	533.8	Plateau	0.23	0.21	0.38	2.11	0.62	0.36	0.69	0.80	0.72	0.30	0.04	0.09
OMZ670	526.9	Plateau	0.25	0.24	0.46	1.27	0.74	0.31	0.87	0.92	0.81	0.23	0.01	0.04
OMZ667	510.8	Plateau	0.22	0.20	0.44	2.25	0.67	0.24	0.72	0.82	0.71	0.26	0.04	0.08
OMZ666	507.8	Plateau	0.26	0.22	0.37	1.93	0.79	0.25	0.67	0.79	0.73	NA	NA	NA
OMZ663	495.8	Plateau	0.22	0.24	0.46	2.19	0.59	0.20	0.72	0.84	0.73	0.30	0.03	0.08
OMZ662	488.6	Plateau	0.23	0.24	0.49	2.66	0.64	0.26	0.68	0.81	0.75	0.28	0.03	0.10
OMZ660	481.8	Plateau	0.26	0.23	0.35	2.04	0.69	0.33	0.78	0.88	0.78	0.23	0.02	0.05
OMZ659	474.0	Plateau	0.26	0.19	0.37	2.06	0.58	0.37	0.67	0.78	0.71	0.29	0.05	0.11
OMZ657	462.3	Plateau	0.21	0.24	0.43	2.73	0.70	0.39	0.81	0.87	0.76	0.28	0.02	0.07
OMZ656	453.7	Plateau	0.21	0.25	0.38	1.48	0.75	0.37	0.59	0.73	0.65	0.27	0.04	0.07
OMZ655	443.6	Plateau	0.25	0.21	0.42	1.64	0.50	0.32	0.69	0.76	0.73	0.29	0.04	0.11
OMZ654	438.0	Plateau	0.22	0.26	0.39	1.63	0.71	0.27	0.76	0.83	0.74	0.23	0.06	0.15
OMZ653	428.7	Plateau	0.20	0.25	0.39	1.99	0.68	0.30	0.77	0.85	0.77	0.25	0.02	0.06
OMZ652	416.4	Plateau	0.23	0.23	0.45	2.43	0.66	0.25	0.76	0.84	0.79	0.28	0.03	0.11
OMZ651	413.0	Plateau	0.28	0.19	0.39	1.95	0.73	0.37	0.83	0.85	0.79	NA	NA	NA
OMZ649	399.5	Plateau	0.24	0.25	0.43	1.62	0.71	0.18	0.70	0.80	0.79	0.27	0.04	0.13
OMZ647	389.9	Plateau	0.21	0.25	0.36	2.02	0.71	0.36	0.72	0.80	0.67	0.29	0.03	0.06
OMZ645	377.8	Plateau	0.23	0.22	0.38	1.71	0.58	0.46	0.67	0.82	0.69	NA	NA	NA
OMZ644	368.0	Plateau	0.18	0.23	0.47	2.11	0.45	0.35	0.63	0.81	0.66	NA	NA	NA
OMZ643	364.0	Plateau	0.16	0.23	0.44	3.17	0.61	0.29	0.77	0.87	0.81	0.27	0.03	0.10
OMZ641	349.7	Plateau	0.21	0.24	0.81	2.09	0.57	0.47	0.78	0.87	0.78	0.25	0.02	0.06
OMZ640	340.1	Plateau	0.22	0.22	0.36	1.90	0.64	0.44	0.76	0.86	0.71	0.25	0.02	0.05
OMZ638	325.9	Plateau	0.22	0.19	0.36	1.82	0.50	0.47	0.76	0.84	0.72	0.28	0.03	0.07
OMZ637	317.3	Plateau	0.21	0.20	0.39	1.95	0.64	0.55	0.73	0.81	0.71	0.26	0.02	0.06
OMZ635	307.2	Plateau	0.21	0.21	0.38	1.63	0.59	0.64	0.83	0.82	0.64	0.28	0.03	0.05
OMZ633	294.0	2nd-BU	0.23	0.19	0.42	1.64	0.65	0.44	0.83	0.90	0.79	0.26	0.01	0.04
OMZ632	291.5	2nd-BU	0.22	0.20	0.85	2.52	0.69	0.34	0.62	0.71	0.64	0.23	0.06	0.10
OMZ006	279.8	2nd-BU	0.21	0.19	0.54	1.82	0.55	0.19	0.65	0.75	0.73	0.26	0.05	0.13
OMZ009	271.3	2nd-BU	0.23	0.22	0.44	1.76	0.71	0.19	0.70	0.83	0.74	NA	NA	NA
OMZ012	262.9	2nd-BU	0.16	0.21	0.43	2.98	0.65	0.27	0.60	0.66	0.65	0.25	0.06	0.11
OMZ016	253.0	2nd-BU	0.21	0.23	0.45	1.77	0.49	0.14	0.51	0.57	0.67	0.27	0.11	0.19
OM053	239.3	Trough	0.21	0.24	0.41	2.03	0.69	0.33	0.19	0.30	0.05	NA	NA	NA
OM044	232.7	Trough	0.21	0.22	0.38	2.06	0.77	0.23	0.47	0.58	0.85	0.21	0.09	0.35
OM039	228.3	Trough	0.20	0.23	0.40	2.25	0.67	0.39	0.33	0.51	0.42	0.29	0.05	0.04
OM033	223.4	Trough	0.16	0.23	0.38	2.48	0.64	0.38	0.40	0.54	0.73	0.22	0.10	0.23
OM026	218.8	Trough	0.24	0.22	0.41	2.04	0.52	0.49	0.35	0.49	0.72	0.25	0.13	0.27
OM019	214.1	Trough	0.22	0.22	0.42	2.15	0.57	0.43	0.52	0.68	0.87	0.23	0.05	0.25
OM001	204.5	Trough	0.20	0.20	0.47	2.45	0.62	0.48	0.79	0.89	0.68	NA	NA	NA
OM006	199.0	Trough	0.18	0.22	0.39	2.11	0.57	0.58	0.77	0.88	0.78	NA	NA	NA
OM010	195.2	Trough	0.21	0.21	0.38	1.75	0.61	0.54	0.50	0.66	0.45	0.25	0.06	0.05
OM015	190.6	Trough	0.16	0.20	0.34	1.81	0.55	0.58	0.50	0.62	0.53	0.25	0.07	0.09
OM016	189.8	Trough	0.25	0.18	0.48	2.18	0.44	0.52	0.67	0.80	0.69	0.34	0.04	0.09
OM018	188.1	Trough	0.24	0.22	0.38	1.85	0.50	0.56	0.61	0.73	0.82	0.24	0.04	0.17
OM056	186.6	1st-BU	0.20	0.20	0.42	1.90	0.56	0.51	0.40	0.61	0.06	NA	NA	NA
OM060	183.9	1st-BU	0.18	0.25	0.40	2.44	0.73	0.38	0.44	0.61	0.77	0.23	0.07	0.20
OM064	180.6	1st-BU	0.19	0.24	0.34	2.54	0.78	0.28	0.63	0.77	0.55	NA	NA	NA
OM066	179.6	1st-BU	0.16	0.24	0.39	1.89	0.77	0.29	0.65	0.79	0.76	0.24	0.03	0.09
OM067	178.9	1st-BU	0.18	0.22	0.38	2.22	0.71	0.26	0.55	0.69	0.88	0.23	0.05	0.30
OM068	177.5	1st-BU	0.16	0.24	0.34	2.99	0.77	0.24	0.39	0.51	0.62	0.23	0.12	0.18
OM069	176.9	1st-BU	0.17	0.25	0.39	2.80	0.76	0.25	0.47	0.60	0.20	NA	NA	NA
OM070	176.0	1st-BU	0.13	0.22	0.38	2.63	0.79	0.23	0.43	0.56	0.67	0.25	0.10	0.19
OM071	175.2	1st-BU	0.21	0.23	0.41	1.64	0.75	0.26	0.46	0.58	0.86	0.22	0.08	0.37
OM076	171.4	1st-BU	0.17	0.22	0.31	2.80	0.81	0.24	0.74	NA	0.20	NA	NA	NA
OM080	167.2	1st-BU	0.20	0.25	0.41	2.28	0.72	0.27	0.62	0.76	0.46	NA	NA	NA
OM085	162.5	1st-BU	0.20	0.25	0.40	2.22	0.69	0.35	0.45	0.67	0.31	NA	NA	NA
OM090	159.1	1st-BU	0.19	0.24	0.41	1.75	0.70	0.42	0.51	0.67	0.78	0.24	0.06	0.18
OMZ508	147.4	Pre-excursion	0.19	0.22	0.38	2.90	0.74	0.30	0.77	0.87	0.79	0.26	0.03	0.09
OMZ512	138.4	Pre-excursion	0.21	0.22	0.39	2.99	0.71	0.28	0.71	0.85	0.75	0.29	0.03	0.09
OMZ517	128.3	Pre-excursion	0.21	0.22	0.37	1.44	0.72	0.26	0.48	0.38	0.12	NA	NA	NA
OMZ525	113.4	Pre-excursion	0.23	0.21	0.44	2.32	0.56	0.44	0.77	0.88	0.78	0.26	0.02	0.08
OMZ526	102.5	Pre-excursion	0.19	0.23	0.43	2.95	0.65	0.30	0.58	0.72	0.69	0.24	0.06	0.12
OMZ531	95.2	Pre-excursion	0.18	0.24	0.42	2.98	0.79	0.26	0.67	0.80	0.65	0.29	0.03	0.05
OMZ603	84.6	pre-OAE	0.19	0.24	0.45	2.47	0.62	0.35	0.76	0.88	0.76	0.29	0.03	0.09
OMZ606	75.5	pre-OAE	0.24	0.22	0.68	2.20	0.67	0.38	0.71	0.83	0.69	0.25	0.03	0.05
OMZ610	64.6	pre-OAE	0.21	0.21	0.46	2.01	0.54	0.44	0.70	0.83	0.73	0.28	0.03	0.08
OMZ614	49.7	pre-OAE	0.17	0.21	0.42	2.57	0.67	0.48	0.82	0.91	0.80	0.26	0.01	0.06
OMZ616	40.8	pre-OAE	0.23	0.22	0.48	2.20	0.61	0.19	0.69	0.79	0.77	0.28	0.05	0.16
OMZ618	30.5	pre-OAE	0.25	0.22	0.42	2.13	0.64	0.26	0.61	0.78	0.69	0.29	0.04	0.06
OMZ621	22.2	pre-OAE	0.30	0.20	0.37	1.32	0.70	0.48	0.77	0.80	0.71	0.26	0.03	0.06
OMZ625	10.4	pre-OAE	0.25	0.18	0.46	2.06	0.49	0.40	0.80	0.83	0.79	0.27	0.04	0.13
OMZ627	3.6	pre-OAE	0.21	0.20	0.38	1.27	0.50	0.48	0.84	0.78	0.81	0.25	0.03	0.00

Table 3.2. List of indicator values used in this chapter in the NFCC section

Sampl No.	depth(m)	Phase	S/(S+R) C$_{32}$ hopane	ββhopan ratio	C$_{27}$/(C$_{27}$+C$_{29}$)STN	Pr/Ph	ar-AGI	HPP	Perylene/(Perylene+Pyrene)	Perylene/(Perylene+Phenanthrene)	Perylene/(Perylene+ar-DT+ar-TT)	1-/(1-,2-,3-,4-MDBF) ration	1-MDBF/(1-MDBF+Perylene)	1-MDBF/(1-MDBF+ar-DT+ar-TT)
US096	425.5	post-OAE	0.32	0.38	0.19	1.62	0.20	0.59	0.52	0.65	0.34	0.30	0.09	0.05
US094	400	post-OAE	0.22	0.42	0.21	3.50	0.25	0.67	0.60	0.76	0.51	0.28	0.03	0.03
US093	382.5	post-OAE	0.27	0.37	0.22	1.73	0.31	0.49	0.67	0.79	0.56	0.33	0.03	0.04
US092	338.5	post-OAE	0.27	0.41	0.17	1.24	0.30	0.47	0.63	0.70	0.52	0.23	0.04	0.05
US913	328	post-OAE	0.26	0.34	0.20	1.36	0.12	0.83	0.49	0.78	0.16	0.42	0.04	0.01
US091	315	Recovery	0.24	0.36	0.21	1.68	0.23	0.54	0.63	0.73	0.45	0.33	0.06	0.05
US907	308	Recovery	0.23	0.36	0.20	2.34	0.23	0.39	0.65	0.75	0.46	0.32	0.05	0.04
US906	306	Recovery	0.22	0.41	0.20	2.53	0.23	0.64	0.67	0.80	0.48	0.34	0.03	0.03
US904	299	Recovery	0.22	0.40	0.21	0.72	0.18	0.59	0.66	0.80	0.48	0.27	0.03	0.03
US090	291	Recovery	0.24	0.35	0.33	1.80	0.26	0.07	0.17	0.08	0.27	0.27	0.63	0.38
US603	282.5	Recovery	0.28	0.39	0.21	0.67	0.25	0.30	0.51	0.58	0.38	0.31	0.13	0.08
US605	276.1	Recovery	0.19	0.35	0.31	2.56	0.31	0.09	0.37	0.32	0.30	0.33	0.33	0.17
US608	270.7	Recovery	0.21	0.33	0.31	2.00	0.28	0.11	0.15	0.07	0.15	0.29	0.74	0.33
US611	263.6	Recovery	0.14	0.38	0.17	2.52	0.76	0.07	0.88	0.94	0.86	0.36	0.03	0.15
US615	257.6	Recovery	0.12	0.36	0.19	2.60	0.76	0.22	0.75	0.80	0.64	0.37	0.03	0.05
US619	250.2	Plateau	0.12	0.32	0.11	2.80	0.51	0.14	0.64	0.83	0.64	0.32	0.05	0.08
US620	249.2	Plateau	0.20	0.33	0.20	2.90	0.50	0.26	0.77	0.81	0.71	0.34	0.05	0.12
US622	241.8	Plateau	0.13	0.44	0.20	1.75	0.56	0.21	0.75	0.82	0.81	0.31	0.04	0.14
US624	234	Plateau	0.16	0.35	0.12	2.07	0.70	0.13	0.78	0.84	0.76	0.27	0.05	0.13
US087	224	Plateau	0.10	0.31	0.13	1.94	0.74	0.10	0.85	0.87	0.84	0.33	0.03	0.15
US631	215.1	Plateau	0.13	0.34	0.18	2.58	0.65	0.22	0.70	0.81	0.59	0.30	0.06	0.09
US635	204	Plateau	0.15	0.37	0.12	3.12	0.48	0.37	0.70	0.84	0.57	0.29	0.04	0.05
US086	194.5	Plateau	0.15	0.41	0.23	3.50	0.37	0.36	0.74	0.81	0.64	0.27	0.04	0.07
US642	183.8	Plateau	0.11	0.33	0.18	1.45	0.56	0.30	0.70	0.80	0.67	0.30	0.05	0.09
US647	177.5	Plateau	0.12	0.36	0.13	2.31	0.66	0.09	0.73	0.82	0.75	0.32	0.05	0.14
US650	170.2	Plateau	0.15	0.40	0.20	1.86	0.53	0.29	0.73	0.84	0.77	0.24	0.02	0.08
US652	162	Plateau	0.15	0.32	0.15	2.52	0.53	0.33	0.74	0.85	0.75	0.26	0.03	0.09
US655	150	Plateau	0.11	0.43	0.22	3.67	0.62	0.17	0.77	0.82	0.89	0.27	0.02	0.14
US656	148	Plateau	0.11	0.33	0.18	2.20	0.72	0.23	0.70	0.83	0.70	0.24	0.03	0.08
US658	139.2	Plateau	0.15	0.36	0.21	1.46	0.47	0.24	0.72	0.74	0.77	0.24	0.05	0.16
US661	127	Plateau	0.16	0.34	0.24	2.44	0.64	0.15	0.72	0.86	0.76	0.29	0.03	0.09
US664	115	Plateau	0.12	0.48	0.28	3.45	0.71	0.16	0.85	0.91	0.89	0.25	0.02	0.11
US665	110.7	2nd BU	0.07	0.35	0.26	2.32	0.58	0.19	0.70	0.85	0.70	0.30	0.04	0.09
US667	100.8	2nd BU	0.12	0.34	0.20	1.60	0.32	0.33	0.76	0.83	0.70	0.23	0.02	0.05
US669	96.4	2nd BU	0.16	0.42	0.23	1.82	0.28	0.43	0.73	0.85	0.69	0.27	0.03	0.06
US672	92.7	2nd BU	0.14	0.32	0.16	1.82	0.39	0.31	0.68	0.75	0.65	0.24	0.05	0.09
US673	90.1	2nd BU	0.18	0.33	0.21	2.88	0.42	0.42	0.66	0.83	0.61	0.32	0.05	0.08
US061	82	2nd BU	0.20	0.33	0.36	1.25	0.51	0.17	0.68	0.74	0.79	0.27	0.04	0.15
US676	78.9	Trough	0.18	0.28	0.22	1.34	0.55	0.10	0.55	0.71	0.71	0.34	0.10	0.21
US678	72.3	Trough	0.14	0.40	0.26	0.87	0.46	0.12	0.71	0.72	0.83	0.25	0.06	0.24
US062	68.5	Trough	0.43	0.18	0.54	1.12	0.35	0.20	0.64	0.57	0.75	0.27	0.08	0.21
US679	65	Trough	0.18	0.39	0.30	1.92	0.55	0.11	0.75	0.63	0.82	0.30	0.07	0.25
US680	60.7	Trough	0.13	0.44	0.16	3.02	0.37	0.40	0.71	0.88	0.74	0.29	0.02	0.06
US682	59.9	Trough	0.13	0.33	0.23	1.85	0.30	0.11	0.42	0.56	0.45	0.32	0.08	0.07
US684	58.9	1st BU	0.12	0.38	0.31	1.32	0.47	0.10	0.60	0.57	0.64	0.30	0.10	0.17
US688	55.71	1st BU	0.15	0.47	0.27	1.92	0.58	0.10	0.76	0.82	0.86	0.25	0.03	0.16
US066	54.2	1st BU	0.14	0.34	0.28	1.56	0.41	0.09	0.63	0.74	0.69	0.34	0.07	0.15
US691	51.6	1st BU	0.10	0.30	0.29	0.82	0.53	0.26	0.80	0.93	0.72	0.42	0.02	0.05
US693	49	1st BU	0.13	0.42	0.26	2.65	0.35	0.23	0.77	0.86	0.74	0.26	0.02	0.05
US070	47.7	1st BU	0.11	0.39	0.22	1.83	0.52	0.09	0.59	0.65	0.71	0.31	0.08	0.18
US071	45.2	Negative shift	0.11	0.37	0.24	1.42	0.60	0.11	0.70	0.83	0.79	0.37	0.05	0.17
US1001	43.3	Negative shift	0.13	0.39	0.27	1.74	0.59	0.21	0.79	0.85	0.80	0.27	0.02	0.08
US074	38.5	Negative shift	0.11	0.37	0.24	1.35	0.38	0.26	0.62	0.73	0.66	0.40	0.06	0.12
US1006	36.7	Pre excursion	0.10	0.35	0.12	2.38	0.48	0.28	0.81	0.78	0.82	0.25	0.02	0.08
US1009	27	Pre excursion	0.14	0.35	0.23	2.43	0.42	0.26	0.76	0.81	0.77	0.21	0.03	0.08
US1011	22.1	Pre excursion	0.15	0.30	0.21	2.53	0.45	0.34	0.81	0.92	0.77	0.33	0.01	0.03
US076	11	Pre excursion	0.20	0.38	0.26	1.81	0.52	0.21	0.75	0.81	0.77	0.20	0.02	0.07
US077	0	Pre excursion	0.11	0.33	0.24	2.69	0.56	0.23	0.73	0.87	0.78	0.35	0.03	0.10

CHAPTER 4

Reconstruction of fungal flora changes by fungal palynomorph analysis in the sediments deposited during the Cretaceous Oceanic Anoxic Events

4.1. Introduction

Fungi, which associate with many species as decomposers or symbionts in terrestrial ecosystems, have been reported to be the dominant strata in Earth's history immediately after several mass extinction events known as the Fungal spike, which is interpreted as a surge of fungi as decomposers on land after the devastation of the (Vajda & McLoughlin, 2004; Rampino & Eshet, 2018). On the other hand, it has been suggested that even under normal conditions, fungi, which account for a large biomass in terrestrial ecosystems, may have had a significant impact on the carbon cycle (Pieńkowski et al., 2016; Taylor et al., 2009, 2011). Thus, reconstructing changes in terrestrial ecosystems, including the behavior of fungi, will be important in discussing terrestrial paleoenvironments. In this study, organic microfossils (palynomorphs) were isolated from sedimentary rocks that recorded Oceanic Anoxic Events (OAEs), known as major environmental disturbance events that occurred multiple times during the Mid-Cretaceous, and fluorescence microscopic observations were made with particular attention to the transition of the fungal flora.

4.2. Samples and methods

4.2.1. OAE samples from southern France

Preparation of kerogen-treated samples provided by Dr. Takuto Ando of Akita University was used for the analysis, and light to dark gray marls and black shales from the Marbourg Formation (Aptian-early Cenomanian) in southeastern France were used for the OAE1a~1d strata. Of the OAE1a (Goguel level) and OAE1b formations, outcrop samples from the Sauzeries area were used for the Jacob and Leenhardt formations, core samples collected in 2004 at St. Andre-les Alpes were used for the Kilian Formation, and samples from the Paquier and OAE1d, OAE2 (Thomel) samples are massive limestone to marl and black shale samples collected from outcrops in the Lambruisse area (Fig. 4.1).

4.2.2. OAE samples from Brazil

The preparation of kerogen-treated samples provided by Dr. Takuto Ando of Akita University was used for the analysis. Sedimentary rock samples were from the Santana Formation of the Araripe Basin,

which corresponds to the OAE1b level in Estiva, provided by Dr. Heimhofer of the University of Hannover, Germany. The lithology is sandy, and the sedimentary field is predicted to have been very close to land (Fig. 4.2).

4.2.3. OAE samples from Japan and North America

The samples from the Yezo Formation in Japan and the Great Valley Sequence in North America are the same as those used in Chapter 3 and are not described here. For the Yezo Formation, samples from the Hakkin-gawa and Shumarinai-gawa sections, which are also OAE2 stratigraphic sections, were also used for comparison, in addition to the OMZ section.

4.2.4. Kerogen separation

Crushed rock samples (5-10 g) were extracted with ultrasonication by subsequent treatment with methanol and dichloromethane. After that, residues were treated sequentially in a water bath shaker as follows: HCl 6M (100 ml, 60 ℃, 6 h), HCl 12 M/HF 46% (1/1 v/v) (100 ml, 60 ℃, 48 h). After each treatment, the supernatant was removed after centrifugation (3000 rpm, 10 min). The residue, kerogen, was sequentially and repeatedly washed with distilled water.

4.2.5. Methods of identification

In this study, we used grazing incidence differential interference observation and transmission/ fluorescence microscopy to identify the fungi in our analysis of fungal palynomorphs. Matsuoka (1992) reported that the fluorescent color of fungal palynomorphs by the UV excitation method did not show autofluorescence (blackish brown), and in this study, neither mycelium nor spores showed autofluorescence. In addition to the characteristics mentioned above, the presence or absence of septa and the structure of the spore surface were observed using grazing differential interferometry to identify the fungal palynomorphs. Unlike the present fungi, fungal spores in palynomorphs are broadly classified based on the number and shape of spore-forming cells. The classification method summarized by Taylor et al. (2015) was applied in this study (Fig. 4.3).

4.3. Results and discussion

4.3.1. Effects of changes in sedimentary environments on fungal palynomorphs

In the Vocontian Basin of southeastern France, few fungal palynomorphs were observed from OAE1a (Goguel level), and more mycelia and spores were observed in OAE1b (Kilian and

Paquier level), OAE1d (Breistroffer) and OAE2 (Thomel). Fungal palynomorphs, such as mycelia and fungal spores, were abundant in the OAE1d (Breistroffer) and OAE2 (Thomel) (Fig 4.4, Fig. 4.5). Biomarker and palynomorph analyses have reported that in the Vocontian Basin, the contribution of terrestrial source organic matter was small in OAE1a and large in OAE1b, especially at Killian and Paquier levels (Herrle et al. ., 2003; Okano et al. 2007; Ando, 2016). In addition, at Breistroffer level (OAE 1d), terrestrial origin palynomorphs increased in the black shale layer, suggesting that terrestrial organic matter transport may have increased with the humidification of the terrestrial environment (Bornemann et al., 2005). It is inferred that the increase or decrease in fungal palynomorphs in this study is particularly influenced by terrestrial runoff. In particular, the black shales of OAE1d, where the contribution of terrestrial sources is considered high, also produced microspores and fruiting bodies similar to *Callimothallus* spp. and showed a high diversity of fungal palynomorphs. The same trend was observed in the OAE1b stage (Estiva section) in Brazil, which was a sedimentary field closer to land than the southeastern French section, strongly suggesting that the increase and decrease of fungal palynomorph are high attributable to the inflow of terrestrial organic matter.

4.3.2. Effects of changes in terrestrial paleoenvironment on fungal palynomorphs

As discussed in the previous chapter, the results showed that the increase in fungal palynomorphs is strongly influenced by the amount of terrestrial runoff. On the other hand, even among the same Vocontian basin sediments, the observed trends of fungal palynomorphs differed significantly, with the majority of mycelia up to OAE1b having septate walls characteristic of basidiomycetes and ascomycetes. In contrast, only more primitive, septate-free mycelia were produced after OAE1d (Fig. 4.9). The appearance of capsular pollen during the same period, and the prominence of septate mycelium in the Yezo Group, which is thought to have been forest vegetation in contrast to Thomel, where the hinterland was predominantly herbaceous vegetation during OAE2, suggest that the change in fungal flora in the fungal palynomorphs reflects the change in vegetation (Fig. 4.6)

In the GVS, previous studies such as pollen reported that herbaceous savanna vegetation had spread in the hinterland. The biomarker results indicate that the vegetation changed to woody dominated with the spread of conifers at the end of the OAE, and the mycelial changes observed in the GVS were associated with this conifer expansion, which may indicate that the coccolithophores and basidiomycetes associated with woody vegetation expanded with the

vegetation change in the hinterland (Fig. 4.8). This may indicate that the presence of woody plant-associated coccolithophores and basidiomycetes has been accompanied by vegetation changes in the hinterland.

In OMZ, unlike the fungal palynomorphs OAE1d-2 in VB and the first half of OAE2 in GVS, a mycelium with septate walls was detected through OAE2. This suggests that the hinterland of the Yezo Formation at that time was forest vegetation (see Chapter 3), and that the contribution of the ascomycetes and basidiomycetes (with their characteristic septate mycelia) in the forest vegetation was significant.

The appearance of septate mycelia in the fungal palynomorphs was sympathetic to the expansion of woody vegetation in terrestrial environments. It was interpreted as an increase in basidiomycetes and ascomycetes, such as wood-degrading fungi and ectomycorrhiza, while not necessarily consistent with the reconstruction using fungal biomarkers.

4.4. Conclusions

During OAEs, the increase in fungal palynomorphs was generally sympatric with the influx of terrestrial sources, especially in strata where the contribution of terrestrial sources was significant, and the variety of fungal palynomorphs, including not only mycelia but also spores and fruiting bodies, was diverse. In OAE2 of each section, fungal palynomorphs were significantly more abundant during normal periods than during periods of environmental disturbance, suggesting that they may reflect changes in the terrestrial environment. The appearance of septate mycelia in the fungal palynomorphs was synchronous with the expansion of woody vegetation in terrestrial environments and was interpreted as an increase in basidiomycetes and ascomycetes such as wood decay fungi and ectomycorrhizas. On the other hand, although the timing of the increase and decrease was synchronous with the fungal biomarker reconstruction, the increase and decrease in contribution did not always coincide with the fungal biomarker reconstruction.

Although more detailed studies are needed in the future, the results indicate the possibility of vividly reconstructing environmental changes in terrestrial environments by comparing fungal biomarkers and palynomorph analysis.
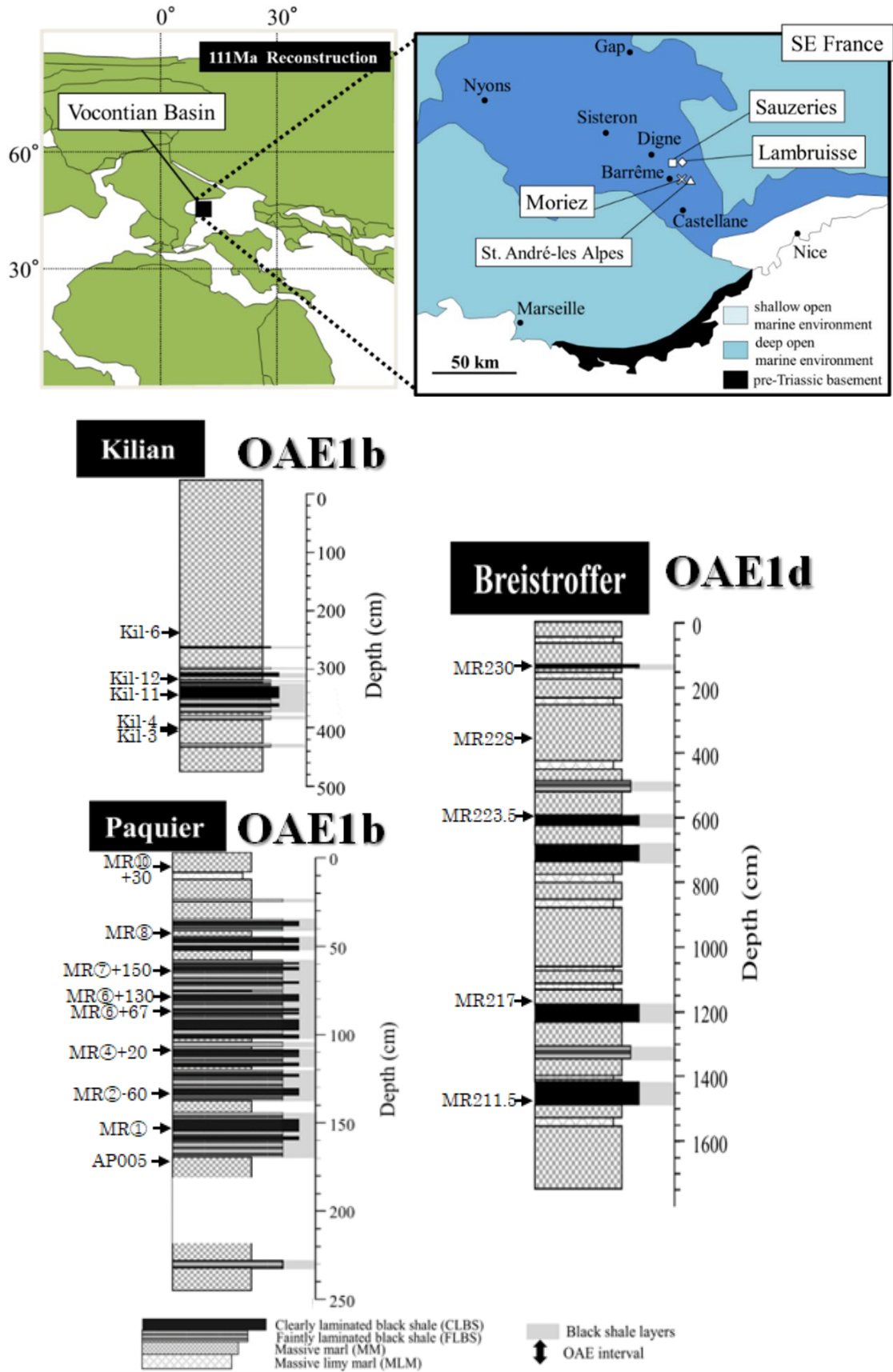
Fig.4.1. Index map showing location of Vocontian basin in southeastern France (Upper) and Columnar diagram of each layer level and samples used in this study (Lower) (Ando et al., 2017).
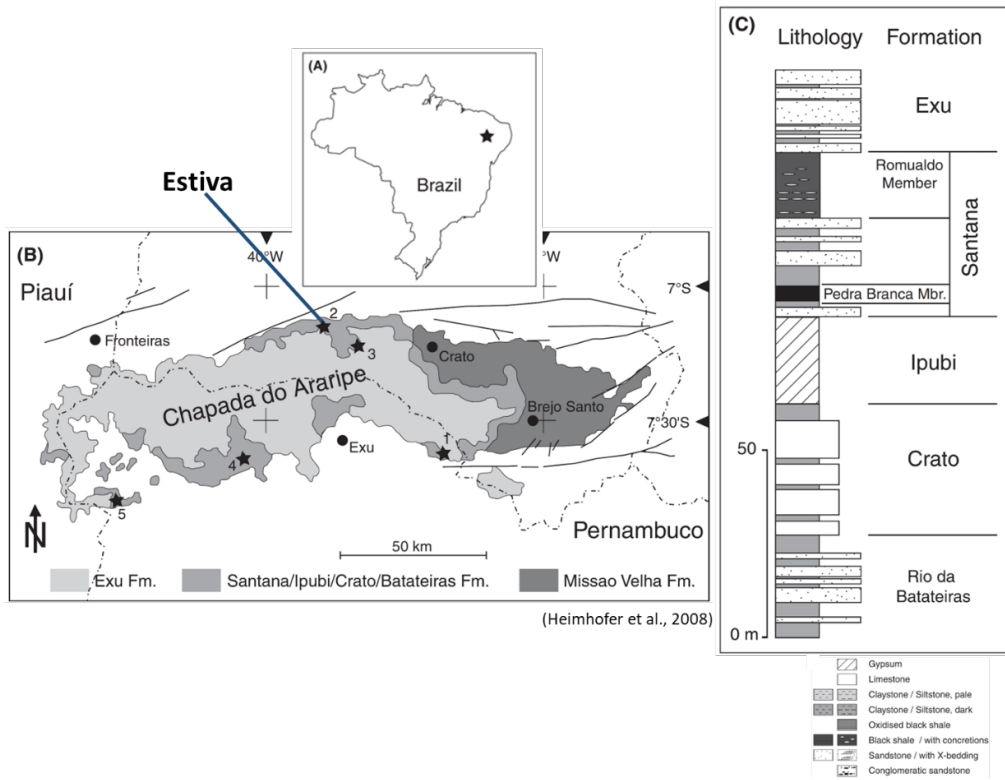
Fig.4.2. Index map showing location of Estiva area of Brazil and schematic geological map of study area (modified from Heimhofer et al., 2008).
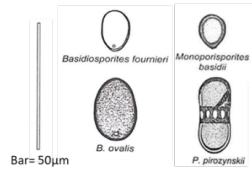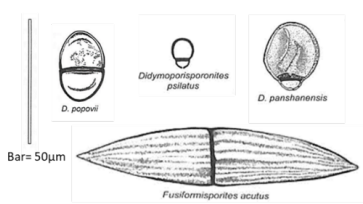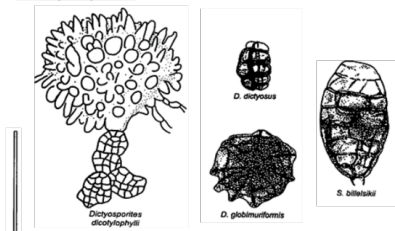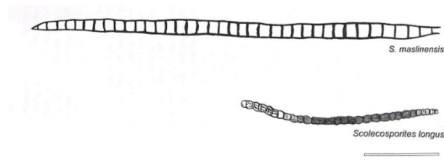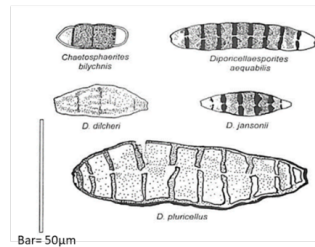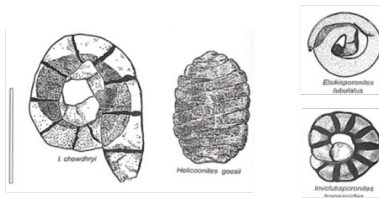
Fungal spore
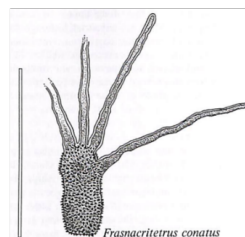
Fig.4.2. Fungal spore taxonomic groups used in this study (Taylor et al., 2015).

OAE1a

Goguel

Not detected

OAE1b

Kilian

Paquier

50.0 μm

50.0 μm

OAE1d

Breistroffer

Black shale

20.0 μm   20.0 μm

Callimothallus sp.?

20.0 μm   20.0 μm

Dicellaesporites sp.?

20.0 μm   20.0 μm

Amerospore

OAE1b   Estiva

20.0 μm

20.0 μm

μm

20.0 μm

20.0 μm

Metacapnodium sp.?
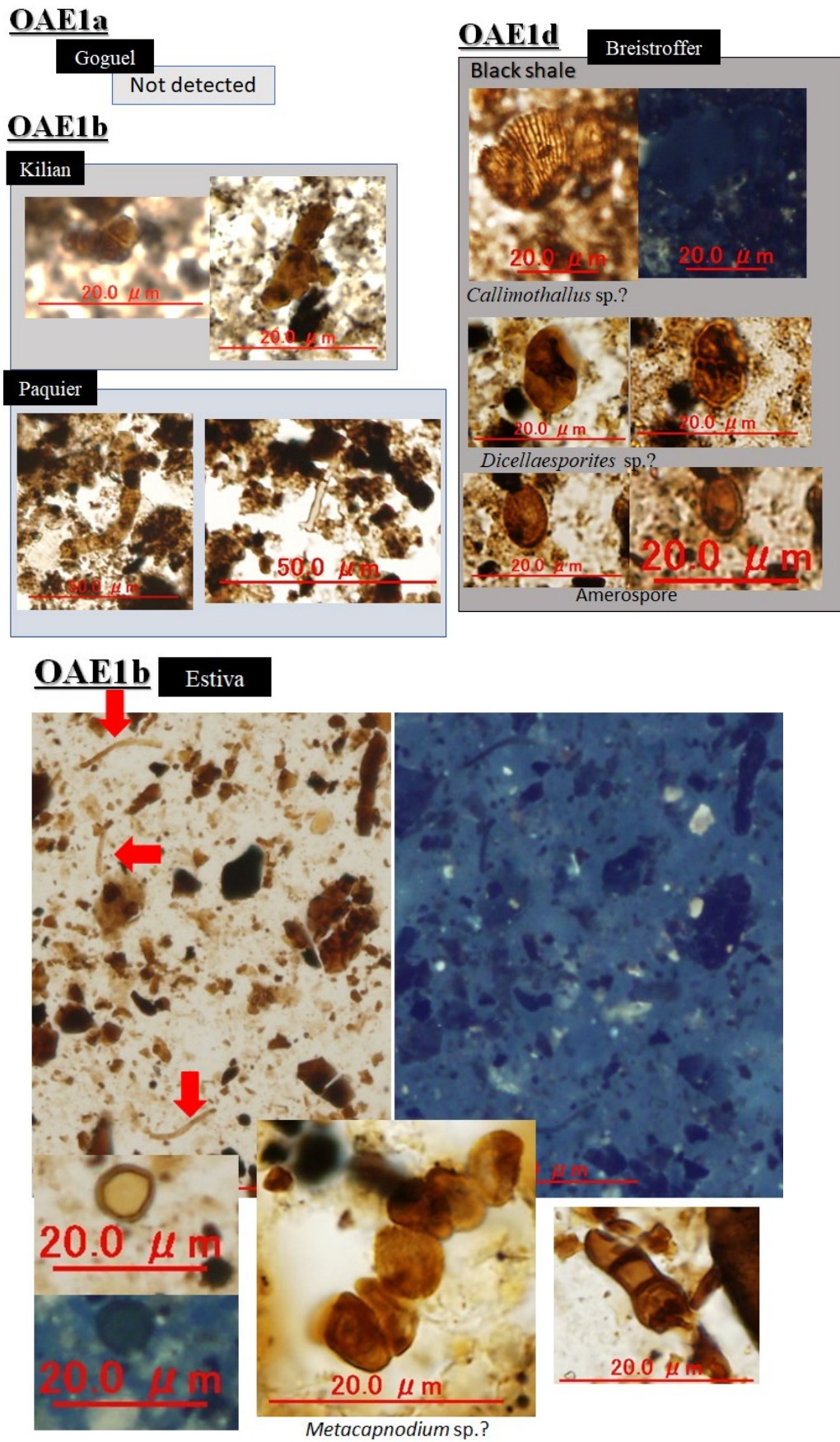
Fig.4.4. Fungal palynomorphs detected in OAE1a-1d samples.

5 8

Thomel, VB <u>**OAE2**</u>

(Takashima et al.,2009)

-:ND **+**:Detected **++**:rich **+++**:high abundant
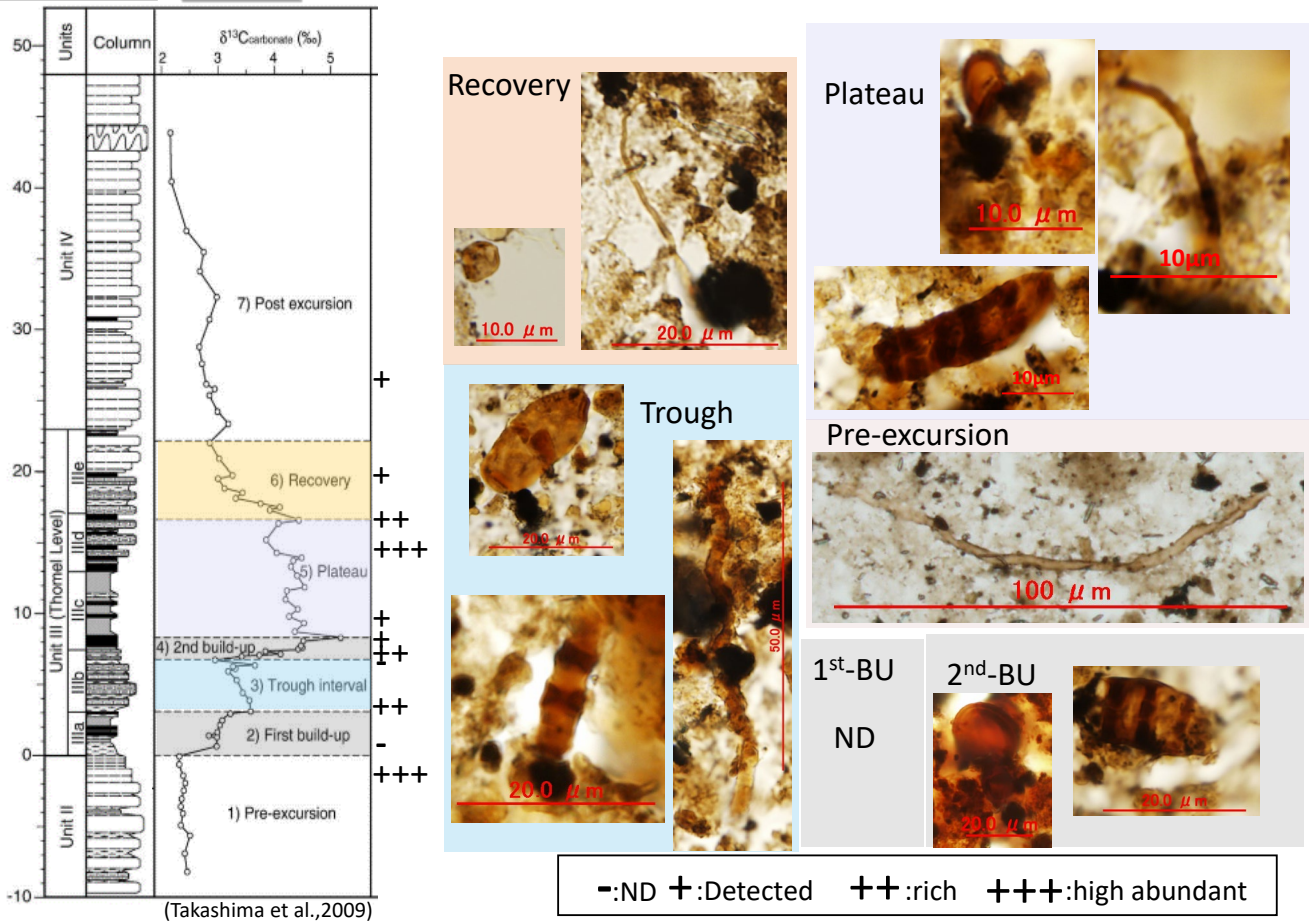
Fig.4.5. Fungal palynomorphs detected in Thomel samples

★ Vocontian basin

Closed canopy, broad leaved, moist evergreen forest	
Savanna: dry, low understory with sparse broad leaved overstory	

(modified from Sewall et al., 2007)
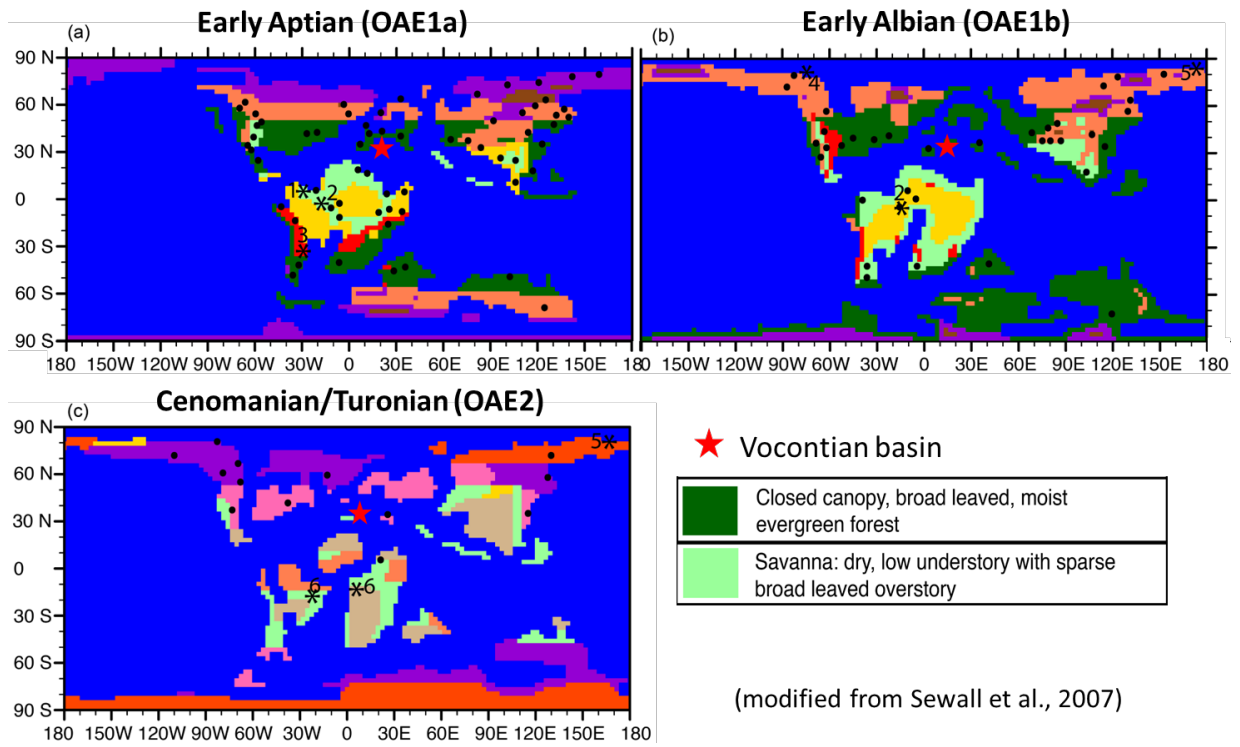
Fig.4.6. Vegetation biome changes from OAE1a to OAE2
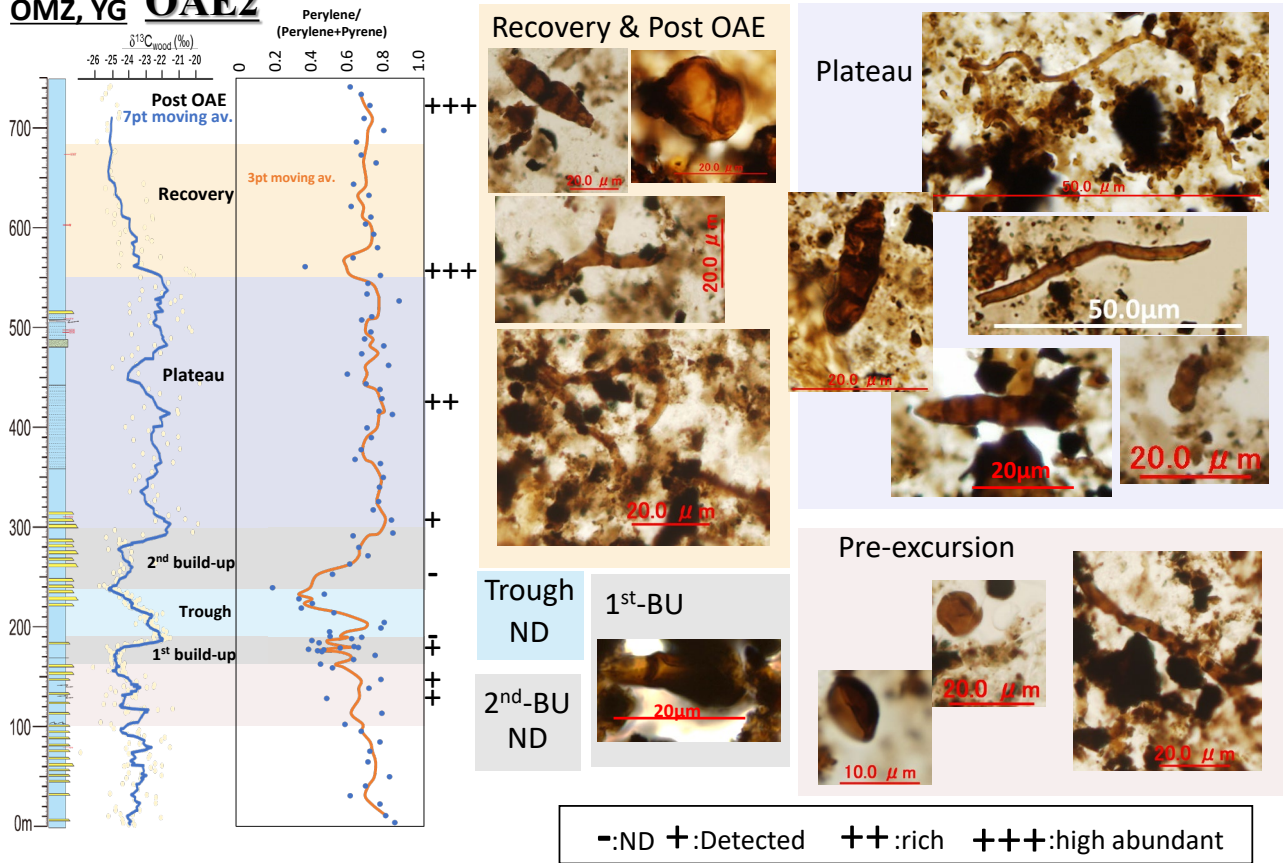
Fig.4.7. Changes in fungal contribution recovered from fungal palynomorphs detected in each phase of OAE2 and biomarker indicators in the OMZ section.
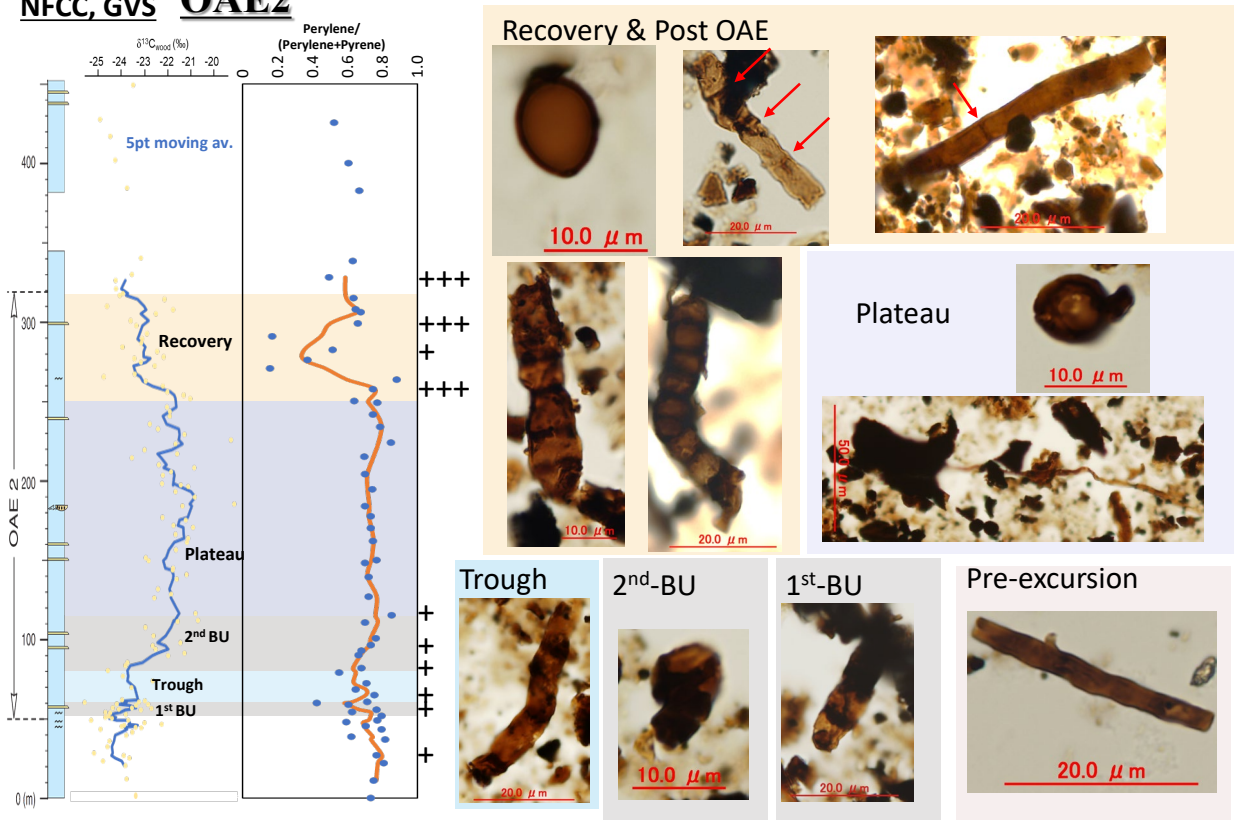
Fig.4.8. Changes in fungal contributions recovered from fungal palynomorphs detected in each phase of OAE2 and biomarker indices in the NFCC section.

6 0
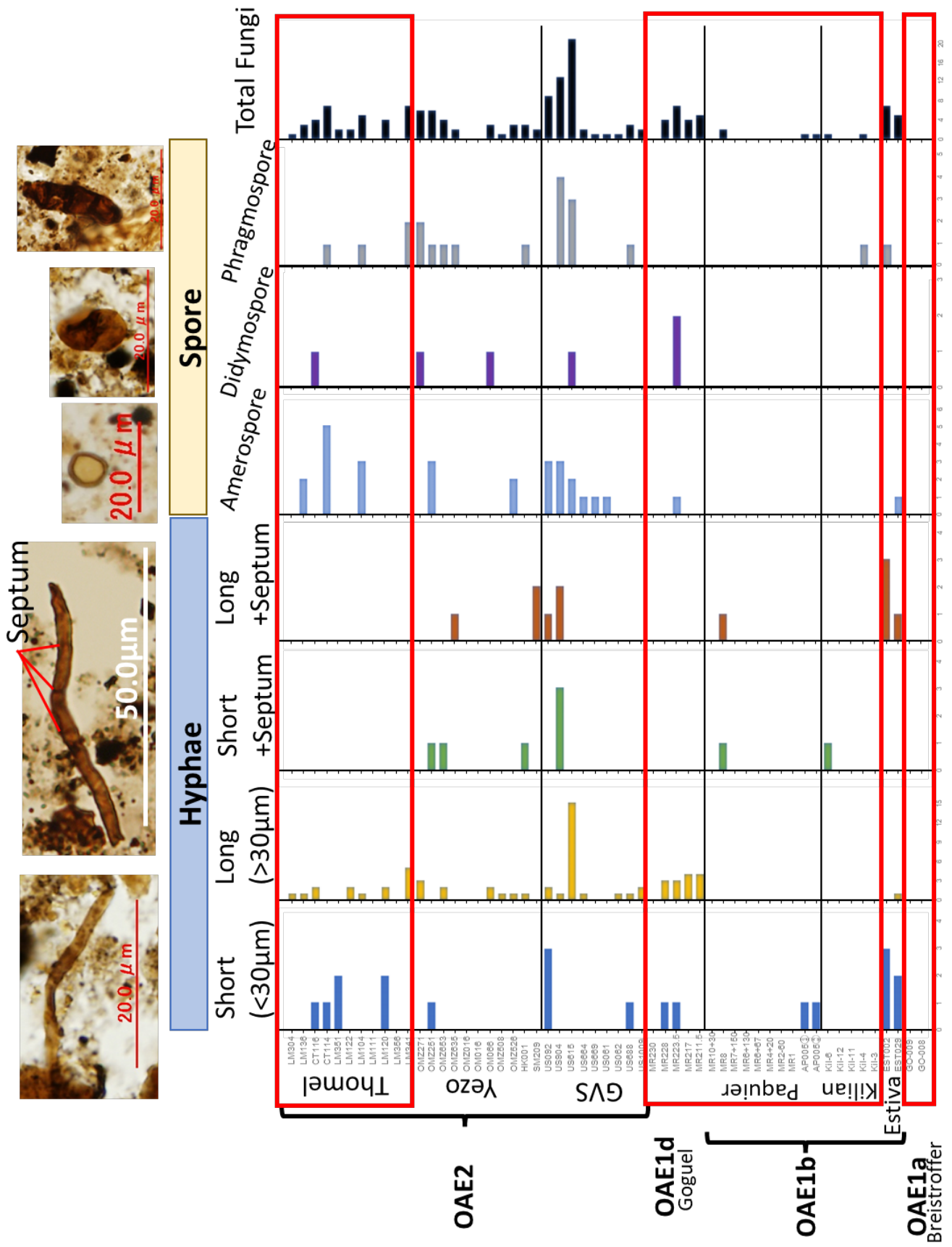
Fig.4.9. Type and number of fungal palynomorphs detected in each sample. Red boxes indicate data from the Vocontian Basin.

CHAPTER 5
The evolutionary history of lichens using molecular fossils: Possibility of terrestrial life in the Proterozoic

5.1. Introduction

The Proterozoic (2500-541 Ma) is considered the era of major breakthroughs in the evolution of the global environment and life, including the atmosphere and oceans (Craig et al., 2013). The Proterozoic is divided into three eras (Paleoproterozoic, Mesoproterozoic, and Neoproterozoic) and further divided into ten periods with names reflecting large-scale tectonic depositional events. In the Paleoproterozoic (2500-1600 Ma) and Neoproterozoic (1000-541 Ma), the distribution of glacial deposits has been reported worldwide, suggesting that multiple global glacial events (Snowball Earth) may have occurred (e.g., Hoffman and Schrag, 2002; Tang and Chen, 2013). Likewise, two atmospheric oxygen-elevation events have been reported to have occurred in these epochs: the Great Oxidation Event (GOE), which occurred about 2.5-2.0 Ga, and the Neoproterozoic Oxygenation Event (NOE), which occurred 700-500 Ma (e.g., Kump, 2008; Lyons et al., 2014). In recent years, the link between these global events and the emergence and evolution of eukaryotes has been actively discussed based on molecular clocks, fossil records, biomarkers, and geochemical studies (e.g., Craig et al., 2013; Cohen and Kodner, 2022)(Fig. 5.1). Thus, while the Paleoproterozoic and Neoproterozoic are known to have been major events in the global environment and life evolution, the Mesoproterozoic (1600-1000 Ma) is considered to have been a very stable period, characterized by the fact that no events that dramatically changed the global environment were recorded. Because of this and the lack of geochemical variations such as carbon isotope ratios, Buick et al. (1995) called the Mesoproterozoic "The dullest time in Earth's history." The Mesoproterozoic is considered a very warm period, as glacial sediments were rarely found for over 600 million years (Young, 2018). The middle Proterozoic (1.8 - 0.8 Ga), which was sandwiched between two major oxidation events (GOE and NOE), has also been called the "barren billion" because of the lack of carbon isotope excursions and glaciations (Young, 2013). However, molecular phylogenetic analyses suggest that the emergence and rapid dispersal of a common eukaryotic ancestor occurred (Parfrey et al., 2011; Eme et al., 2014), and geochemical evidence suggests that microbes may have preceded higher plants on land during this period, promoting terrestrial weathering (e.g., Kump, 2014). In the present study, we discuss the origin of aromatic furans detected in Mesoproterozoic sedimentary rocks in northwestern

Greenland and their potential as biomarkers.

5.2. Samples and methods

5.2.1 Samples

The shaley mudstones of the Qaanaaq Formation, Baffin Bay Group, distributed in northwestern Greenland, were used for the biomarker analysis in this study. The Qaanaaq Formation is composed of sand-dominated sand and mud alternations. Previous studies suggest it is considered dep an alluvial plain to marine shoreline deposit in the late Mesoproterozoic (ca 1.2-1.0 Ga) (Samuelsson et al., 1999; Dawes, 2006).

These were surveyed and collected by Dr. Takuto Ando in July and August 2018 and 2019 as part of the Arctic Challenge for Sustainability (ArCS) project. The Thule Supergroup, which includes the Qaanaaq Formation, is a widely preserved middle Mesoproterozoic to early Neoproterozoic deposit extending into western Canada, with a maximum thickness of 6 km. The Thule Basin was formed on the Laurentia. The Qaanaaq Formation is the uppermost member of the Baffin Bay Group in the Thule Basin and consists of weakly weathered sandstone, shale, and siltstone. Based on these lithologies, it is considered to be deposited in a coastal plain and an alluvial plain. Furthermore, the clay layer increases upward upper of the Qaanaaq Formation and gradually shifts to the Dundas Formation, composed of deltaic sediments immediately above it. This suggests a continuous change in the depositional environment (Dawes, 1997). On the other hand, a reddish layer above the Qaanaaq Formation in the northern outcrop suggests that a regional retreat may have occurred (Dawes, 2006). The outcrops in the study area (Fig. 5.2) consist mainly of thick sandstone layers and sandstone-shale-mudstone alternations, and the shale-mudstone part was used for analysis. The continuous sandstone-mudstone alternation between thick sandstone layers was defined as BSI-1 through BSI-5 from the bottom; BSI-2 and BSI-3 are thick beds of mudstone interbedded with thin sandstone layers, so they were numbered U for the upper part and L for the lower part. Samples of the same stratigraphic level but collected in different years were analyzed as separate samples rather than the same sample.

5.2.2. Biomarker analysis

Extraction and separation of bitumen were performed as described by Sawada et al. (1996). Sediments were extracted with methanol (MeOH), dichloromethane (DCM) and DCM/MeOH (1/1, v/v). As an internal standard, tetracosane-d50 was added, and the extract was dried in a rotary

evaporator and re- dissolved in hexane. The hexane extract was passed through a silica gel column (95% activated); the aliphatic and aromatic hydrocarbon fractions were eluted consecutively with hexane and hexane/toluene (3/1, v/v) and analyzed using gas chromatography-mass spectrometry (GC-MS). Lipids were identified by GC-MS using an Agilent 7890B GC instrument equipped with a 30 m × 0.25 mm i.d. DB-5HT fused silica column (Agilent, Santa Clara, CA, USA) directly coupled to an Agilent 5977A MSD quadruple mass spectrometer (electron voltage, 70 eV; scan range, *m/z* 50–650 in 1.3 s). The oven temperature was programmed as follows: 50°C (held for 4 min) to 310 C at 4°C/min (held for 20 min). The injection temperature was 310°C and the instrument was run in splitless mode with helium as the carrier gas.

5.3. Results and discussion

5.3.1. Effect of sample maturity on isomer ratios of aromatic furans

In these samples, T_{max} varies from about 500 °C to 450 °C from the lower to the upper levels, and the degree of maturation is 2.0 (Ro %) in the lower level and 1.0 (Ro %) in the upper level, indicating a gradual change in the degree of maturation within the 70m level. The thin sections of the samples show chlorite, suggesting that metamorphism itself is relatively low (Fig. 5.3).

Although their distribution varied, several aromatic furans, which are oxygen-containing aromatic compounds, were detected in each sample (Fig. 5.4, Fig. 5.5).

Due to the high degree of maturity in this sample, it is likely that the original information on the position of methyl groups and isomer ratios of MDBF, as discussed in Chapter 3, is not preserved due to methyl shifts. Among MDBFs, 1-MDBF and 4-MDBF have been reported to gradually undergo a methyl shift to 1-MDBF, especially in the higher maturity range, due to the difference in thermal stability of the isomers. However, a cross plot of the 1-MDBF/4-MDBF ratio versus maturity for this sample showed no change with maturity(Fig. 5.5). This result suggests that the variation in isomeric diversity of these aromatic furans may be other than due to differences in maturation.

5.3.2. Origin of the aromatic furans

The origin of dibenzofurans, in particular, has been discussed in several ways, including lignin from higher plants and polysaccharides from terrestrial soils (Sephton et al., 2005; Fenton et al., 2007; Wang & Visscher, 2007) and secondary metabolites from lichens (Radke, 2000; Watson et al., 2005; Sawada et al., 2012). Fullana and Sidhu (2005) reported that dibenzofurans are produced

from fluorene and biphenyl in catalytic combustion experiments. As a natural product, dibenzofurans have been reported as antimicrobial agents produced by higher plants (Kokubun et al., 1995; Dixon, 2001) and lichens (e.g., Millot et al., 2016). In this sample, the origin of higher plants can be dismissed among these theories. Watanabe (2000) reported that dibenzofurans were produced from cellulose, lignin, and saccharide in heating experiments simulating maturation in sediments. However, dibenzofurans with alkyl groups were not produced. Therefore, we believe that the origin of polysaccharides is also unlikely.

  In addition, the distribution of isomers of alkyl dibenzofurans fluctuates each sample, suggesting that they may be derived from compounds that originally have aromatic furan structures and thus from specific organisms of origin. When looking at changes in the concentration of aromatic furans, TOC increases upward. However, these oxygen-containing aromatic furans are higher in the lower stratigraphic levels and become lower or undetectable in the upper levels (Fig. 5.6). Previous studies using organic microfossils have indicated that the inflow of terrestrial water is high in the lower stratigraphic levels and that the upper stratigraphic levels are transitioning to a more marine environment (Hara, 2022). The change in concentration itself from lower to higher is more consistent with the oxygen-containing aromatic furans detected being produced from terrestrial sources or near terrestrial areas. In addition, in the present sample, we found microfossils similar to the oldest fungi described from Canadian Mesoproterozoic-Neoproterozoic sedimentary rocks in Loron et al. (2019). Of course, there is no direct evidence that these fungi are the organisms of origin for dibenzofurans. However, it does indicate that the hinterland where the samples were collected was a habitat that could support these fungi.

5.3.3. Lichens as a possible origin of aromatic furans

As mentioned above, fungi and slime molds are known to produce dibenzofurans in nature, in addition to higher plants. However, these species produce only a minimal number of dibenzofurans, and only a few species are known to produce dibenzofurans. The major dibenzofuran-producing species in nature today are lichens, which are known to produce a great variety of dibenzofurans (Millot et al., 2016).

Extant lichens are composed of higher fungi, basidiomycetes, and ascomycetes. Until the early 2000s, their molecular phylogeny indicates that they appeared during the Carboniferous to the Permian. However, the oldest known fossil lichens are from the lower Devonian, and their structural characteristics indicate that more primitive fungi and cyanobacteria formed the lichens

at that time. In particular, these results suggest that the fungi could be lichenized even before the appearance of the fungi, or at least the common ancestor of basidiomycetes and ascomycetes. In light of the above case, Nelsen et al. (2019), based on a new age calibration in the molecular clock, which also takes into account the appearance of primitive lichens, concluded that the appearance of lichens was after the appearance of terrestrial vascular plants (Silurian). Dibenzofurans act as growth inhibitors to other organisms and UV protectants from intense solar radiation. Dibenzofurans are known to be ubiquitous in extant lichens. The timing of the acquisition of the ability of lichens to produce dibenzofurans is unknown, but they were likely capable of doing so from very early times.

The results suggested by this study are much older than the age range given by Nelsen et al. (2019), so the possibility that there were extinct species that synthesized aromatic furans cannot be dismissed. However, although lichen fossils are not currently recognized, some fossils from the Neoproterozoic suggest the possibility of symbiosis between fungi and algae (Yuan et al., 2005), so it is not surprising that "lichens" exist in the context of fungal-algal symbiosis. As mentioned in the introduction to this paper, many studies consider the appearance of early terrestrial life forms to be during the Mesoproterozoic to Neoproterozoic periods and point to lichens as the early life forms (e.g., Kennedy et al., 2006) et al. In any case, although more detailed studies are needed, the present results may suggest that the existence of early terrestrial life forms could have been dibenzofuran-producing, possibly lichen-like, life forms.

5.4. Conclusions

Various aromatic furans were detected in the Mesoproterozoic (1.2-1.0 Ga) sedimentary rocks of the Qaanaaq Fm. in northwestern Greenland. The isomer ratios and abundances of the aromatic furans detected vary from stratigraphic level to stratigraphic level, and are more likely due to changes in the contribution of the source material at the time of deposition than to the effect of maturity. Many previous studies have suggested that aromatic furans are of terrestrial origin (especially higher plants). In this sample, however, the higher plant origin is dismissed, and other life forms that produce these aromatic furan compounds are assumed. In particular, the fact that fossils similar to the oldest fungal fossils reported by Loron et al. (2019) were found at this study site and that the results of palynomorph analysis showed higher concentrations of aromatic furans in the lower layers, where the environment was more influenced by terrestrial, suggest that a terrestrial ecosystem may have already been formed. At this stage, it is not possible to identify the

organisms from which these compounds originated. However, there may have been organisms similar to lichens, which are the primary producers of aromatic furans found in the present.

Although more detailed studies are needed in the future, these compounds from the Mesoproterozoic (Boring Billion) may provide important evidence in discussing the evolutionary history of ecosystems and life at that time.
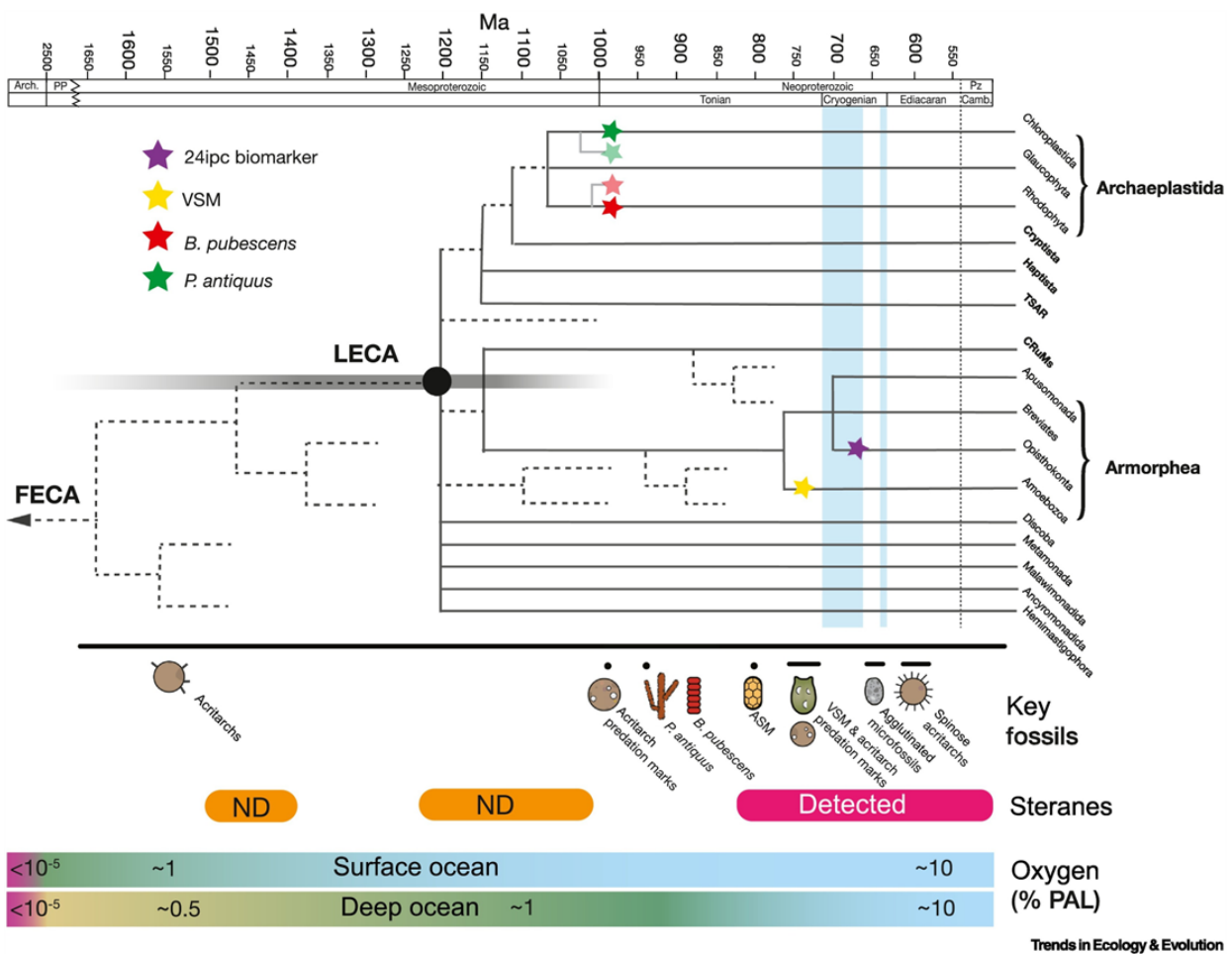
Fig.5.1. Overview of major trends and proxies in the Proterozoic evolution of eukaryotes (Cohen and Kodner, 2022)

6 7
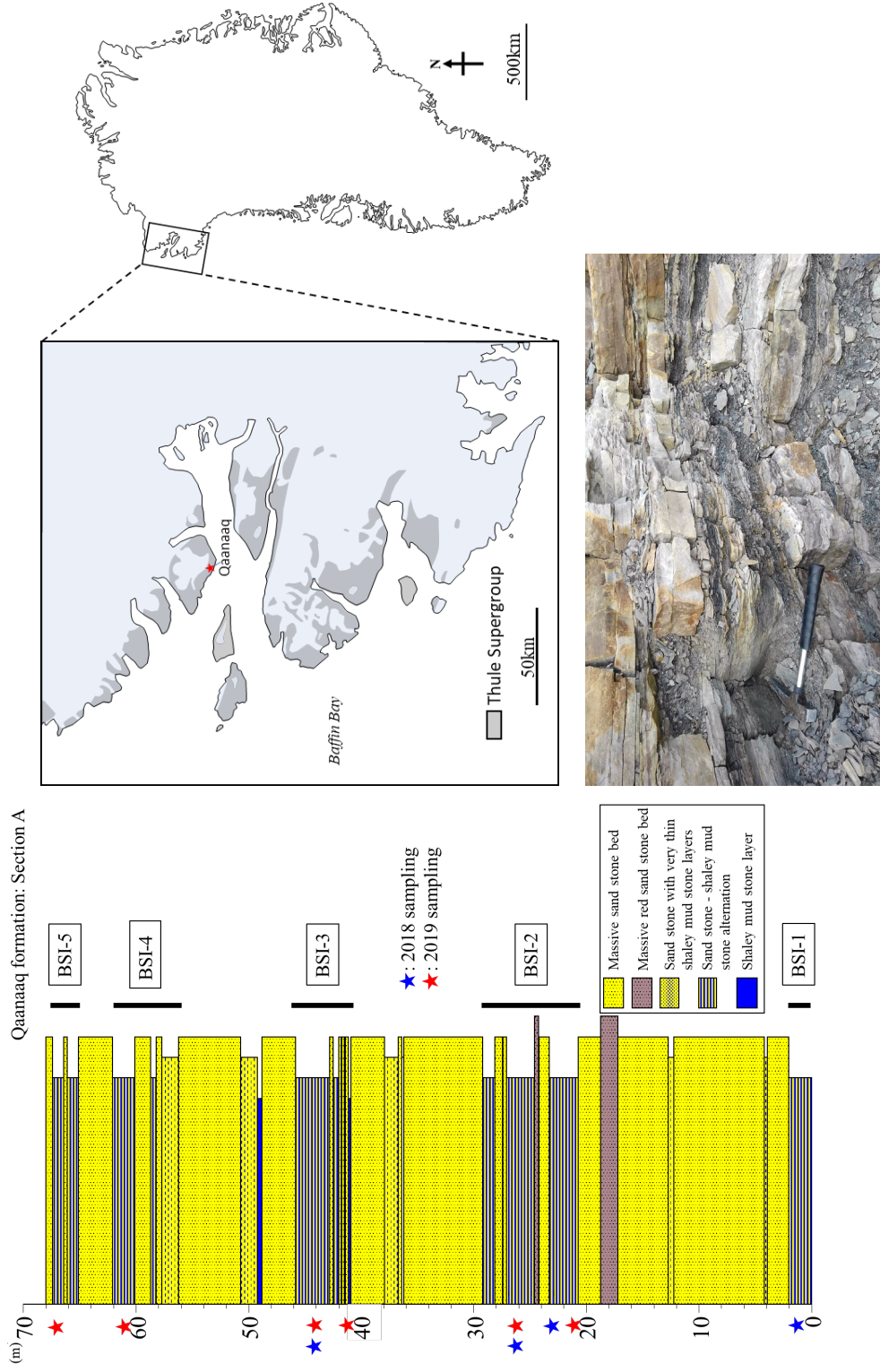
Fig.5.2. Index map showing the location of the Qaanaaq region of Greenland and columnar map of outcrops
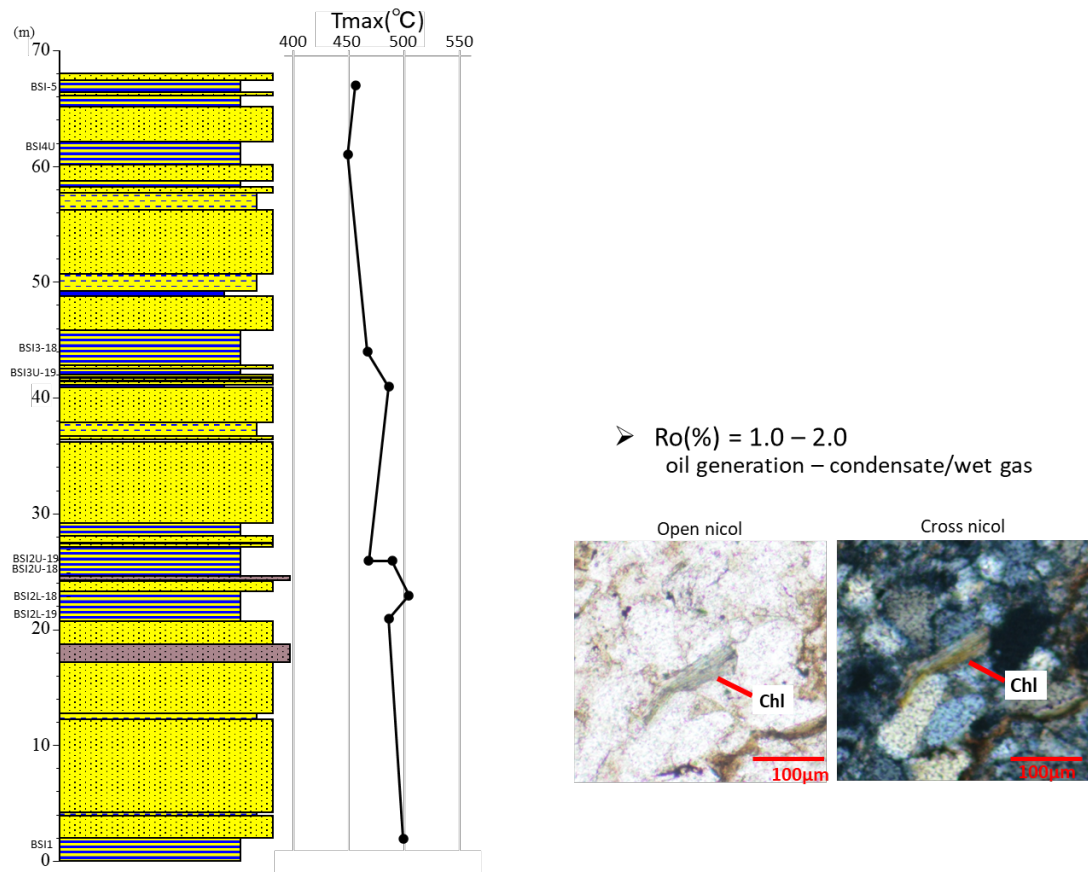
Fig.5.3. Maturity (Tmax) of the sample and chlorite observed by thin section observation

Ro(%) = 1.0 – 2.0
oil generation – condensate/wet gas
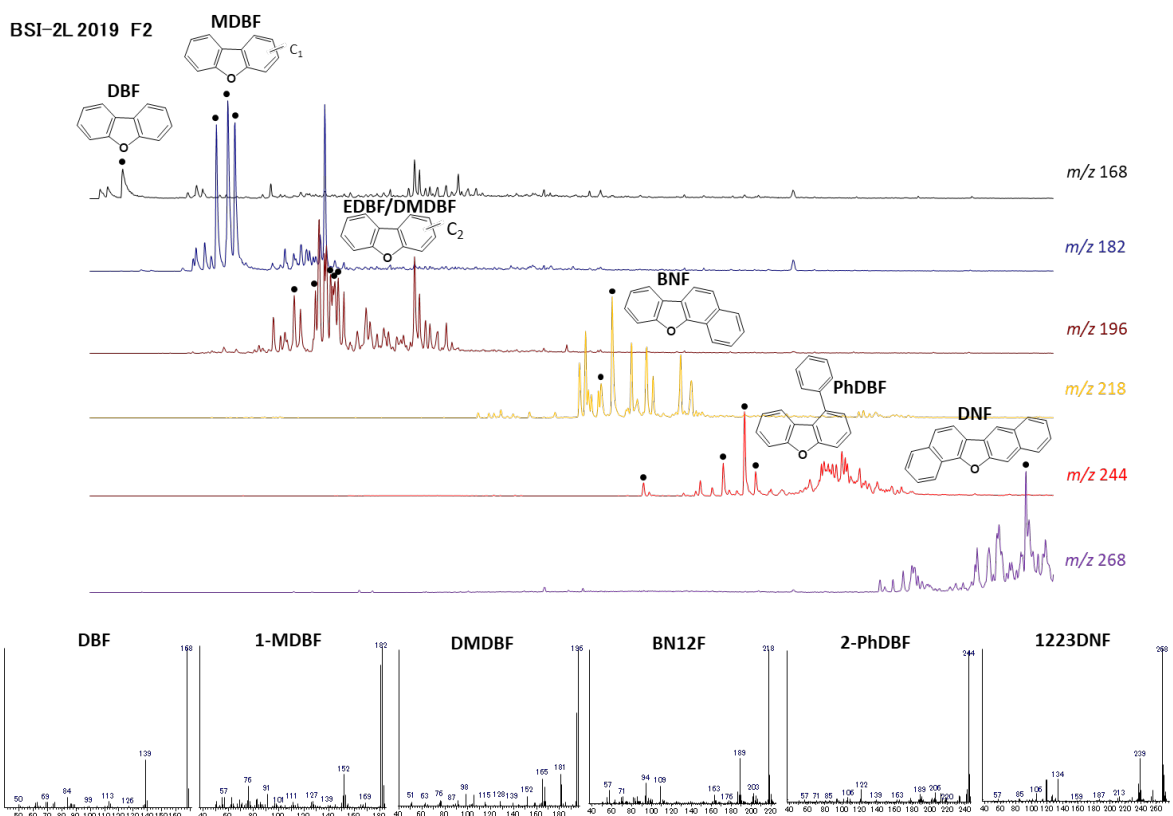
Fig.5.4. Selected ion chromatograms and major mass fragmentograms of aromatic furans detected in the samples.
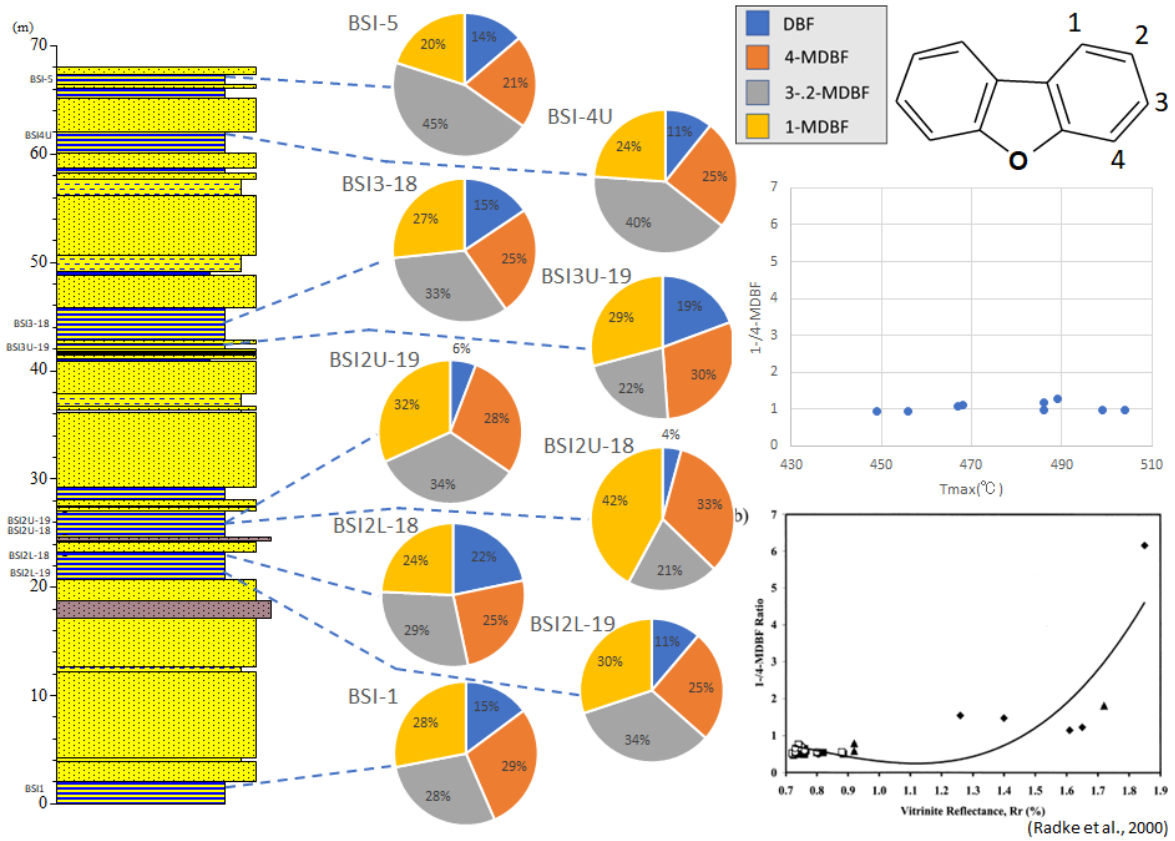
Fig.5.5. Selected ion chromatograms and major mass fragmentograms of aromatic furans detected in the samples.

(Radke et al., 2000)
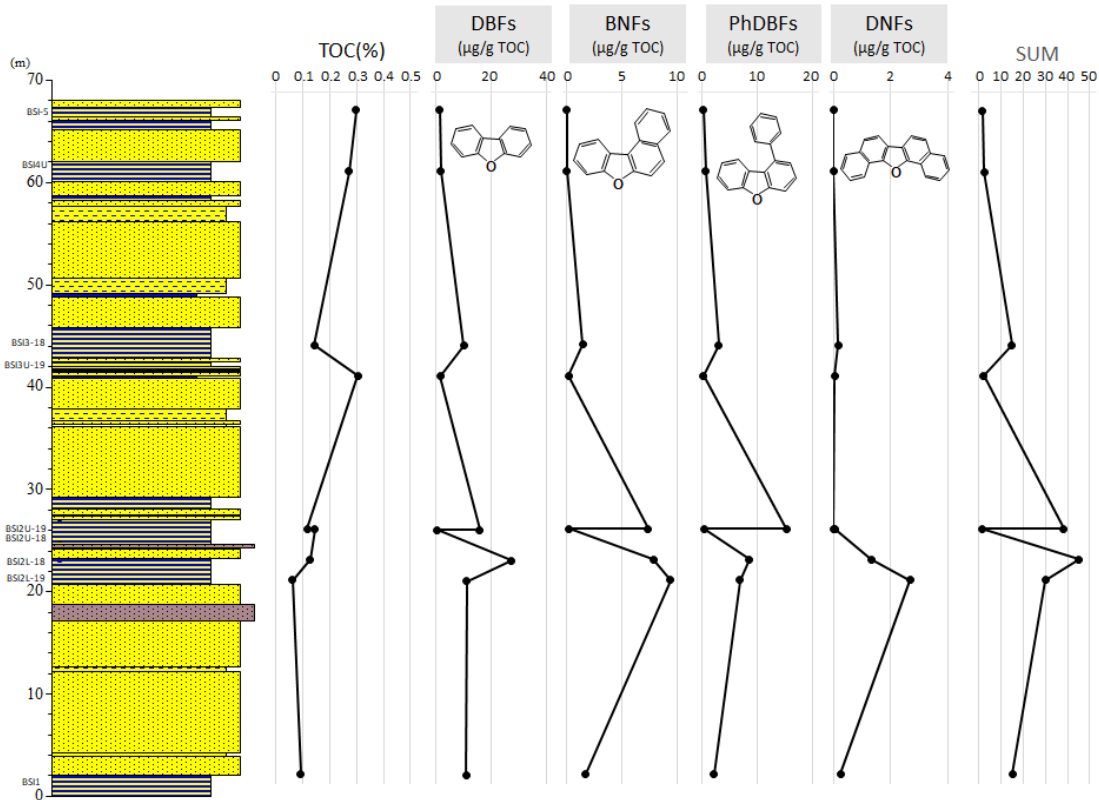
Fig.5.6. Variation of TOC and each aromatic furan concentration (µg/g TOC) in samples.
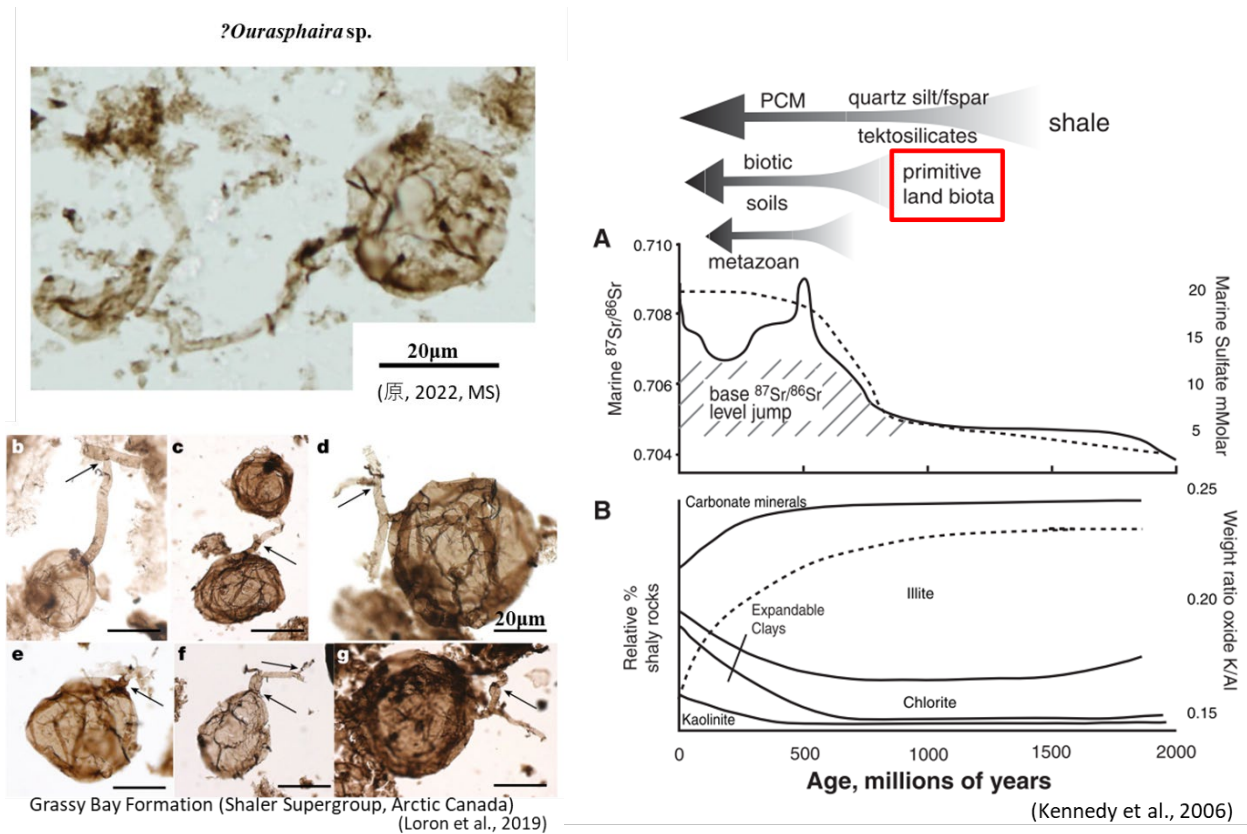
Fig.5.7. Palynomorphs tentatively identified as *Ourasphaira* sp. detected in this sample(Top left) and the oldest fossil fungi reported in Loron et al. (2019)(Bottom left)

7 1

Table.5.1. TOC (%), Tmax and aromatic furans composition (μg/g TOC) for each sample

Sample name	depth(m)	Total Organc Carbon(%)	Tmax(°C)	μg/g TOC										
				BN21F	BN12F	1223DNF	1-PhDBF	4-PhDBF	2-PhDBF	3-PhDBF	DBF	4-MDBF	3-+2-MDBF	1-MDBF
BSI-5	67	0.30	456	ND	ND	ND	0.02	0.04	0.18	0.04	0.16	0.24	0.52	0.23
BSI4U	61	0.27	449	ND	ND	ND	0.04	0.13	0.50	0.07	0.17	0.40	0.66	0.39
BSI3-18	44	0.14	467	ND	1.46	0.16	0.15	0.42	2.08	0.47	1.57	2.48	3.33	2.69
BSI3U19	41	0.30	486	ND	0.19	0.03	0.03	0.06	0.19	0.05	0.30	0.46	0.34	0.45
BSI2U19	26	0.12	468	ND	7.36	ND	0.58	2.27	9.47	3.02	0.91	4.49	5.28	4.98
BSI2U18	26	0.14	489	ND	0.25	0.04	0.03	0.08	0.23	0.06	0.02	0.15	0.09	0.19
BSI2L18	23	0.13	504	1.47	6.36	1.33	0.48	1.39	5.10	1.65	5.93	6.80	7.95	6.63
BSI2L19	21	0.06	486	2.17	7.21	2.67	0.61	1.53	3.49	1.27	1.24	2.79	3.68	3.32
BSI-1	2	0.09	499	ND	1.73	0.24	0.21	0.53	1.22	0.31	1.61	3.12	3.10	3.05

List of Figures

on the heatmap with a value one order of magnitude smaller than the smallest value.

7 5

List of Tables

References

Ageta, H., Arai, Y., 1983. Fern constituents: pentacyclic triterpenoids isolated from *Polypodium niponicum* and *P. formosanum*. Phytochemistry 22, 1801–1808.

Ahmadjian, V., 1988. The lichen alga Trebouxia: does it occur free-living? Plant Systematics and Evolution 158, 243–247.

Ahmadjian, V., 1988. The lichen alga *Trebouxia*: does it occur free-living? Plant Systematics and Evolution 158, 243–247.

Ahmadjian, V. 1993. The lichen symbiosis. John Wiley & Sons, New York.

Amon, R.M.W., Fitznar, H.P., Benner, R., 2001. Linkages among the bioreactivity, chemical composition, and diagenetic state of marine dissolved organic matter. Limnology and Oceanography 46, 287–297.

Ando, T., 2016. Organic biogeochemical study on marine ecosystems in the mid-Cretaceous oceanic anoxic events in SE France and Hokkaido, Japan. PhD thesis, Hokkaido Univ. Sapporo, .

Ando, T., Sawada, K., Nakamura, H., Omatsu, K., Takashima, R., Nishi, H., 2017. Depositional environments and maturity evaluated by biomarker analyses of sediments deposited across the Cenomanian–Turonian boundary in the Yezo Group, Tomamae area, Hokkaido, Japan. Island Arc 26, 1–17.

Ando, T., Sawada, K., Okano, K., Takashima, R., Nishi, H., 2017. Marine primary producer community during the mid-Cretaceous oceanic anoxic events (OAEs) 1a, 1b and 1d in the Vocontian Basin (SE France) evaluated from triaromatic

steroids in sediments. Organic Geochemistry 106, 13–24.

Asahina, Y., Shibata, S., 1954. Chemistry of lichen substances. Japan Society for the Promotion of Science, Tokyo.

Asplund, J., Wardle, D.A., 2017. How lichens impact on terrestrial community and ecosystem properties. Biological Reviews 92, 1720–1738.

Bates, S.T., Cropsey, G.W.G., Caporaso, J.G., Knight, R., Fierer, N., 2011. Bacterial communities associated with the lichen symbiosis. Applied and Environmental Microbiology 77, 1309–1314.

Beck, A., Friedl, T., Rambold, G., 1998. Selectivity of photobiont choice in a defined lichen community: Inferences from cultural and molecular studies. New Phytologist 139, 709–720.

Beimforde, C., Feldberg, K., Nylinder, S., Rikkinen, J., Tuovila, H., Dörfelt, H., Gube, M., Jackson, D.J., Reitner, J., Seyfullah, L.J., Schmidt, A.R., 2014. Estimating the Phanerozoic history of the Ascomycota lineages: Combining fossil and molecular data. Molecular Phylogenetics and Evolution 77, 307–319.

Berbee, M.L., Strullu-Derrien, C., Delaux, P.M., Strother, P.K., Kenrick, P., Selosse, M.A., Taylor, J.W., 2020. Genomic and fossil windows into the secret lives of the most ancient fungi. Nature Reviews Microbiology 18, 717–730.

Bernier, U.R., Carlson, D.A., Geden, C.J., 1998. Gas chromatography/mass spectrometry analysis of the cuticular hydrocarbons from parasitic wasps of the genus *Muscidifurax*. Journal of the American Society for Mass Spectrometry 9, 320–332.

Bi, X., Sheng, G., Feng, Y., Fu, J., Xie, J., 2005. Gas- and particulate-phase specific

tracer and toxic organic compounds in environmental tobacco smoke. Chemosphere 61, 1512–1522.

Biswas, R.K., Kaiho, K., Saito, R., Tian, L., Shi, Z., 2020. Terrestrial ecosystem collapse and soil erosion before the end-Permian marine extinction: Organic geochemical evidence from marine and non-marine records. Global and Planetary Change 195, 103327.

Blackwell, M., 2011. The fungi: 1, 2, 3 … 5.1 million species? American Journal of Botany 98, 426–438.

Blomquist, G.J., Kearney, G.P., 1976. Biosynthesis of internally branched monomethylalkanes in the cockroach *Periplaneta fuliginosa*. Archives of Biochemistry and Biophysics 173, 546–553.

Born, J.G.P., Louw, R., Mulder, P., 1989. Formation of dibenzodioxins and dibenzofurans in homogenous gas-phase reactions of phenols. Chemosphere 19, 401–406.

Bornemann, A., Pross, J., Reichelt, K., Herrle, J.O., Hemleben, C., Mutterlose, J., 2005. Reconstruction of short-term palaeoceanographic changes during the formation of the Late Albian 'Niveau Breistroffer' black shales (Oceanic Anoxic Event 1d, SE France). Journal of the Geological Society 162, 623–639.

Boustie, J., Tomasi, S., Grube, M., 2011. Bioactive lichen metabolites: Alpine habitats as an untapped source. Phytochemistry Reviews 10, 287–307.

Brassell, S.C., Comet, P.A., Eglinton, G., Isaacson, P.J., McEvoy, J., Maxwell, J.R., Thomson, I.D., Tibbetts, P.J.C., Volkman, J.K., 1980. The origin and fate of lipids in the Japan Trench. Physics and Chemistry of the Earth 12, 375–392.

Brassell, S.C., Eglinton, G., 1981. Steroids and triterpenoids in deep sea sediments as environmental and diagenetic indicators. Advances in Organic Geochemistry, 684–697.

Buick, R., Des Marais, D.J., Knoll, A.H., 1995. Stable isotopic compositions of carbonates from the Mesoproterozoic Bangemall group, northwestern Australia. Chemical Geology 123, 153–171.

Cardinale, M., Puglia, A.M., Grube, M., 2006. Molecular analysis of lichen-associated bacterial communities. FEMS Microbiology Ecology 57, 484–495.

Cardinale, M., Vieira De Castro, J., Müller, H., Berg, G., Grube, M., 2008. *In situ* analysis of the bacterial community associated with the reindeer lichen *Cladonia arbuscula* reveals predominance of *Alphaproteobacteria*. FEMS Microbiology Ecology 66, 63–71.

Cardoso, J.N., Gaskell, S.J., Quirk, M.M., Eglinton, G., 1983. Hydrocarbon and fatty acid distributions in Rostherne lake sediment (England). Chemical Geology 38, 107–128.

Carlson, D.A., Roan, C.S., Yost, R.A., Hector, J., 1989. Dimethyl disulfide derivatives of long chain alkenes, alkadienes, and alkatrienes for gas chromatography/mass spectrometry. Analytical Chemistry 61, 1564–1571.

Chaffee, A.L., Hoover, D.S., Johns, R.B., Scheweighardt, F.M., 1986. Biological markers extractable from coal, In: Johns, R.B. (Ed.), Biological Markers in the Sedimentary Record. Elsevier, Amsterdam, pp. 311–345.

Cheng, Q., Guanghui, H., Zhang, M., Wenjun, Z., Xi, L., 2019. Distribution and source significance of 2-methylalkanes in coal-measure source rocks, northwest China.

Journal of Petroleum Science and Engineering 174, 257–267.

Coates, R.C., Podell, S., Korobeynikov, A., Lapidus, A., Pevzner, P., Sherman, D.H., Allen, E.E., Gerwick, L., Gerwick, W.H., 2014. Characterization of cyanobacterial hydrocarbon composition and distribution of biosynthetic pathways. PLoS ONE 9, e85140.

Cohen, P.A., Kodner, R.B., 2022. The earliest history of eukaryotic life: uncovering an evolutionary story through the integration of biological and geological data. Trends in Ecology and Evolution 37, 246–256.

Corbier, B., Teisseire, P., 1974. Contribution to the knowledge of absolute oakmoss oil. Recherches 19, 291–294.

Cornejo, C., Scheidegger, C., 2015. Multi-gene phylogeny of the genus *Lobaria*: Evidence of species-pair and allopatric cryptic speciation in east asia. American Journal of Botany 102, 2058–2073.

Craig, J., Biffi, U., Galimberti, R.F., Ghori, K.A.R., Gorter, J.D., Hakhoo, N., Le Heron, D.P., Thurow, J., Vecoli, M., 2013. The palaeobiology and geochemistry of Precambrian hydrocarbon source rocks. Marine and Petroleum Geology 40, 1–47.

Cranwell, P.A., Eglinton, G., Robinson, N., 1987. Lipids of aquatic organisms as potential contributors to lacustrine sediments-II. Organic Geochemistry 11, 513–527.

Czeczuga, B., Czeczuga-semeniuk, E., 2002. Seasonal changes in the size of phyco- and photobiont cells in some lichen species of the Knyszyǹska Forest (N-E Poland). The Journal of the Hattori Botanical Laboratory 92, 261–275.

Dahlkild, Å., Källersjö, M., Lohtander, K., Tehler, A., 2001. Photobiont diversity in the Physciaceae (Lecanorales). Bryologist 104, 527–536.

Dal Grande, F., Beck, A., Cornejo, C., Singh, G., Cheenacharoen, S., Nelsen, M.P., Scheidegger, C., 2014. Molecular phylogeny and symbiotic selectivity of the green algal genus *Dictyochloropsis* s.l. (Trebouxiophyceae): A polyphyletic and widespread group forming photobiont-mediated guilds in the lichen family Lobariaceae. New Phytologist 202, 455–470.

Dawes, P.R., 1997. The Proterozoic Thule Supergroup, Greenland and Canada: history, lithostratigraphy and development, Geology of Greenland Survey Bulletin.

Dawes, P.R., 2006. Explanatory notes to the Geological map of Greenland, 1:500 000, Thule, Sheet 5.

Dembitsky, V.M., Rezanka, T., Bychek, I.A., 1994a. Seasonal variation of lipids and fatty acids from tree-growing lichens of the genus *Physcia*. Phytochemistry 36, 601–608.

Dembitsky, V.M., Rezanka, T., Bychek, I.A., 1994b. Seasonal variability of lipids and fatty acids in the tree-growing lichen *Xanthoria parientina* L.. Journal of Experimental Botany 45, 403–408.

de Mesmay, R., Grossi, V., Williamson, D., Kajula, S., Derenne, S., 2007. Novel mono-, di- and tri-unsaturated very long chain (C_{37}-C_{43}) *n*-alkenes in alkenone-free lacustrine sediments (Lake Masoko, Tanzania). Organic Geochemistry 38, 323–333.

Didyk, B.M., Simoneit, B.R.T., Brassell, S.C., Eglinton, G., 1978. Organic geochemical indicators of paleoenvironmental conditions of sedimentation. Nature 272, 216–221.

Dixon, R.A., 2001. Natural products and plant disease resistance. Nature 411, 843–847.

Douka, E., Koukkou, A.I., Drainas, C., Grosdemange-Billiard, C., Rohmer, M., 2001. Structural diversity of the triterpenic hydrocarbons from the bacterium *Zymomonas mobilis*: The signature of defective squalene cyclization by the squalene/hopene cyclase. FEMS Microbiology Letters 199, 247–251.

Du Vivier, A.D.C., Selby, D., Condon, D.J., Takashima, R., Nishi, H., 2015. Pacific ^{187}Os/^{188}Os isotope chemistry and U-Pb geochronology: Synchroneity of global Os isotope change across OAE 2. Earth and Planetary Science Letters 428, 204–216.

Eaton, J.G., Kirkland, J.I., Hutchison, J.H., Denton, R., O'Neill, R.C., Parrish, J.M., 1997. Nonmarine extinction across the Cenomanian-Turonian boundary, southwestern Utah, with a comparison to the Cretaceous-Tertiary extinction event. Bulletin of the Geological Society of America 109, 560–567.

Elbert, W., Weber, B., Burrows, S., Steinkamp, J., Büdel, B., Andreae, M.O., Pöschl, U., 2012. Contribution of cryptogamic covers to the global cycles of carbon and nitrogen. Nature Geoscience 5, 459–462.

Eldrett, J.S., Ma, C., Bergman, S.C., Lutz, B., Gregory, F.J., Dodsworth, P., Phipps, M., Hardas, P., Minisini, D., Ozkan, A., Ramezani, J., Bowring, S.A., Kamo, S.L., Ferguson, K., Macaulay, C., Kelly, A.E., 2015. An astronomically calibrated stratigraphy of the Cenomanian, Turonian and earliest Coniacian from the Cretaceous Western Interior Seaway, USA: Implications for global chronostratigraphy. Cretaceous Research 56, 316–344.

Eme, L., Sharpe, S.C., Brown, M.W., Roger, A.J., 2014. On the Age of Eukaryotes: Evaluating Evidence from Fossils and Molecular Clocks. Cold Spring Harbor Perspectives in Biology 6.

Eriksson, O.V.E.E., 2005. Origin and evolution of Ascomycota – the protolichenes hypothesis. Svensk Mykolisk Tidskrift 26, 30-33.

Eshet, Y., Rampino, M.R., Visscher, H., 1995. Fungal event and palynological record of ecological crisis and recovery across the Permian-Triassic boundary. Geology 23, 967–970.

Fenton, S., Grice, K., Twitchett, R.J., Böttcher, M.E., Looy, C. V., Nabbefeld, B., 2007. Changes in biomarker abundances and sulfur isotopes of pyrite across the Permian-Triassic (P/Tr) Schuchert Dal section (East Greenland). Earth and Planetary Science Letters 262, 230–239.

Fernando, A.G.S., Nishi, H., Tanabe, K., Moriya, K., Iba, Y., Kodama, K., Murphy, M.A., Okada, H., 2011. Calcareous nannofossil biostratigraphic study of forearc basin sediments: Lower to Upper Cretaceous Budden Canyon Formation (Great Valley Group), northern California, USA. Island Arc 20, 346–370.

Feuerer, T., Hawksworth, D.L., 2007. Biodiversity of lichens, including a world-wide analysis of checklist data based on Takhtajan's floristic regions. Biodiversity and Conservation 16, 85–98.

Ficken, K.J., Barber, K.E., Eglinton, G., 1998. Lipid biomarker, δ^{13}C and plant macrofossil stratigraphy of a Scottish montane peat bog over the last two millennia. Organic Geochemistry 28, 217–237.

Forster, A., Schouten, S., Moriya, K., Wilson, P.A., Damsté, J.S.S., 2007. Tropical warming and intermittent cooling during

the Cenomanian/Turonian oceanic anoxic event 2: Sea surface temperature records from the equatorial Atlantic. Paleoceanography 22, 1–14.

Francis, G.W., Veland, K., 1981. Alkylthiolation for the determination of double-bond positions in linear alkenes. Journal of Chromatography A 219, 379–384.

Fukushima, K., Mochizuki, M., Hayashi, H., Ishikawa, R., Uemura, H., Ogura, K., Tanaka, A., 1996. Long-chain anteiso compound series found in acidified freshwater lake sediments in Japan: Lake Tazawa-ko. Geochemical Journal 30, 111–130.

Fukushima, K., Yoda, A., Kayama, M., Miki, S., 2005. Implications of long-chain *anteiso* compounds in acidic freshwater lake environments: Inawashiro-ko in Fukushima Prefecture, Japan. Organic Geochemistry 36, 311–323.

Fullana, A., Sidhu, S.S., 2005. Fate of PAHs in the post-combustion zone: Partial oxidation of PAHs to dibenzofuran over CuO. Journal of Analytical and Applied Pyrolysis 74, 479–485.

Gaskell, S.J., Eglinton, G., Bruun, T., 1973. Hydrocarbon constituents of three species of Norwegian lichen: *Cetraria nivalis*, *C. crispa*, *Siphula ceratites*. Phytochemistry 12, 1174–1176.

Gavin, J., Nicollier, G., Tabacchi, R., 1978. Volatile components of "oak moss" (*Evernia prunastri* (L.) ACH.) 3rd communication. Helvetica Chimica Acta 61, 352–357 (in French with English abstract).

Gaya, E., Fernández-Brime, S., Vargas, R., Lachlan, R.F., Gueidan, C., Ramírez-Mejía, M., Lutzoni, F., 2015. The adaptive radiation of lichen-forming Teloschistaceae is associated with

sunscreening pigments and a bark-to-rock substrate shift. Proceedings of the National Academy of Sciences 112, 11600–11605.

Gelpi, E., Schneider, H., Mann, J., Oró, J., 1970. Hydrocarbons of geochemical significance in microscopic algae. Phytochemistry 9, 603–612.

Cohen, P.A., Kodner, R.B., 2022. The earliest history of eukaryotic life: uncovering an evolutionary story through the integration of biological and geological data. Trends in Ecology and Evolution 37, 246–256.

Graham, L.E., Trest, M.T., Cook, M.E., 2017. Acetolysis resistance of modern fungi: Testing attributions of enigmatic proterozoic and early paleozoic fossils. International Journal of Plant Sciences 178, 330–339.

Grice, K., Lu, H., Atahan, P., Asif, M., Hallmann, C., Greenwood, P., Maslen, E., Tulipani, S., Williford, K., Dodson, J., 2009. New insights into the origin of perylene in geological samples. Geochimica et Cosmochimica Acta 73, 6531–6543.

Guiry, M.D., Guiry, G.M., 2020. AlgaeBase [WWW Document]. AlgaeBase. URL https://www.algaebase.org (accessed 11.6.22).

Hallbauer, D.K., Jahns, H.M., Beltmann, H.A., 1977. Morphological and anatomical observations on some precambrian plants from the Witwatersrand, South Africa. Geologische Rundschau 66, 477–491.

Hanke, U.M., Lima-Braun, A.L., Eglinton, T.I., Donnelly, J.P., Galy, V., Poussart, P., Hughen, K., McNichol, A.P., Xu, L., Reddy, C.M., 2019. Significance of perylene for source allocation of terrigenous organic matter in aquatic sediments. Environmental Science and Technology 53, 8244–8251.

Hara, Y., 2022. Biogeochemical significance of molecular fossils and organic-walled microfossils in the Mesoproterozoic sedimentary rocks from northwestern Greenland. Master Thesis of Department of Science, Hokkaido University (in Japanese).

Harris, L.I., Moore, T.R., Roulet, N.T., Pinsonneault, A.J., 2018. Lichens: A limit to peat growth? Journal of Ecology 106, 2301–2319.

Hasegawa, T., 2001. Predominance of terrigenous organic matter in Cretaceous marine fore-arc sediments, Japan and Far East Russia. International Journal of Coal Geology 47, 207–221.

Hasegawa, T., 2003. Cretaceous terrestrial paleoenvironments of northeastern Asia suggested from carbon isotope stratigraphy: Increased atmospheric pCO_2-induced climate. Journal of Asian Earth Sciences 21, 849–859.

Hatcher, P.G., Clifford, D.J., 1997. The organic geochemistry of coal: From plant materials to coal. Organic Geochemistry 27, 251–257.

Hautevelle, Y., Michels, R., Lannuzel, F., Malartre, F., Trouiller, A., 2006. Confined pyrolysis of extant land plants: A contribution to palaeochemotaxonomy. Organic Geochemistry 37, 1546–1561.

Hawksworth, D.L., Lücking, R., 2017. Fungal Diversity Revisited: 2.2 to 3.8 million Species. Microbiology Spectrum 5, 79–95.

Hay, W.W., Floegel, S., 2012. New thoughts about the Cretaceous climate and oceans. Earth-Science Reviews 115, 262–272.

He, D., Simoneit, B.R.T., Jara, B., Jaffé, R., 2015. Occurrence and distribution of monomethylalkanes in the freshwater wetland ecosystem of the Florida Everglades. Chemosphere 119, 258–266.

Hedges, J.I., Cowie, G.L., Ertel, J.R., Barbour, R.J., Hatcher, P.G., 1985. Degradation of carbohydrates and lignins in buried woods. Geochimica et Cosmochimica Acta 49, 701–711.

Heimhofer, U., Hesselbo, S.P., Pancost, R.D., Martill, D.M., Hochuli, P.A., Guzzo, J.V.P., 2008. Evidence for photic-zone euxinia in the Early Albian Santana Formation (Araripe Basin, NE Brazil). Terra Nova 20, 347–354.

Heimhofer, U., Wucherpfennig, N., Adatte, T., Schouten, S., Schneebeli-Hermann, E., Gardin, S., Keller, G., Kentsch, S., Kujau, A., 2018. Vegetation response to exceptional global warmth during Oceanic Anoxic Event 2. Nature Communications 9.

Hennig, C., 2020. fpc: Flexible procedures for clustering.

Herrle, J.O., Pross, J., Friedrich, O., Kößler, P., Hemleben, C., 2003. Forcing mechanisms for mid-Cretaceous black shale formation: Evidence from the Upper Aptian and Lower Albian of the Vocontian Basin (SE France). Palaeogeography, Palaeoclimatology, Palaeoecology 190, 399–426.

Hoffman, P.F., Schrag, D.P., 2002. The snowball Earth hypothesis: Testing the limits of global change. Terra Nova 14, 129–155.

Honegger, R., 2008. Mycobionts, In: T. H. Nash, T.H. (Ed.), Lichen biology, 2nd ed. Cambridge University Press, Cambridge. pp. 27-39

Honegger, R., 2018. Fossil lichens from the Lower Devonian and their bacterial and fungal epi- and endobionts. In: Blanz, P. (Ed.), Biodiversity and Ecology of fungi, lichens and mosses. Kerner von Marilaun Workshop 2015 in memory of Josef Poelt. Biosystematics and Ecology Series

34. Verlag der Österreichischen Akademie der Wissenschaften, Wien, 547-563.

Honegger, R., Axe, L., Edwards, D., 2013a. Bacterial epibionts and endolichenic actinobacteria and fungi in the Lower Devonian lichen *Chlorolichenomycites salopensis*. Fungal Biology 117, 512–518.

Honegger, R., Edwards, D., Axe, L., 2013b. The earliest records of internally stratified cyanobacterial and algal lichens from the Lower Devonian of the Welsh Borderland. New Phytologist 197, 264–275.

Huang, J.-P., Kraichak, E., Leavitt, S.D., Nelsen, M.P., Lumbsch, H.T., 2019. Accelerated diversifications in three diverse families of morphologically complex lichen-forming fungi link to major historical events. Scientific Reports 9, 8518.

Huang, X., Wang, C., Xue, J., Meyers, P.A., Zhang, Z., Tan, K., Zhang, Zhiqi, Xie, S., 2010. Occurrence of diploptene in moss species from the Dajiuhu Peatland in southern China. Organic Geochemistry 41, 321–324.

Huang, X., Xue, J., Guo, S., 2012. Long chain *n*-alkanes and their carbon isotopes in lichen species from western Hubei Province: implication for geological records. Frontiers of Earth Science 6, 95–100.

Huneck, S., Yoshimura, I., 1996. Identification of Lichen Substances. Springer-Vrlag Berlin Heidelberg, Berlin.

Ikeda, M.A., Nakamura, H., Sawada, K., 2018. Aliphatic hydrocarbons identified in lichen genus *Cladonia* and *Xanthoria* : Potential for their chemotaxonomic and environmental indicators. Researches in Organic Geochemistry 34, 15–28 (in Japanese with English abstract).

Ikeda, M.A., Nakamura, H., Sawada, K., 2021. Long-chain alkenes and alkadienes of eight lichen species collected in Japan. Phytochemistry 189, 112823.

Itoh, N., Sakagami, N., Torimura, M., Watanabe, M., 2012. Perylene in Lake Biwa sediments originating from *Cenococcum geophilum* in its catchment area. Geochimica et Cosmochimica Acta 95, 241–251.

Jaffé, R., Hausmann, K.B., 1995. Origin and early diagenesis of arborinone/isoarborinol in sediments of a highly productive freshwater lake. Organic Geochemistry 22, 231–235.

Jenkyns, H.C., Dickson, A.J., Ruhl, M., van den Boorn, S.H.J.M., 2017. Basalt-seawater interaction, the Plenus Cold Event, enhanced weathering and geochemical change: deconstructing Oceanic Anoxic Event 2 (Cenomanian–Turonian, Late Cretaceous). Sedimentology 64, 16–43.

Jia, G., Dungait, J.A.J., Bingham, E.M., Valiranta, M., Korhola, A., Evershed, R.P., 2008. Neutral monosaccharides as biomarker proxies for bog-forming plants for application to palaeovegetation reconstruction in ombrotrophic peat deposits. Organic Geochemistry 39, 1790–1799.

Jiang, C., Alexander, R., Kagi, R.I., Murray, A.P., 2000. Origin of perylene in ancient sediments and its geological significance. Organic Geochemistry 31, 1545–1559.

Jones, M.M., Sageman, B.B., Oakes, R.L., Parker, A.L., Leckie, R.M., Bralower, T.J., Sepúlveda, J., Fortiz, V., 2019. Astronomical pacing of relative sea level during Oceanic Anoxic Event 2: Preliminary studies of the expanded SH#1 Core, Utah, USA. Bulletin of the

Geological Society of America 131, 1702–1722.

Joppa, L.N., Roberts, D.L., Pimm, S.L., 2011. How many species of flowering plants are there? Proceedings of the Royal Society B: Biological Sciences 278, 554–559.

Kaiser, J., Ön, B., Arz, H.W., Akçer-Ön, S., 2016. Sedimentary lipid biomarkers in the magnesium rich and highly alkaline Lake Salda (south-western Anatolia). Journal of Limnology 75, 581–596.

Karatygin, I. V, Snigirevskaya, N.S., Vikulin, S. V, 2009. The most ancient terrestrial lichen *Winfrenatia reticulata*: A new find and new interpretation. Paleontological Journal 43, 107–114.

Kaasalainen, U., Schmidt, A.R., Rikkinen, J., 2017. Diversity and ecological adaptations in Palaeogene lichens. Nature Plants 3, 1–8.

Kavouras, I.G., Stratigakis, N., Stephanou, E.G., 1998. *Iso-* and *anteiso*-alkanes: Specific tracers of environmental tobacco smoke in indoor and outdoor particle-size distributed urban aerosols. Environmental Science and Technology 32, 1369–1377.

Kenig, F., Sinninghe Damsté, J.S., Kock-van Dalen, A.C., Rijpstra, W.I.C., Huc, A.Y., de Leeuw, J.W., 1995. Occurrence and origin of mono-, di-, and trimethylalkanes in modern and Holocene cyanobacterial mats from Abu Dhabi, United Arab Emirates. Geochimica et Cosmochimica Acta 59, 2999–3015.

Kennedy, M., Droser, M., Mayer, L.M., Pevear, D., Mrofka, D., 2006. Supporting Online Material for Late precambrian oxygenation; inception of the clay mineral factory. Science 311, 1446–1449.

Kokubun, T., Harborne, J.B., Eagles, J., Waterman, P.G., 1995. Dibenzofuran phytoalexins from the sapwood of Cotoneaster acutifolius and five related species. Science 38, 5–8.

Kolde, R., 2019. pheatmap: Pretty Heatmaps.

Kraichak, E., Divakar, P.K., Crespo, A., Leavitt, S.D., Nelsen, M.P., Lücking, R., Lumbsch, H.T., 2015. A tale of two hyper-diversities: Diversification dynamics of the two largest families of lichenized fungi. Scientific Reports 5, 10028.

Kump, L.R., 2008. The rise of atmospheric oxygen. Nature 451, 277–278.

Kump, L.R., 2014. Hypothesized link between Neoproterozoic greening of the land surface and the establishment of an oxygen-rich atmosphere. Proceedings of the National Academy of Sciences of the United States of America 111, 14062–14065.

Kuypers, M.M.M., Pancost, R.D., Sinninghe Damsté, J.S., 1999. A large and abrupt fall in atmospheric CO_2 concentration during cretaceous times. Nature 399, 342–345.

Ladygina, N., Dedyukhina, E.G., Vainshtein, M.B., 2006. A review on microbial synthesis of hydrocarbons. Process Biochemistry 41, 1001–1014.

Larson, D. W., 1987. The absorption and release of water by lichens. Bibliotheca Lichenologica 25, 351-360.

Leavitt, S.D., Kraichak, E., Nelsen, M.P., Altermann, S., Divakar, P.K., Alors, D., Esslinger, T.L., Crespo, A., Lumbsch, T., 2015. Fungal specificity and selectivity for algae play a major role in determining lichen partnerships across diverse ecogeographic regions in the lichen-forming family Parmeliaceae (Ascomycota). Molecular Ecology 24, 3779–3797.

Li, Y.X., Montañez, I.P., Liu, Z., Ma, L., 2017. Astronomical constraints on global

carbon-cycle perturbation during Oceanic Anoxic Event 2 (OAE2). Earth and Planetary Science Letters 462, 35–46.

Li, J., Xue, J., Naafs, B.D.A., Yang, Y., Yang, H., Liu, D., 2022. Distribution and carbon isotopic composition of diploptene from epiphytic bryophytes in Wuhan, central China. Organic Geochemistry 173, 104506.

Liu, A., Zhu, T., Lu, X., Song, L., 2013. Hydrocarbon profiles and phylogenetic analyses of diversified cyanobacterial species. Applied Energy 111, 383–393.

Loron, C.C., François, C., Rainbird, R.H., Turner, E.C., Borensztajn, S., Javaux, E.J., 2019. Early fungi from the Proterozoic era in Arctic Canada. Nature 570, 232–235.

Lücking, R., Hodkinson, B.P., Leavitt, S.D., 2016. The 2016 classification of lichenized fungi in the Ascomycota and Basidiomycota – Approaching one thousand genera. The Bryologist 119, 361–416.

Lücking, R., Huhndorf, S., Pfister, D.H., Plata, E.R., Lumbsch, H.T., 2009. Fungi evolved right on track. Mycologia 101, 810–822.

Lücking, R., Nelsen, M.P. (2018). Ediacarans, protolichens, and lichen-derived Penicillium: A critical reassessment of the evolution of lichenization in fungi. In: Krings, M., Harper, C.J., Cúneo, M.R., Rothwell, G.W. (Eds.), Transformative paleobotany. London, UK: Academic Press, 551-590.

Lyons, T.W., Reinhard, C.T., Planavsky, N.J., 2014. The rise of oxygen in Earth's early ocean and atmosphere. Nature 506, 307–315.

Maffei, M., 1994. Discriminant analysis of leaf wax alkanes in the Lamiaceae and four other plant families. Biochemical Systematics and Ecology 22, 711–728.

Marynowski, L., Smolarek, J., Bechtel, A., Philippe, M., Kurkiewicz, S., Simoneit, B.R.T., 2013. Perylene as an indicator of conifer fossil wood degradation by wood-degrading fungi. Organic Geochemistry 59, 143–151.

Marynowski, L., Smolarek, J., Hautevelle, Y., 2015. Perylene degradation during gradual onset of organic matter maturation. International Journal of Coal Geology 139, 17–25.

Matsumoto, G.I., Akiyama, M., Watanuki, K., Torii, T., 1990. Unusual distributions of long-chain n-alkanes and n-alkenes in Antarctic soil. Organic Geochemistry 15, 403–412.

Matsumoto, G.I., Friedmann, E.I., Watanuki, K., Ocampo-Friedmann, R., 1992. Novel long-chain anteiso-alkanes and anteiso-alkanoic acids in Antarctic rocks colonized by living and fossil cryptoendolithic microorganisms. Journal of Chromatography A 598, 267–276.

Matsunaga, K.K.S., Stockey, R. a, Tomescu, A.M.F., 2013. Honeggeriella complexa gen. et sp. nov., a heteromerous lichen from the Lower Cretaceous of Vancouver Island (British Columbia, Canada). American journal of botany 100, 450–459.

Matsuoka, K., 1992. Seasonal variability of palynomorphs in a JT-03 sediment trap setteled in the Japan Trench. Bulletin of the Faculty of Liberal Arts, Nagasaki University. Natural science 32, 221–233 (In Japanese).

Méjanelle, L., Rivière, B., Pinturier, L., Khripounoff, A., Baudin, F., Dachs, J., 2017. Aliphatic hydrocarbons and triterpenes of the Congo deep-sea fan.

Deep-Sea Research Part II: Topical Studies in Oceanography 142, 109–124.

Miadlikowska, J., Kauff, F., Hofstetter, V., Fraker, E., Grube, M., Hafellner, J., Reeb, V., Hodkinson, B.P., Kukwa, M., Lücking, R., Hestmark, G., Otalora, M.G., Rauhut, A., Büdel, B., Scheidegger, C., Timdal, E., Stenroos, S., Brodo, I., Perlmutter, G.B., Ertz, D., Diederich, P., Lendemer, J.C., May, P., Schoch, C.L., Arnold, A.E., Gueidan, C., Tripp, E., Yahr, R., Robertson, C., Lutzoni, F., 2006. New insights into classification and evolution of the Lecanoromycetes (Pezizomycotina, Ascomycota) from phylogenetic analyses of three ribosomal RNA- and two protein-coding genes. Mycologia 98, 1088–1103.

Miadlikowska, J., Kauff, F., Högnabba, F., Oliver, J.C., Molnár, K., Fraker, E., Gaya, E., Hafellner, J., Hofstetter, V., Gueidan, C., Otálora, M.A.G., Hodkinson, B., Kukwa, M., Lücking, R., Björk, C., Sipman, H.J.M., Burgaz, A.R., Thell, A., Passo, A., Myllys, L., Goward, T., Fernández-Brime, S., Hestmark, G., Lendemer, J., Lumbsch, H.T., Schmull, M., Schoch, C.L., Sérusiaux, E., Maddison, D.R., Arnold, A.E., Lutzoni, F., Stenroos, S., 2014. A multigene phylogenetic synthesis for the class Lecanoromycetes (Ascomycota): 1307 fungi representing 1139 infrageneric taxa, 317 genera and 66 families. Molecular Phylogenetics and Evolution 79, 132–168.

Millot, M., Dieu, A., Tomasi, S., 2016. Dibenzofurans and derivatives from lichens and ascomycetes. Natural Product Reports 33, 801–811.

Moya, P., Škaloud, P., Chiva, S., García-Breijo, F.J., Reig-Armiñana, J., Vančurová, L., Barreno, E., 2015. Molecular phylogeny and ultrastructure of the lichen microalga *Asterochloris mediterranea* sp. nov. from Mediterranean and Canary Islands ecosystems. International Journal of Systematic and Evolutionary Microbiology 65, 1838–1854.

MycoBank Fungal Databases Nomenclature and Species Bank, 2022.[WWW Document] International Mycological Association. URL https://www.mycobank.org (accessed 11.6.22).

Myllys, L., Stenroos, S., Thell, A., Kuusinen, M., 2007. High cyanobiont selectivity of epiphytic lichens in old growth boreal forest of Finland. New Phytologist 173, 621–629.

Nakagawa, Y., Legrand, J., Bôle, M., Hori, R.S., Kuroda, J., Hasegawa, H., Ikeda, M., 2022. Terrestrial and marine organic matter evidence from a Cretaceous deep-sea chert of Japan: Implications for enhanced hydrological cycle during the Aptian OAE 1a. Global and Planetary Change 215, 103886.

Nakamura, H., Sawada, K., Araie, H., Suzuki, I., Shiraiwa, Y., 2015. *n*-Nonacosadienes from the marine haptophytes *Emiliania huxleyi* and *Gephyrocapsa oceanica*. Phytochemistry 111, 107–113.

Nakamura, H., Sawada, K., Takahashi, M., 2010. Aliphatic and aromatic terpenoid biomarkers in Cretaceous and Paleogene angiosperm fossils from Japan. Organic Geochemistry 41, 975–980.

Nelson, D.R., Dillwith, J.W., Blomquist, G.J., 1981. Cuticular hydrocarbons of the house fly, *Musca domestica*. Insect Biochemistry 11, 187–197.

Nelsen, M.P., Lücking, R., Boyce, C.K., Lumbsch, H.T., Ree, R.H., 2020. No support for the emergence of lichens prior

to the evolution of vascular plants. Geobiology 18, 3–13.

Norris, R.D., Bice, K.L., Magno, E.A., Wilson, P.A., 2002. Jiggling the tropical thermostat in the Cretaceous hothouse. Geology 30, 299–302.

Nyati, S., Scherrer, S., Werth, S., Honegger, R., 2014. Green-algal photobiont diversity (*Trebouxia* spp.) in representatives of Teloschistaceae (Lecanoromycetes, lichen-forming ascomycetes). The Lichenologist 46, 189–212.

O'Brien, C.L., Robinson, S.A., Pancost, R.D., Sinninghe Damsté, J.S., Schouten, S., Lunt, D.J., Alsenz, H., Bornemann, A., Bottini, C., Brassell, S.C., Farnsworth, A., Forster, A., Huber, B.T., Inglis, G.N., Jenkyns, H.C., Linnert, C., Littler, K., Markwick, P., McAnena, A., Mutterlose, J., Naafs, B.D.A., Püttmann, W., Sluijs, A., van Helmond, N.A.G.M., Vellekoop, J., Wagner, T., Wrobel, N.E., 2017. Cretaceous sea-surface temperature evolution: Constraints from TEX$_{86}$ and planktonic foraminiferal oxygen isotopes. Earth-Science Reviews 172, 224–247.

O'Brien, H.E., Miadlikowska, J., Lutzoni, F., 2005. Assessing host specialization in symbiotic cyanobacteria associated with four closely related species of the lichen fungus *Peltigera*. European Journal of Phycology 40, 363–378.

O'Connor, L.K., Jenkyns, H.C., Robinson, S.A., Remmelzwaal, S.R.C., Batenburg, S.J., Parkinson, I.J., Gale, A.S., 2020. A Re-evaluation of the Plenus Cold Event, and the Links Between CO2, Temperature, and Seawater Chemistry During OAE 2. Paleoceanography and Paleoclimatology 35, 1–23.

Opsahl, S., Benner, R., 1999. Characterization of carbohydrates during early diagenesis of five vascular plant tissues. Organic Geochemistry 30, 83–94.

Otálora, M.A.G., Martínez, I., O'Brien, H., Molina, M.C., Aragón, G., Lutzoni, F., 2010. Multiple origins of high reciprocal symbiotic specificity at an intercontinental spatial scale among gelatinous lichens (Collemataceae, Lecanoromycetes). Molecular Phylogenetics and Evolution 56, 1089–1095.

Okano K., Sawada K., Takashima R., Nishi H. and Okada H. (2007) Depositional environments revealed from biomarkers in sediments deposited during the mid-Cretaceous oceanic anoxic events (OAEs) in the Vocontian Basin (SE France). Okada, H., Mawatari, S.F., Suzuki, N. and Gautam, P. (eds.), Origin and Evolution of Natural Diversity, Proceedings of International Symposium "The Origin and Evolution of Natural Diversity", 1–5 October 2007, Sapporo, pp. 233-238.

Palmqvist, K., Dahlman, L., 2006. Responses of the green algal foliose lichen *Platismatia glauca* to increased nitrogen supply. New Phytologist 171, 343–356.

Panagiotopoulos, C., Sempéré, R., 2007. Sugar dynamics in large particles during *in vitro* incubation experiments. Marine Ecology Progress Series 330, 67–74.

Pankratov, T.A., 2018. Bacterial complexes of Khibiny Mountains lichens revealed in *Cladonia uncialis*, *C. portentosa*, *Alectoria ochroleuca*, and *Nephroma arcticum*. Microbiology (Russian Federation) 87, 70–78.

Parfrey, L.W., Lahr, D.J.G., Knoll, A.H., Katz, L.A., 2011. Estimating the timing of early eukaryotic diversification with multigene molecular clocks. Proceedings of the National Academy of Sciences of the

United States of America 108, 13624–13629.

Paton, A.J., 2008. Towards target 1 of the global strategy for plant conservation: A working list of all known plant species - Progress and prospects. Taxon 57, 602-611.

Paull, R., Michaelsen, B.H., McKirdy, D.M., 1998. Fernenes and other triterpenoid hydrocarbons in *Dicroidium*-bearing Triassic mudstones and coals from South Australia. Organic Geochemistry 29, 1331–1343.

Payette, S., Delwaide, A., 2018. Tamm review: The North-American lichen woodland. Forest Ecology and Management 417, 167–183.

Peksa, O., Škaloud, P., 2011. Do photobionts influence the ecology of lichens? A case study of environmental preferences in symbiotic green alga *Asterochloris* (Trebouxiophyceae). Molecular Ecology 20, 3936–3948.

Pieńkowski, G., Hodbod, M., Ullmann, C. V., 2016. Fungal decomposition of terrestrial organic matter accelerated Early Jurassic climate warming. Scientific Reports 6, 1–11.

Piervittori, R., Alessio, F., Usai, L., Maffei, M., 1995. Seasonal variations in lipids of *Xanthoria parietina* growing at high elevations. Phytochemistry 40, 717–723.

Piervittori, R., Usai, L., Alessio, F., Maffei, M., 1996. Surface *n*-alkane variability in *Xanthoria parietina*. The Lichenologist 28, 79–87.

Pino-Bodas, R., Stenroos, S., 2021. Global biodiversity patterns of the photobionts associated with the genus *Cladonia* (Lecanorales, Ascomycota). Microbial Ecology 82, 173–187.

Powell, T. G., 1988. Pristane/phytane ratio as environmental indicator. Nature 333, 604.

Prieto, M., Wedin, M., 2013. Dating the diversification of the major lineages of Ascomycota (Fungi). PLoS ONE 8, e65576.

Printzen, C., Lumbsch, H.T., 2000. Molecular evidence for the diversification of extant lichens in the Late Cretaceous and tertiary. Molecular Phylogenetics and Evolution 17, 379–387.

R Core Team, 2022. R: A language and environment for statistical computing. R Foundation for Statistical Computing, Vienna, Austria.

Radke, M., Vriend, S.P., Ramanampisoa, L.R., 2000. Alkyldibenzofurans in terrestrial rocks: Influence of organic facies and maturation. Geochimica et Cosmochimica Acta 64, 275–286.

Rafat, A., Ridgway, H.J., Cruickshank, R.H., Buckley, H.L., 2015. Isolation and co-culturing of symbionts in the genus *Usnea*. Symbiosis 66, 123–132.

Rampino, M.R., Eshet, Y., 2018. The fungal and acritarch events as time markers for the latest Permian mass extinction: An update. Geoscience Frontiers 9, 147–154.

Redecker, D., Kodner, R., Graham, L.E., 2000. Glomalean fungi from the Ordovician. Science 289, 1920–1921.

Reis, R.A., Iacomini, M., Gorin, P.A.J., Souza, L.M., Grube, M., Cortes Cordeiro, L.M., Sassaki, G.L., 2005. Fatty acid composition of the tropical lichen *Teloschistes flavicans* and its cultivated symbionts. FEMS Microbiology Letters 247, 1–6.

Retallack, G.J., 1994. Were the Ediacaran fossils lichens? Paleobiology 20, 523–544.

Retallack, G.J., 1995. Ediacaran lichens-A reply to Waggoner. Paleontological Society 21, 398–399.

Retallack, G.J., 2007. Growth, decay and burial compaction of *Dickinsonia*, an iconic Ediacaran fossil. Alcheringa 31, 215–240.

Retallack, G.J., 2013. Ediacaran life on land. Nature 493, 89–92.

Rieley, G., Teece, M.A., Peakman, T.M., Raven, A.M., Greene, K.J., Clarke, T.P., Murray, M., Leftley, J.W., Campbell, C.N., Harris, R.P., Parkes, R.J., Maxwell, J.R., 1998. Long-chain alkenes of the haptophytes *Isochrysis galbana* and *Emiliania huxleyi*. Lipids 33, 617–625.

Rikkinen, J., Oksanen, I., Lohtander, K., 2002. Lichen guilds share related cyanobacterial symbionts. Science 297, 357.

Rogge, W.F., Hildemann, L.M., Mazurek, M.A., Cass, G.R., Simonelt, B.R.T., 1994. Sources of fine organic aerosol. 6. cigarette smoke in the urban atmosphere. Environmental Science and Technology 28, 1375–1388.

Sageman, B.B., Meyers, S.R., Arthur, M.A., 2006. Orbital time scale and new C-isotope record for Cenomanian-Turonian boundary stratotype. Geology 34, 125–128.

Samuelsson, J., Dawes, P.R., Vidal, G., 1999. Organic-walled microfossils from the Proterozoic Thule Supergroup, Northwest Greenland. Precambrian Research 96, 1–23.

Santos, L.S., Soriano, M. del P.C., Mirabal-Gallardo, Y., Carrasco-sanchez, V., Nachtigall, F.M., Pereira, I., Pereira, E., 2015. Chemotaxonomic fingerprinting of Chilean lichens through maldi and electrospray ionization mass spectrometry. Brazilian Archives of Biology and Technology 58, 244–253.

Sassaki, G.L., Cruz, L.M., Gorin, P.A.J., Iacomini, M., 2001. Fatty acid composition of lipids present in selected lichenized fungi: A chemotyping study. Lipids 36, 167–175.

Sawada, K., 2006. Organic facies wand geochemical aspects in Neogene neritic sediments of the Takafu syncline area of Central Japan: Paleoenviromental and sedimentological reconstructions. Island Arc 15, 517–536.

Sawada, K., Kaiho, K., Okano, K., 2012. Kerogen morphology and geochemistry at the Permian-Triassic transition in the Meishan section, South China: Implication for paleoenvironmental variation. Journal of Asian Earth Sciences 54–55, 78–90.

Sawada, K., Nakamura, H., Arai, T., Tsukagoshi, M., 2013. Evaluation of paleoenvironment using terpenoid biomarkers in lignites and plant fossil from the Miocene Tokiguchi Porcelain Clay Formation at the Onada mine, Tajimi, central Japan. International Journal of Coal Geology 107, 78–89.

Schellekens, J., Bradley, J.A., Kuyper, T.W., Fraga, I., Pontevedra-Pombal, X., Vidal-Torrado, P., Abbott, G.D., Buurman, P., 2015. The use of plant-specific pyrolysis products as biomarkers in peat deposits. Quaternary Science Reviews 123, 254–264.

Sephton, M.A., Looy, C. V., Brinkhuis, H., Wignall, P.B., de Leeuw, J.W., Visscher, H., 2005. Catastrophic soil erosion during the end-Permian biotic crisis. Geology 33, 941–944.

Sephton, M.A., Visscher, H., Looy, C. V., Verchovsky, A.B., Watson, J.S., 2009. Chemical constitution of a Permian-Triassic disaster species. Geology 37, 875–878.

Sepkoski, J.J., 1989. Periodicity in extinction and the problem of catastrophism in the

history of life. Journal of Geological Society of London 146, 7-19.

Sewall, J.O., Van De Wal, R.S.W., Van Der Zwan, K., Van Oosterhout, C., Dijkstra, H.A., Scotese, C.R., 2007. Climate model boundary conditions for four Cretaceous time slices. Climate of the Past 3, 647–657.

Shibamoto, S., Murata, T., Yamamoto, K., 2016. Determination of double bond positions and geometry of methyl linoleate isomers with dimethyl disulfide adducts by GC/MS. Lipids 51, 1077–1081.

Shiea, J., Brassell, S.C., Ward, D.M., 1990. Mid-chain branched mono- and dimethyl alkanes in hot spring cyanobacterial mats: A direct biogenic source for branched alkanes in ancient sediments? Organic Geochemistry 15, 223–231.

Silva, M., Hoeneisen, M., Sammes, P.G., 1972. Some constituents of *Podocarpus saligna*. Phytochemistry 11, 433–434.

Škaloud, P., Friedl, T., Hallmann, C., Beck, A., Dal Grande, F., 2016. Taxonomic revision and species delimitation of coccoid green algae currently assigned to the genus *Dictyochloropsis* (Trebouxiophyceae, Chlorophyta). Journal of phycology 52, 599–617.

Škaloud, P., Peksa, O., 2010. Evolutionary inferences based on ITS rDNA and actin sequences reveal extensive diversity of the common lichen alga *Asterochloris* (Trebouxiophyceae, Chlorophyta). Molecular Phylogenetics and Evolution 54, 36–46.

Solberg, Y., 1986. Chemical constituents of the lichen species *Cetraria islandica*. The Journal of the Hattori Botanical Laboratory 60, 391–406.

Solberg, Y., 1987. Chemical constituents of the lichens *Cetraria delisei*, *Lobaria pulmonaria*, *Stereocaulon tomentosum* and *Usnea hirta*. The Journal of the Hattori Botanical Laboratory 63, 357–366.

Sorigué, D., Légeret, B., Cuiné, S., Morales, P., Mirabella, B., Guédeney, G., Li-Beisson, Y., Jetter, R., Peltier, G., Beisson, F., 2016. Microalgae synthesize hydrocarbons from long-chain fatty acids via a light-dependent pathway. Plant Physiology 171, 2393–2405.

Stein, W. E., Harmon, G. D., Hueber, F. M., 1993. Spongiophyton from the Lower Devonian of North America reinterpreted as a lichen. American Journal of Botany, 80, 93.

Steiner, M.B., Eshet, Y., Rampino, M.R., Schwindt, D.M., 2003. Fungal abundance spike and the Permian-Triassic boundary in the Karoo Supergroup (South Africa). Palaeogeography, Palaeoclimatology, Palaeoecology 194, 405–414.

Summons, R.E., Powell, T.G., Boreham, C.J., 1988. Petroleum geology and geochemistry of the Middle Proterozoic McArthur Basin, Northern Australia: III. Composition of extractable hydrocarbons. Geochimica et Cosmochimica Acta 52, 1747–1763.

Suzuki, N., Yessalina, S., Kikuchi, T., 2010. Probable fungal origin of perylene in Late Cretaceous to Paleogene terrestrial sedimentary rocks of northeastern Japan as indicated from stable carbon isotopes. Organic Geochemistry 41, 234–241.

Takashima, R., Kawabe, F., Nishi, H., Moriya, K., Wani, R., Ando, H., 2004. Geology and stratigraphy of forearc basin sediments in Hokkaido, Japan: Cretaceous environmental events on the north-west Pacific margin. Cretaceous Research 25, 365–390.

Takashima, R., Nishi, H., Yamanaka, T., Tomosugi, T., Fernando, A.G., Tanabe, K., Moriya, K., Kawabe, F., Hayashi, K., 2011. Prevailing oxic environments in the Pacific Ocean during the mid-Cretaceous Oceanic Anoxic Event 2. Nature Communications 2, 234–235.

Tang, H., Chen, Y., 2013. Global glaciations and atmospheric change at ca. 2.3 Ga. Geoscience Frontiers 4, 583–596.

Taylor, L., Banwart, S., Leake, J., Beerling, D.J., 2011. Modeling the evolutionary rise of ectomycorrhiza on sub-surface weathering environments and the geochemical carbon cycle. American Journal of Science 311, 369–403.

Taylor, T.N., Hass, H., Kerp, H., 1997. A cyanolichen from the lower Devonian Rhynie chert. American Journal of Botany 84, 992–1004.

Taylor, T.N., Klavins, S.D., Krings, M., Taylor, E.L., Kerp, H., Hass, H., 2004. Fungi from the Rhynie chert: A view from the dark side. Transactions of the Royal Society of Edinburgh, Earth Sciences 94, 457–473.

Taylor, T. N., Krings, M., 2005. Fungi and lichens. *In* Selley, R.C., Cocks, L.R.M., Plimer, I.R. [eds.], Encyclopedia of geology, vol. 2, 436-443. Elsevier, Amsterdam, Netherlands.

Taylor, T. N., Krings, M., Taylor, E. L., 2015. Fungal Spores. *In* Taylor, T. N., Krings, M., Taylor, E. L. [eds.], Fossil Fungi, 221-238. Elsevier, Amsterdam, Netherlands.

Taylor, L.L., Leake, J.R., Quirk, J., Hardy, K., Banwart, S.A., Beerling, D.J., 2009. Biological weathering and the long-term carbon cycle: Integrating mycorrhizal evolution and function into the current paradigm. Geobiology 7, 171–191.

ter Heide, R., Provatoroff, N., Traas, P.C., de valois, P.J., Van der plasse, N., Wobben, H.J., Timmer, R., 1975. Qualitative analysis of the odoriferous fraction of oakmoss (*Evernia prunastri* (L.) Ach.). Journal of Agricultural and Food Chemistry 23, 950–957.

Theissen, K.M., Zinniker, D.A., Moldowan, J.M., Dunbar, R.B., Rowe, H.D., 2005. Pronounced occurrence of long-chain alkenones and dinosterol in a 25,000-year lipid molecular fossil record from Lake Titicaca, South America. Geochimica et Cosmochimica Acta 69, 623–636.

Tomescu, M.F., Tate, R., Mack, N., Calder, V., 2010. Simulating fossilization to resolve the taxonomic affinities of thalloid fossils in Early Silurian (ca. 425 Ma) terrestrial assemblages. Bibliotheca Lichenologic 105, 183–190.

Torres, A., Dor, I., Rotem, J., Srebnik, M., Dembitsky, V.M., 2003. Characterization of surface *n*-alkanes and fatty acids of the epiphytic lichen *Xanthoria parietina*, its photobiont a green alga *Trebouxia* sp., and its mycobiont, from the Jerusalem hills. European Journal of Biochemistry 270, 2120–2125.

Toyota, M., Masuda, K., Asakawa, Y., 1998. Triterpenoid constituents of the moss *Floribundaria aurea* subsp. *nipponica*. Phytochemistry 48, 297–299.

Vajda, V., McLoughlin, S., 2004. Fungal proliferation at the Cretaceous-Tertiary Boundary. Science 303, 1489.

van Aarssen, B.G.., Alexander, R., Kagi, R.I., 2000. Higher plant biomarkers reflect palaeovegetation changes during Jurassic times. Geochimica et Cosmochimica Acta 64, 1417–1424.

van Bree, L.G.J., Rijpstra, W.I.C., Cocquyt, C., Al-Dhabi, N.A., Verschuren, D., Sinninghe Damsté, J.S., de Leeuw, J.W.,

2014. Origin and palaeoenvironmental significance of C_{25} and C_{27} *n*-alk-1-enes in a 25,000-year lake-sedimentary record from equatorial East Africa. Geochimica et Cosmochimica Acta 145, 89–102.

van Winden, J.F., Talbot, H.M., De Vleeschouwer, F., Reichart, G.J., Sinninghe Damsté, J.S., 2012. Variation in methanotroph-related proxies in peat deposits from Misten Bog, Hautes-Fagnes, Belgium. Organic Geochemistry 53, 73–79.

Venkatesan, M.I., 1988. Diploptene in Antarctic sediments. Geochimica et Cosmochimica Acta 52, 217–222.

Visscher, H., Sephton, M.A., Looy, C. V., 2011. Fungal virulence at the time of the end-Permian biosphere crisis? Geology 39, 883–886.

Volkman, J.K., Allen, D.I., Stevenson, P.L., Burton, H.R., 1986. Bacterial and algal hydrocarbons in sediments from a saline Antarctic lake, Ace Lake. Organic Geochemistry 10, 671–681.

Voytsekhovich, A., Beck, A., 2016. Lichen photobionts of the rocky outcrops of Karadag massif (Crimean Peninsula). Symbiosis 68, 9–24.

Wang, X., Krings, M., Taylor, T.N., 2010. A thalloid organism with possible lichen affinity from the Jurassic of northeastern China. Review of Palaeobotany and Palynology 162, 591–598.

Wang, C., Visscher, H., 2007. Abundance anomalies of aromatic biomarkers in the Permian-Triassic boundary section at Meishan, China - Evidence of end-Permian terrestrial ecosystem collapse. Palaeogeography, Palaeoclimatology, Palaeoecology 252, 291–303.

Waseda, A., Nishita, H., 1998. Geochemical characteristics of terrigenous- and marine-sourced oils in Hokkaido, Japan. Organic Geochemistry 28, 27–41.

Watanabe, T., 2000. Solvent-extractable Furans in Sedimentary rocks: Examination for their Potential Sources. Master Thesis of Department of CHEMISTRY, University of Tsukuba (in Japanese).

Watson, J.S., Sephton, M.A., Looy, C. V., Gilmour, I., 2005. Oxygen-containing aromatic compounds in a Late Permian sediment. Organic Geochemistry 36, 371–384.

Wolff, R.E., Wolff, G., McCloskey, J.A., 1966. Characterization of unsaturated hydrocarbons by mass spectrometry. Tetrahedron 22, 3093–3101.

Xu, H., Wang, L., Feng, X., Gong, X., 2022. Core taxa and photobiont-microbial interaction within the lichen *Heterodermia obscurata* (Physcsiaceae, *Heterodermia*). Symbiosis 86, 187–204.

Yamamoto, Y., 2017. Lichen of Japan. Sankeisha, Nagoya (In Japanese).

Yamamoto, K., Shibahara, A., Nakayama, T., Kajimoto, G., 1991. Determination of double-bond positions in methylene-interrupted dienoic fatty acids by GC-MS as their dimethyl disulfide adducts. Chemistry and Physics of Lipids 60, 39–50.

Yongdong, Z., Yaling, S., Zhengwen, L., Xiangchao, C., Jinlei, Y., Xiaodan, D., Miao, J., 2015. Long-chain *n*-alkenes in recent sediment of Lake Lugu (SW China) and their ecological implications. Limnologica 52, 30–40.

Yoshimura, I., 1994. Lichen flora of Japan in color, 6th ed. Hoikusha, Osaka (In Japanese).

Young, G.M., 2013. Precambrian supercontinents, glaciations, atmospheric oxygenation, metazoan evolution and an impact that may have changed the second

half of Earth history. Geoscience Frontiers 4, 247–261.

Yuan, X., Xiao, S., Taylor, T.., 2005. Lichens-like symbiosis 600 million Years Ago. Science 308, 1017–1020.

Zhang, Z., Metzger, P., Sachs, J.P., 2007. Biomarker evidence for the co-occurrence of three races (A, B and L) of *Botryococcus braunii* in El Junco Lake, Galápagos. Organic Geochemistry 38, 1459–1478.

Zhang, Z., Zhao, M., Yang, X., Wang, S., Jiang, X., Oldfield, F., Eglinton, G., 2004. A hydrocarbon biomarker record for the last 40 kyr of plant input to Lake Heqing, southwestern China. Organic Geochemistry 35, 595–613.

Zygadlo, J.A., Pignata, M.L., Gonzalez, C.M., Levin, A., 1993. Alkanes in lichens. Phytochemistry 32, 1453–1456.

Table S1

Compositions and concentrations of alkanes in lichen samples (μg/g dry wt). Mean ± SD.

Name	C_{13}		C_{14}		C_{15}		C_{16}		C_{17}		C_{18}		C_{19}		C_{20}	
	mean	*s.d.*	*mean*	*s.d.*	*mean*	*s.d.*	*mean*	*s.d.*	*mean*	*s.d.*	*mean*	*s.d.*	*mean*	*s.d.*	*mean*	*s.d.*
Platismatia interrupta (n = 1)					0.46	NA	0.22	NA	0.36	NA	0.30	NA	0.53	NA	0.60	NA
Flavoparmelia caperata (n = 3)					0.23	± 0.07	0.31	± 0.02	0.75	± 0.03	0.28	± 0.07	0.42	± 0.09	0.47	± 0.13
Parmotrema clavuliferum (n = 1)									0.24	NA	0.24	NA	0.19	NA	0.16	NA
Usnea bismolliuscula (n = 1)					0.05	NA	0.14	NA	0.10	NA	0.11	NA	0.14	NA
Usnea rubrotincta (n = 3)	0.02	± 0.01	0.02	± 0.02	0.04	± 0.01	0.06	± 0.01	0.15	± 0.04	0.11	± 0.03	0.12	± 0.03	0.08	± 0.03
Usnea mutabilis (n = 3)	0.01	± 0.01	0.02	± 0.01	0.03	± 0.01	0.05	± 0.01	0.17	± 0.03	0.12	± 0.03	0.13	± 0.02	0.10	± 0.01
Cladonia scabriuscula (n = 1)			0.09	NA	0.08	NA	0.19	NA	1.58	NA	0.94	NA	0.92	NA	0.65	NA
Cladonia vulcani (n = 1)			0.03	NA	0.08	NA	0.12	NA	0.82	NA	0.20	NA	0.49	NA	0.23	NA
Cladonia fruticulosa (n = 3)			0.02	± 0.02	0.11	± 0.03	0.09	± 0.01	2.69	± 0.46	0.13	± 0.03	0.59	± 0.06	0.46	± 0.04
Cladonia stellaris (n = 3)			0.01	± 0.01	0.04	± 0.01	0.04	± 0.01	0.60	± 0.08	0.11	± 0.02	0.17	± 0.02	0.17	± 0.03
Cladonia cryptochlorophaea (n = 3)			0.01	± 0.02	0.16	± 0.06	0.16	± 0.04	2.67	± 0.60	0.79	± 0.11	2.43	± 0.33	2.50	± 0.34
Cladonia ramulosa (n = 3)			0.02	± 0.02	0.18	± 0.08	0.15	± 0.05	2.27	± 0.35	0.54	± 0.11	1.65	± 0.24	1.63	± 0.28
Cladonia rangiferina (n = 3)					0.04	± 0.01	0.03	± 0.00	0.68	± 0.07	0.07	± 0.00	0.30	± 0.01	0.25	± 0.02
Stereocaulon japonicum (n = 1)			0.05	NA	1.05	NA	0.42	NA	8.96	NA	0.55	NA	1.47	NA	1.53	NA
Ramalina sinensis (n = 3)							0.10	± 0.02	1.56	± 0.27	0.25	± 0.04	1.37	± 0.16	0.41	± 0.05
Ramalina yasudae (n = 1)							0.17	NA	0.19	NA	0.19	NA	0.20	NA	0.15	NA
Xanthoria mandschurica **1** (n = 1)			0.09	NA	0.57	NA	0.56	NA	1.44	NA	0.50	NA	0.74	NA	1.02	NA
Xanthoria mandschurica **2** (n = 3)			0.13	± 0.04	2.76	± 0.58	0.82	± 0.35	3.05	± 0.70	1.74	± 0.54	3.59	± 0.88	5.99	± 1.52
Pyxine endochrysina (n =1)	3.28	NA	9.19	NA	0.45	NA	0.42	NA	1.26	NA	0.50	NA	0.42	NA	0.68	NA
Heterodermia subascendens (n = 1)					0.70	NA			3.04	NA	0.73	NA	1.49	NA	1.11	NA
Heterodermia obscurata (n = 1)							0.38	NA	1.71	NA			0.42	NA	0.38	NA
Anaptychia isidiza (n = 1)	0.23	NA	0.59	NA	0.63	NA	1.65	NA	2.67	NA	3.02	NA	1.84	NA	1.78	NA
Lobaria spathulata (n = 4)					0.14	± 0.08	0.19	± 0.11	11.70	± 1.74	0.16	± 0.12	0.18	± 0.11	0.32	± 0.18
Lobaria orientalis **1** (n = 1)			0.79	NA	1.10	NA	0.48	NA	7.37	NA	0.24	NA	0.68	NA	0.63	NA
Lobaria orientalis **2** (n = 3)			0.02	± 0.01	0.07	± 0.05	0.07	± 0.05	2.96	± 0.45	0.12	± 0.06	0.27	± 0.22	0.14	± 0.02
Lobaria tuberculata (n = 3)					0.10	± 0.03	0.15	± 0.04	11.24	± 1.87	0.08	± 0.02	0.10	± 0.01	0.11	± 0.01
Peltigera degenii (n = 1)					0.07	NA	0.26	NA	30.56	NA	0.96	NA	0.41	NA	0.27	NA
Collema furfuraceum (n = 3)	0.04	± 0.05	0.07	± 0.10	0.57	± 0.15	1.57	± 0.29	225.28	± 53.27	1.14	± 0.15	0.66	± 0.13	0.33	± 0.13
Collema complanatum (n = 3)					0.34	± 0.26	1.60	± 1.05	192.07	± 125.41	2.01	± 1.09	1.01	± 0.62	0.56	± 0.37

C$_{21}$		C$_{22}$		C$_{23}$		C$_{24}$		C$_{25}$		C$_{26}$		C$_{27}$		C$_{28}$		C$_{29}$		C$_{30}$	
mean	*s.d.*	*mean*	*s.d.*	*mean*	*s.d.*	*mean*	*s.d.*	*mean*	*s.d.*	*mean*	*s.d.*	*mean*	*s.d.*	*mean*	*s.d.*	*mean*	*s.d.*	*mean*	*s.d.*
2.30	NA	1.06	NA	13.46	NA	0.53	NA	3.55	NA	0.43	NA	7.63	NA	0.47	NA	4.79	NA	0.25	NA
0.86	± 0.15	0.73	± 0.19	0.88	± 0.24	0.37	± 0.10	1.11	± 0.35	0.18	± 0.08	1.59	± 0.66	0.19	± 0.10	2.67	± 1.23	0.14	± 0.12
0.33	NA	0.27	NA	0.40	NA	0.19	NA	0.51	NA	0.10	NA	0.64	NA	0.15	NA	1.59	NA		
0.23	NA	0.17	NA	0.27	NA	0.15	NA	0.37	NA	0.17	NA	0.64	NA			1.08	NA	0.18	NA
0.15	± 0.04	0.12	± 0.03	0.19	± 0.06	0.06	± 0.03	0.18	± 0.06	0.04	± 0.02	0.25	± 0.12	0.03	± 0.01	0.27	± 0.11	0.02	± 0.01
0.24	± 0.04	0.19	± 0.03	0.55	± 0.11	0.10	± 0.02	0.30	± 0.07	0.06	± 0.02	0.36	± 0.10	0.07	± 0.02	0.28	± 0.09	0.04	± 0.01
0.81	NA	0.60	NA	0.99	NA	0.48	NA	1.04	NA	0.55	NA	2.09	NA	0.75	NA	3.71	NA	0.47	NA
0.43	NA	0.66	NA	0.51	NA	0.12	NA	0.32	NA	0.07	NA	0.58	NA	0.07	NA	0.48	NA		
1.40	± 0.12	1.18	± 0.11	2.96	± 0.33	1.25	± 0.14	2.90	± 0.51	1.37	± 0.29	3.76	± 1.05	1.57	± 0.37	5.14	± 1.46	0.65	± 0.10
0.28	± 0.05	0.30	± 0.05	0.30	± 0.05	0.15	± 0.02	0.33	± 0.04	0.16	± 0.02	0.61	± 0.12	0.26	± 0.08	1.85	± 0.56	0.33	± 0.14
5.24	± 0.67	5.29	± 0.65	5.40	± 0.54	3.55	± 0.40	4.85	± 0.61	4.79	± 0.68	8.09	± 1.29	7.61	± 1.66	17.44	± 5.52	3.67	± 1.26
3.74	± 0.59	3.68	± 0.60	4.27	± 0.69	2.11	± 0.31	2.63	± 0.40	2.29	± 0.34	3.52	± 0.49	2.41	± 0.37	3.64	± 0.71	0.63	± 0.12
0.65	± 0.07	0.69	± 0.06	1.02	± 0.10	0.39	± 0.03	0.97	± 0.08	0.48	± 0.06	2.22	± 0.26	0.62	± 0.06	7.38	± 4.43	0.55	± 0.06
4.75	NA	3.67	NA	4.77	NA	2.30	NA	3.09	NA	0.98	NA	3.37	NA	1.34	NA	13.59	NA	1.01	NA
0.96	± 0.08	0.96	± 0.13	1.44	± 0.16	0.43	± 0.06	4.22	± 0.90	0.48	± 0.08	8.92	± 1.82	0.53	± 0.09	4.88	± 0.83	0.15	± 0.07
0.54	NA	0.27	NA	0.89	NA	0.22	NA	1.05	NA	0.14	NA	0.79	NA	0.12	NA	1.41	NA		
3.64	NA	2.97	NA	3.25	NA	0.71	NA	1.80	NA	0.55	NA	2.07	NA	0.47	NA	1.79	NA	0.46	NA
20.03	± 2.04	14.48	± 2.38	9.78	± 1.60	1.21	± 0.36	1.38	± 0.18	0.21	± 0.05	0.97	± 0.30	0.06	± 0.02	0.54	± 0.21		
1.44	NA	1.10	NA	2.26	NA	0.66	NA	2.20	NA	0.79	NA	6.09	NA	1.49	NA	18.64	NA	1.70	NA
2.54	NA	2.10	NA	3.54	NA	1.24	NA	3.46	NA	0.61	NA	5.29	NA	0.96	NA	20.57	NA	0.92	NA
1.17	NA	0.67	NA	2.45	NA			1.54	NA	0.26	NA	1.66	NA			2.29	NA		
2.34	NA	1.75	NA	1.95	NA	0.72	NA	1.74	NA	0.80	NA	3.37	NA	1.01	NA	6.67	NA	1.39	NA
1.02	± 0.34	0.81	± 0.33	1.65	± 0.68	0.43	± 0.18	1.70	± 0.72	0.12	± 0.08	0.97	± 0.63	0.08	± 0.09	1.80	± 0.37	0.03	± 0.04
2.37	NA	1.06	NA	0.96	NA														
0.46	± 0.06	0.30	± 0.03	0.61	± 0.08	0.13	± 0.02	0.59	± 0.08	0.09	± 0.02	1.04	± 0.30	0.12	± 0.03	2.08	± 0.75	0.05	± 0.02
0.41	± 0.05	0.29	± 0.04	0.53	± 0.04	0.18	± 0.01	0.72	± 0.06	0.25	± 0.03	1.27	± 0.29	0.42	± 0.12	1.78	± 0.54	0.15	± 0.05
0.52	NA	0.30	NA	2.49	NA	0.27	NA	5.50	NA	0.50	NA	12.21	NA	0.46	NA	6.97	NA	0.09	NA
0.63	± 0.08	0.48	± 0.04	0.96	± 0.04	0.28	± 0.11	0.68	± 0.15	0.26	± 0.12	1.56	± 0.39	0.36	± 0.08	3.75	± 1.26	0.34	± 0.16
0.52	± 0.17	0.27	± 0.13	0.41	± 0.12	0.06	± 0.05	0.15	± 0.11	0.01	± 0.02	0.08	± 0.11			0.24	± 0.34		

C$_{31}$		C$_{32}$		C$_{33}$		C$_{34}$		C$_{35}$		C$_{36}$		C$_{37}$		C$_{38}$		C$_{39}$		C$_{40}$	
mean	s.d.	mean	s.d.	mean	s.d.	mean	s.d.	mean	s.d.	mean	s.d.	mean	s.d.	mean	s.d.	mean	s.d.	mean	s.d.
3.24	NA	0.11	NA	0.47	NA														
1.27	± 1.02	0.06	± 0.09	0.10	± 0.14														
0.71	NA																		
0.72	NA			0.22	NA														
0.09	± 0.04	0.01	± 0.01	0.03	± 0.02														
0.12	± 0.04	0.02	± 0.01	0.06	± 0.02														
2.97	NA	0.18	NA	0.69	NA														
0.32	NA																		
3.07	± 0.57	0.22	± 0.03	1.80	± 0.68	0.03	± 0.02	0.33	± 0.18	0.02	± 0.03								
5.84	± 2.36	0.10	± 0.04	0.75	± 0.38														
15.09	± 5.93	0.79	± 0.37	3.48	± 1.83														
3.55	± 1.23	0.19	± 0.08	1.53	± 0.83														
9.23	± 1.31	0.27	± 0.06	3.30	± 1.01														
15.66	NA	0.48	NA	5.17	NA														
2.83	± 0.85	0.06	± 0.03	0.28	± 0.21														
0.57	NA																		
1.45	NA	0.33	NA	0.43	NA	0.20	NA	0.15	NA	0.12	NA	0.09	NA	0.06	NA	0.03	NA	0.04	NA
0.07	± 0.11			0.04	± 0.06														
17.87	NA	1.15	NA	3.03	NA														
9.61	NA	0.44	NA	1.68	NA														
1.19	NA																		
8.53	NA	0.87	NA	1.83	NA														
0.58	± 0.16																		
0.67	± 0.29	0.01	± 0.01	0.06	± 0.05														
0.44	± 0.14	0.01	± 0.01	0.01	± 0.01														
3.25	NA	0.05	NA	0.32	NA														
3.83	± 1.34	0.10	± 0.14	0.88	± 0.23														

C_{41}		C_{42}		Total alkane conc. (μg/g dry wt)	
mean	*s.d.*	*mean*	*s.d.*	*mean*	*s.d.*
				40.75	NA
				12.61	± 4.50
				5.71	NA
				4.73	NA
				2.05	± 0.67
				3.02	± 0.61
				19.77	NA
				5.55	NA
				31.74	± 4.87
				12.40	± 4.05
				94.01	± 22.11
				40.62	± 5.78
				29.14	± 6.72
				74.20	NA
				29.83	± 4.99
				6.92	NA
0.02	NA	0.02	NA	25.59	NA
				66.84	± 10.54
				74.61	NA
				60.05	NA
				14.12	NA
				45.39	NA
				21.87	± 4.97
				15.67	NA
				9.86	± 2.25
				18.24	± 1.56
				65.47	NA
				243.770	± 49.98
				199.35	± 128.43

Table S2

Compositions and concentrations of alkenes in lichen samples (μg/g dry wt). Mean ± SD. tr.; trace

Samples	C16:1								C17:4		C17:3				C17:2									
	C16:1_1		C16:1_2		C16:1_3		C16:1_4		C17:1_4		C17:3_1		C17:3_2		1,8-C17:2		6,9-C17:2		C17:2_3		C17:2_4		C17:2_5	
	mean	s.d.	mean	s.d.	mean	s.d.	mean	s.d.	mean	s.d.	mean	s.d.	mean	s.d.	mean	s.d.	mean	s.d.	mean	s.d.	mean	s.d.	mean	s.d.
Platismatia interrupta (n = 1)	0.33	NA	tr.	NA	tr.	NA					0.08	NA			41.93	NA								
Flavoparmelia caperata * (n = 3)	0.31	± 0.14					0.26	± 0.04			0.18	± 0.04			67.93	± 3.19							2.48	± 0.41
Parmotrema clavuliferum (n = 1)	0.29	NA			tr.	NA									56.68	NA							0.98	NA
Usnea bismolliuscula * (n = 1)	0.26	NA									0.18	NA			58.47	NA							0.71	NA
Usnea rubrotincta (n = 3)															70.41	± 16.09							2.87	± 1.91
Usnea mutabilis (n = 3)															98.55	± 10.87								
Cladonia scabriuscula * (n = 1)							0.09	NA									5.28	NA	tr.	NA				
Cladonia vulcani (n = 1)																	10.61	NA	tr.	NA				
Cladonia fruticulosa (n = 3)																	3.08	± 1.53						
Cladonia stellaris (n = 3)																	12.18	± 2.28			1.40	± 0.36		
Cladonia cryptochlorophaea (n = 3)																	2.06	± 0.64						
Cladonia ramulosa (n = 3)																	4.75	± 1.13						
Cladonia rangiferina (n = 3)																	4.50	± 0.68						
Stereocaulon japonicum (n = 1)	0.10	NA	tr.	NA	tr.	NA											16.48	NA	tr.	NA				
Ramalina sinensis (n = 3)	0.20	± 0.05							tr.	NA	1.18	± 0.45			14.81	± 2.50								
Ramalina yasudae * (n = 1)	0.21	NA													30.33	NA							0.61	NA
Xanthoria mandschurica **1** * (n = 1)															37.71	NA								
Xanthoria mandschurica **2** (n = 3)											0.33	± 0.24			145.74	± 63.96								
Pyxine endochrysina (n =1)	0.59	NA									0.08	NA			37.32	NA								
Heterodermia subascendens (n = 1)	0.85	NA											0.65	NA	27.08	NA								
Heterodermia obscurata (n = 1)													1.22	NA	30.94	NA								
Anaptychia isidiza (n = 1)															19.24	NA							1.76	NA
Lobaria spathulata * (n = 4)																	46.55	± 7.54			5.25	± 3.74		
Lobaria orientalis **1** (n = 1)																	30.87	NA			5.10	NA		
Lobaria orientalis **2** (n = 3)																	27.59	± 3.26			1.06	± 0.36		
Lobaria tuberculata (n = 3)																	44.38	± 3.32			2.91	± 0.59		
Peltigera degenii * (n = 1)																								
Collema furfuraceum * (n = 3)																								
Collema complanatum (n = 3)																								

*modified from Ikeda et al., 2021

| C17:2_6 | | 8-,7-C17:1 | | 1-C17:1 | | 3-C17:1 | | C17:1_4 | | C17:1_5 | | C17:1_6 | | C17:1_7 | | 1-C18:1 | | 4-C18:1 | | C18:1_3 | | C18:1_4 | | C18:1_5 | | C18:1_6 | |
mean	s.d.	mean	s.d.	mean	s.d.	mean	s.d.	mean	s.d.	mean	s.d.	mean	s.d.	mean	s.d.	mean	s.d.	mean	s.d.	mean	s.d.	mean	s.d.	mean	s.d.	mean	s.d.
				1.07	NA			0.65	NA							0.04	NA	0.11	NA								
				1.32	± 0.13																						
				2.24	NA																						
				2.77	NA																						
tr.	NA			0.93	± 0.26																						
tr.	NA			0.61	± 0.10									3.59	± 1.59												
		17.43	NA					0.31	NA																	tr.	NA
		22.20	NA					0.85	NA																	tr.	NA
		16.68	± 6.40	0.08	± 0.00			0.28	± 0.02																	tr.	NA
		18.47	± 2.78																					0.12	± 0.03		
		9.77	± 2.62	0.18	± 0.07			0.22	± 0.07																		
		12.21	± 2.83	0.19	± 0.01			0.22	± 0.01																		
		26.31	± 1.81	0.06	± 0.01			0.18	± 0.03															0.05	± 0.00		
		15.79	NA	0.45	NA	1.67	NA	0.27	NA							0.30	NA	0.26	NA								
				1.30	± 0.23			0.25	± 0.03									0.03	± 0.01								
				0.96	NA																						
				1.05	NA	0.65	NA	0.45	NA			0.25	NA														
				2.05	± 0.14	0.28	± 0.12	2.49	± 1.08			0.94	± 0.12											0.23	± 0.04		
				2.26	NA			0.70	NA									0.04	NA							tr.	NA
				1.46	NA																						
				2.50	NA																						
				0.73	NA																						
		19.72	± 1.99													8.07	± 5.22							0.34	± 0.20		
		40.41	NA													6.39	NA							0.53	NA		
		9.83	± 2.51			0.20	± 0.28	0.15	± 0.02							0.26	± 0.36	0.42	± 0.04					0.18	± 0.04		
		15.16	± 3.29			0.39	± 0.55	0.70	± 0.40							1.03	± 0.14	0.71	± 0.59					0.46	± 0.11		
						20.32	NA	0.63	NA									77.47	NA	0.41	NA	3.51	NA				
		2.12	± 0.49							3.17	± 0.81					384.56	± 132.79										
						54.88	± 35.65			3.09	± 1.81					450.80	± 313.15	14.87	± 15.00								

| C18:1 | | | | | | | | | | | | | | C19:2 | | | | | | | | | | | | | |
| C18:1_7 | | C18:1_8 | | C18:1_9 | | C18:1_10 | | C18:1_11 | | C18:1_12 | | C18:1_13 | | C19:2_1 | | C19:2_2 | | C19:2_3 | | 5-C19:1 | | C19:1_2 | | C19:1_3 | | C19:1_4 | |
mean	s.d.	mean	s.d.	mean	s.d.	mean	s.d.	mean	s.d.	mean	s.d.	mean	s.d.	mean	s.d.	mean	s.d.	mean	s.d.	mean	s.d.	mean	s.d.	mean	s.d.	mean	s.d.
								0.10	NA	0.05	NA	0.33	NA														
												0.12	± 0.02					0.07	± 0.01								
												0.13	± 0.02					0.13	± 0.02								
												0.11	± 0.04					0.15	± 0.02								
												0.05	± 0.02					0.05	± 0.00								
				0.15	NA							0.17	NA							0.33	NA						
																0.05	NA										
0.55	± 0.44																	0.39	± 0.24	13.50	± 4.59						
0.36	NA							0.26	NA											0.68	NA						
0.12	± 0.05																	0.22	± 0.02	1.86	± 1.22						
2.52	± 0.85																	0.27	± 0.07	6.14	± 2.30						
				4.29	NA															178.76	NA	0.27	NA	1.94	NA	1.79	NA
		3.73	± 1.99	2.31	± 0.64	8.01	± 4.14							9.92	± 3.59												
0.59	± 0.32			25.13	± 24.14	5.26	± 3.40							76.33	± 49.26	1.91	± 1.36										

| C19:1 | | | | | | | | | | C20:1 | | | | | | | | | | | | | | | | | |
| C19:1_5 | | C19:1_6 | | C19:1_7 | | C19:1_8 | | C19:1_9 | | 6-C20:1 | | C20:1_2 | | C20:1_3 | | C20:1_4 | | C20:1_5 | | C20:1_6 | | C20:1_7 | | C21:1_1 | | C21:1_2 | |
mean	s.d.	mean	s.d.	mean	s.d.	mean	s.d.	mean	s.d.	mean	s.d.	mean	s.d.	mean	s.d.	mean	s.d.	mean	s.d.	mean	s.d.	mean	s.d.	mean	s.d.	mean	s.d.
						0.33	NA															0.12	NA				
						0.76	± 0.46																				
						0.27	± 0.08															0.04	± 0.01				
0.18	± 0.02					0.37	± 0.04															0.16	± 0.01				
0.08	± 0.01					0.26	± 0.05															0.10	± 0.02				
0.03	± 0.00					0.07	± 0.00															0.01	± 0.00				
						0.84	NA															0.10	NA				
						0.13	± 0.02															0.04	± 0.01				
0.07	NA																										
						0.80	NA	0.27	NA													0.27	NA			0.17	NA
						1.34	± 0.33	0.11	± 0.03	0.87	± 1.24											0.52	± 0.11	tr.	NA	0.24	± 0.04
0.05	NA					0.43	NA	0.20	NA											tr.	NA	0.08	NA				
						0.45	NA															0.17	NA				
1.21	NA																										
0.04	± 0.03																										
						0.31	± 0.16																				
								0.98	NA	15.22	NA	0.62	NA	0.17	NA												
0.80	± 0.49	1.32	± 0.60	1.79	± 0.73																						
		2.33	± 1.65			9.78	± 4.72											tr.	NA	tr.	NA					1.01	± 0.29

C21:1_3		C21:1_4		C21:1_5		C21:1_6		C22:1_1		C22:1_2		C22:1_3		C23:1_1		C23:1_2		C24:1_1		C25:1_1		C25:1_2		C25:1_3		C26:1_1	
mean	s.d.	mean	s.d.	mean	s.d.	mean	s.d.	mean	s.d.	mean	s.d.	mean	s.d.	mean	s.d.	mean	s.d.	mean	s.d.	mean	s.d.	mean	s.d.	mean	s.d.	mean	s.d.
				0.12	NA							0.13	NA					0.07	NA							0.06	NA
						0.14	± 0.07																				
						0.06	± 0.01																				
						0.09	± 0.02																				
						0.16	NA																				
						0.21	± 0.00					0.05	± 0.01			0.02	± 0.01	0.04	± 0.03					0.05	± 0.04	0.08	± 0.07
				0.02	± 0.00																						
				0.25	± 0.01							0.21	± 0.01			0.07	± 0.01	0.20	± 0.03					0.17	± 0.05	0.38	± 0.14
				0.20	± 0.05							0.11	± 0.02			0.03	± 0.00	0.08	± 0.01					0.05	± 0.00	0.09	± 0.02
				0.02	± 0.01							0.02	± 0.01			0.01	± 0.00	0.03	± 0.00					0.01	± 0.01	0.08	± 0.03
				0.19	NA							0.09	NA			0.02	NA	0.04	NA					0.03	NA		
				0.09	± 0.01							0.04	± 0.01					0.07	± 0.03								
						0.83	NA																				
		0.12	± 0.01			1.66	± 0.21	0.24	± 0.03	1.40	± 0.12			1.08	± 0.06												
0.06	NA			0.09	NA							0.20	NA					0.02	NA			0.08	NA				
						0.49	NA					0.06	NA														
						0.18	NA																				
						0.11	± 0.06																				
				0.03	± 0.00																						
						0.07	± 0.01																			0.10	± 0.08
		0.14	NA	0.07	NA							0.10	NA					0.12	NA					0.21	NA	0.18	NA
						0.19	± 0.14																				

C27:3		C27:2		C27:1				C28:1				C29:3		C29:2		C29:1				Total alkene conc. (µg/g dry wt)	
C27:3_1		C27:2_1		C27:1_1		C27:1_2		C28:1_1		C28:1_2		C29:3_1		C29:2_1		C29:1_1		C29:1_2			
mean	s.d.	mean	s.d.	mean	s.d.	mean	s.d.	mean	s.d.	mean	s.d.	mean	s.d.	mean	s.d.	mean	s.d.	mean	s.d.	mean	s.d.
																				45.51	NA
																				73.37	± 2.30
																				60.19	NA
																				62.40	NA
																				74.27	± 16.90
																				102.84	± 9.36
																				23.52	NA
																				33.82	NA
																				20.87	± 7.85
																				32.37	± 5.44
						0.30	± 0.13			0.30	± 0.18									15.07	± 4.00
						0.05	± 0.01													18.69	± 4.02
										0.02	± 0.00									31.51	± 2.45
										0.04	NA									37.31	NA
																				18.14	± 3.23
																				32.18	NA
																tr.	NA			42.29	NA
																				159.67	± 63.32
0.12	NA	0.42	NA	0.10	NA	1.10	NA	0.08	NA	0.12	NA	0.03	NA	0.63	NA			0.10	NA	44.95	NA
																				31.22	NA
																				34.85	NA
																				22.95	NA
																				94.49	± 11.05
																				84.60	NA
																				41.95	± 4.54
																				75.14	± 10.30
		0.41	NA											0.19	NA					307.79	NA
																				417.74	± 146.01
																				646.17	± 441.24